

**Elucidating Mechanisms of Sulfamethoxazole Sorption onto Bentonite in the  
Presence of Fresh Liquid Swine Manure Dissolved Organic Carbon**

By

Charitha K. Hansima

A Thesis submitted to the Faculty of Graduate Studies of

The University of Manitoba

in Partial fulfillment of the requirements for the degree of

MASTER OF SCIENCE

Department of Soil Science

University of Manitoba

Winnipeg, Manitoba

Copyright © 2023 by Charitha K. Hansima

## ABSTRACT

Charitha K. Hansima, M.Sc., The University of Manitoba, August 2023. Elucidating Mechanisms of Sulfamethoxazole Sorption onto Bentonite in the Presence of Fresh Liquid Swine Manure Dissolved Organic Carbon. Advisor: Dr. Inoka Amarakoon.

The extensive use of sulfamethoxazole (SMX) as a veterinary antimicrobial in the Canadian swine industry increases its occurrence in manure. Land application of swine manure enhances the dispersal of SMX in the environment, increasing the risk of antibiotic resistance development in bacteria, one of the focal human health emergencies of our times. Humic acid (HA) and fulvic acid (FA) from the dissolved organic carbon (DOC) fraction in fresh liquid swine manure influence the sorption of SMX onto smectite clays, hence the environmental fate.

This research aimed to elucidate the effect of fresh liquid swine manure DOC species in fresh liquid swine manure on SMX sorption onto bentonite. Specific objectives were to (i) elucidate the physicochemical characteristics of HA and FA isolated from fresh liquid swine manure DOC and (ii) assess their contribution to the mechanisms controlling SMX sorption onto bentonite clay.

Humic substances were extracted and characterized for their physicochemical properties. A batch sorption study with a randomized complete block design was used to quantify the SMX sorption, explicit clay-mineral surface and interlayer sorption, and probe fluorescence quenching in humic substances by SMX.

Results showed that FA was the dominant component of DOC in the fresh liquid swine manure examined in this study (10 FA: 1 HA). Thus, FA determined the major portion of organic matter coating on the mineral bentonite and binding of SMX. Spectroscopic analysis revealed that hydrophobicity (53.0% HA, 56.5% FA), hydrophilicity (34.0% HA, 35.1% FA), aromaticity

(34.0% HA, 37.2% FA), and aliphaticity (66.0% HA, 62.7% FA) of the two humic substances were similar despite the differences in their functional groups. Solid state  $^{13}\text{C}$ -NMR data and X-ray Photoelectron Spectroscopic data revealed that the core and the surface of HA and FA secondary structures were substantially different. The orientation of functional groups in clay mineral-bound HA and FA and free aqueous HA and FA determined SMX sorption mechanisms. The abundance of surface-oriented phenolic functional groups in mineral-bound and free FA resulted in fluorophore quencher  $\pi$ - $\pi$  electron-donor-acceptor interactions, cation and water bridging, and H-bonding. In contrast, the relatively high surface amide groups in HA structures allowed non-fluorophore quencher H-bonding, cation, and water-bridging mechanisms with SMX. Sorption data suggested the formation of extractable aqueous FA-SMX residues, whereas SMX complexed to aqueous HA is non-extractable. Spectroscopic data revealed a comparatively higher amount of -COOH functional groups in FA colloids, which made FA-SMX unstable and susceptible to breakdown in aqueous environments. SMX complexed with aqueous FA can be transported in rain and snowmelt runoff and leach into aquatic environments and subsequently desorbed. We suggest the storage of fresh liquid swine manure under aerobic conditions in open lagoons to oxidize FA functional groups or composting of the manure to hinder SMX sorption to FA before land application. Further, the transformation of FA to HA through humification under long-term storage may also contribute to reducing the sorption of SMX onto FA.

Key words: Fresh liquid swine manure, dissolved organic carbon, humic acid, fulvic acid, sulfamethoxazole, sorption mechanisms, bentonite clay

## ACKNOWLEDGEMENTS

First, I would like to express my deepest gratitude to my academic advisor, Dr. Inoka Amarakoon, for her invaluable assistance, guidance, encouragement, and continuous support throughout the program. I am grateful to have a supervisor who expected the best of me and encouraged me to be better. I am also grateful to members of my advisory committee, Dr. Francis Zvomuya, Dr. Annemieke Farenhorst, and Dr. Srimathie Indraratne, for their valuable guidance and ideas to improve the project. In addition, I am grateful to Dr. Amarakoon's research group and collaborators for their contribution to this research by facilitating necessary lab resources and allowing me the flexibility to carry out the research.

I am thankful to the technical staff in the Department of Soil Science, especially Rob Ellis and Fernando Esposito, for their untiring willingness to help with my numerous requests. Further, I would also like to extend my gratitude to Dr. Alistair Brown, Mark Cooper, Ravinder Sidhu, Dr. David Davidson, Jolly Hipolito, Emy Komatsu, John Bachu, and Don Chaput for their technical assistance and guidance during the analysis of my samples. A heartfelt gratitude to my friends Manushi Archana, Viranga Weerasinghe, Dilki Wijekoon, Chamali Kodikara, and many others for their companionship during all the ups and downs.

I gratefully appreciate research funding support from the NSERC Discovery Grant (RGPIN-2022-04497) and stipend support from the University of Manitoba Graduate Fellowship (UMGF) during the first year and Manitoba Zero Tillage Research Association (MZTRA) soil conservation fellowship during the second year of the program.

I extend my heartfelt appreciation to my mother, father, and husband, Manuja Sugathadasa, for giving me unwavering belief, love, and push through tough times and during the lone life far-off from home. Thank you for all you did for me and for seeing the best in me.

## FOREWARD

This thesis contains three chapters and follows the layout in the guidelines of the Department of Soil Science, Faculty of Agricultural and Food Sciences, University of Manitoba. Chapter 1 provides an overview of the literature on the fate of livestock-administered sulfamethoxazole in the environment and the role of clay minerals and organic matter in determining the environmental fate of sulfamethoxazole. Chapter 2 presents the thesis research prepared in the manuscript format for the Environmental Science and Technology journal. Chapter 2 focuses on the physicochemical properties of humic acid and fulvic acid derived from fresh liquid swine manure dissolved organic carbon fraction and their contribution to sulfamethoxazole sorption mechanisms onto bentonite. Chapter 3 is the overall synthesis of the project, including a summary of findings and contributions to knowledge, implications of the research, and knowledge gaps and research recommendations. An extended version of Chapter 1 has been published as a review article in the Science of The Total Environment journal.

Publication based on Chapter 1:

**Hansima, M.A.C.K., F. Zvomuya, and I. Amarakoon. 2023.** Fate of veterinary antimicrobials in Canadian prairie soils - A critical review. *Sci. Total Environ.* 892: 164387. doi: 10.1016/j.scitotenv.2023.164387.

### Contributions of Authors

The contributions of the authors for the published article “Fate of veterinary antimicrobials in Canadian prairie soils - A critical review” based on Chapter 1 are as follows:

- M.A.C.K. Hansima: Conceptualization, writing the original draft.

- Inoka Amarakoon: Conceptualization, funding acquisition, review, and editing
- Francis Zvomuya: Review and editing.

The contributions of the authors for the manuscript, Physicochemical properties of humic and fulvic acid in fresh liquid swine manure and their effect on sulfamethoxazole sorption onto bentonite clay, based on Chapter 2 are as follows:

- M.A.C.K. Hansima: Conceptualization, conducted experiments, data acquisition, analysis, and original draft writing.
- Inoka Amarakoon: Conceptualization, supervision of the project, funding acquisition, review, and editing.
- Francis Zvomuya: Review and editing of the manuscript drafts.
- Srimathie Idraratne: Review and editing of the manuscript drafts.
- Annemieke Farenhorst: Review and editing of the manuscript drafts.

# TABLE OF CONTENTS

ABSTRACT.....	ii
ACKNOWLEDGEMENTS.....	iv
LIST OF TABLES.....	iv
LIST OF FIGURES.....	xii
1. GENERAL INTRODUCTION.....	1
1.1 Occurrence of sulfamethoxazole in the environment.....	1
1.2 Structure-inherent sorption interactions of sulfamethoxazole.....	4
1.2.1 Acid dissociation constants.....	6
1.2.2 Partition coefficients.....	7
1.2.3 Molecular geometry.....	8
1.3 Interaction mechanisms with soil components.....	9
1.3.1 Soil organic matter.....	9
1.3.2 Clay minerals.....	11
1.3.3 Organo-mineral complexes.....	13
1.4 Physiochemical properties of humic substances originated from animal manure.....	15
1.5 Status of animal manure contaminated with sulfamethoxazole.....	19
1.6 Objectives.....	20
1.7 Hypotheses.....	21
1.8 Thesis outline.....	21
1.9 References.....	22
2. PHYSICOCHEMICAL PROPERTIES OF HUMIC AND FULVIC ACID IN FRESH LIQUID SWINE MANURE AND THEIR EFFECT ON SULFAMETHOXAZOLE SORPTION ONTO BENTONITE CLAY.....	29
2.1 Abstract.....	29
2.2 Introduction.....	30
2.3 Materials and Methods.....	32
2.3.1 Isolation and purification of humic and fulvic acid from fresh liquid swine manure dissolved organic carbon fraction.....	32
2.3.2 Analytical methods for characterization of swine manure humic substance.....	35
2.3.3 Sorption study.....	37

2.4 Results and Discussion .....	43
2.4.1 Constituents of fresh liquid swine manure DOC fraction .....	43
2.4.2 Structural characteristics of fresh liquid swine manure humic substances.....	45
2.4.2.1 Solid-state <sup>13</sup> C-CPMAS-NMR spectroscopy .....	45
2.4.2.2 Fourier Transformed Infrared Spectroscopy.....	48
2.4.2.3 X-ray Photoelectron Spectroscopy .....	49
2.4.2.4 Particle size distribution and Zeta potential.....	52
2.4.3 Sorption mechanisms from Freundlich parameters combined with the physicochemical characteristics of the dissolved organic carbon fraction and characteristics of mineral bentonite .....	55
2.4.3.1 Mechanism I - Sorption of sulfamethoxazole to bentonite.....	57
2.4.3.2 Mechanism II - Sorption of sulfamethoxazole to organic matter .....	58
2.4.3.3 Mechanism III - Formation of organic matter-bound bentonite .....	63
2.4.3.4 Mechanism IV - Sorption of sulfamethoxazole to organic matter-bound bentonite .....	66
2.4.3.5 Surface and interlayer sulfamethoxazole sorption onto mineral bentonite.....	67
2.5 Mechanism highlights to illustrate sulfamethoxazole sorption onto bentonite in the presence of fresh liquid swine manure dissolved organic carbon fraction .....	75
2.6 Conclusions and environmental implications .....	77
2.7 References.....	80
3. OVERALL SYNTHESIS.....	86
3.1 Summary of Findings and Contributions to Knowledge .....	86
3.2 Implications of the Research.....	90
3.3 Recommendations for Future Research and Limitations of the Current Research.....	91
3.4 References.....	92
4. APPENDICES.....	94

## LIST OF TABLES

Table	Page
1.1 Physicochemical properties of sulfamethoxazole .....	5
1.2 Summary of elemental composition and C-functional groups for livestock manure-derived organic matter .....	17
2.1 A summary of chemical shifts of major carbon functional groups obtained from <sup>13</sup> C-CPMAS-NMR spectra of fresh liquid swine manure humic acid and fulvic acid and a comparison of their bulk chemical properties .....	47
2.2 Non-linear Freundlich parameters $K_f$ and $n$ for sulfamethoxazole sorption for 20, 40, 60, and 100 $\mu\text{g L}^{-1}$ levels of concentration onto bentonite clay in the presence of dissolved organic carbon (DOC) fraction, fulvic acid (FA), and humic acid (HA) derived from fresh liquid swine manure .....	56
2.3 Statistical significance from Analysis of Variance (ANOVA) for the changes occurred to the Infrared peak position of bentonite (Bt) Si-O vibrations when changing the sulfamethoxazole (SMX) concentration as 0, 20, 40, 60, and 100 $\mu\text{g L}^{-1}$ in the presence of fresh liquid swine manure derived organic matter (dissolved organic carbon fraction (DOC)/fulvic acid (FA)/humic acid (HA)) obtained from equilibrated sorption solids .....	68
2.4 Statistical significance from Analysis of Variance (ANOVA) for the changes that occurred to the full width at half maximum (FAHM) of the basal reflection peak ( $d_{001}$ ) of bentonite X-ray diffraction pattern when changing the sulfamethoxazole (SMX) concentration from 0, 20, 40, 60, to 100 $\mu\text{g L}^{-1}$ in the presence of fresh liquid swine	

manure derived organic matter (dissolved organic carbon fraction (DOC)/fulvic acid (FA)/humic acid (HA)) obtained from equilibrated sorption solids .....	71
A-1 Chemical properties of fresh liquid swine manure slurry and metal ions present in fresh liquid swine manure dissolved organic carbon fraction .....	94
A-2 Peak positions of Infrared bands of bentonite (Bt) Si-O vibrations when changing the sulfamethoxazole (SMX) concentration as 0, 20, 40, 60, and 100 $\mu\text{gL}^{-1}$ in the presence of fresh liquid swine manure-derived organic matter (dissolved organic carbon fraction (DOC)/fulvic acid (FA)/humic acid (HA)) obtained from equilibrated sorption solids .....	95
A-3 Full width at half maximum values of basal reflection peak ( $d_{001}$ ) of bentonite X-ray diffraction pattern when changing the sulfamethoxazole (SMX) concentration as 0, 20, 40, 60, and 100 $\mu\text{gL}^{-1}$ in the presence of fresh liquid swine manure derived organic matter (dissolved organic carbon fraction (DOC)/fulvic acid (FA)/humic acid (HA)) obtained from equilibrated sorption solids .....	97

## LIST OF FIGURES

Figure	Page
2.1 Characterization of swine manure DOC fraction for a) molecular weight distribution by High-Performance Size-Exclusion Chromatography (HPSEC) at $UV_{254}$ , b) identification of their components by Excitation-Emission Matrix spectroscopy and deconvoluted HPSEC spectra for c) humic and fulvic acids, and d) aromatic amino acids. Region I) of b) is for protein-like fluorophores, II) is for fulvic-like fluorophores, III) is for soluble microbial byproduct fluorophores, and IV) is for humic-like fluorophores .....	44
2.2 $^{13}C$ -Cross Polarization Magic-Angle-Spinning Nuclear Magnetic Resonance spectra of a) fulvic acid (FA) and b) humic acid (HA) isolated from fresh liquid swine manure dissolved organic carbon fraction with c) a comparison of relative intensities of carbon functionalities of carboxyl, aromatic, carbohydrate, and aliphatic region .....	46
2.3 Splits of FTIR spectra obtained for fresh liquid swine manure humic substances. High-frequency region of a) humic acid (HA) and d) fulvic acid (FA) to capture O-H and C-H vibrations, mid-frequency region of b) HA and e) FA to capture C=C and C=O vibrations, and low-frequency region of c) HA and f) FA to capture single bond vibrations in their chemical structures .....	49
2.4 a) Survey X-ray Photoelectron spectra illustrating the surface elemental composition of humic acid (HA) and fulvic acid (FA) with high-resolution Gaussian-Lorentzian fitted curves for C-1s status of b) HA and e) FA, O-1s status of c) HA and f) FA, and N-1s status of d) HA and g) FA .....	50

2.5 Variation of intensity weighted particle size distribution with the concentration of a) humic acid (HA) dissolved in 0.01 mg L<sup>-1</sup> NaOH, b) fulvic acid (FA) dissolved in water. Solid phase Scanning Electron Microscopic surface imaging to illustrate c) the rigid-cuboid structure of fulvic acid and e) the spherical humic acid colloids. d) A comparison of mean zeta potentials of humic substances with the concentration to indicate colloidal stability .....54

2.6a 3D-Excitation Emission spectra of fulvic acid (FA) region in a) and b) and humic acid (HA) region in c) and d) to visualize fluorescence reduction when sulfamethoxazole (SMX) concentration varied from 0-100 µg L<sup>-1</sup> from treatments obtained for equilibrated batch sorption solutions. Treatments consisted of fresh liquid swine manure dissolved organic carbon (DOC) fraction with and without bentonite (Bt) to capture fulvic-like fluorescence quenching by FA-SMX complexes and non-fluorescence quencher HA-SMX complexes in the aqueous phase .....62

2.6b Cont. Percent fluorescence intensities calculated by 2D volume integrate (*f<sub>i</sub>* in %) for humic acid (HA)-like and fulvic acid (FA)-like regions .....63

2.7 A comparison of Fourier-Transformed Infrared spectra of potassium saturate bentonite (Bt), humic acid (HA) and fulvic acid (FA), the organic matter (OM) sorbed bentonite to understand the OM-mineral complexation mechanisms. Bt-DOC is fresh liquid swine manure dissolved organic carbon fraction as the OM; Bt-FA is fulvic acid as the OM; and Bt-HA is humic acid as the OM. Scanning Electron Microscopic images of the pure mineral and OM-mineral surfaces to visualize the microstructural changes that arose from the OM complexation .....65

2.8 X-ray diffraction patterns of mineral bentonite obtained from the sorption equilibrium to illustrate changes to the basal reflection $d_{001}$ peak when changing the sulfamethoxazole (SMX) concentration as 0, 20, 40, 60, and 100 $\mu\text{g L}^{-1}$ in the presence or absence of fresh liquid swine manure derived organic matter (dissolved organic carbon fraction (DOC)/fulvic acid (FA)/humic acid (HA)) .....	71
2.9a Scanning Electron Microscopic images of mineral bentonite (Bt) obtained from sorption equilibrium to visualize unaffected flaky crystalline structure with increased sulfamethoxazole (SMX) concentration and effect of swine manure humic acid (HA) to alter their surface morphology and mineral microstructure .....	73
2.9b Cont. Effect of swine manure fulvic acid (FA) and swine manure dissolved organic carbon (DOC) fraction to alter the surface morphology and mineral microstructure .....	74
2.10 Schematic illustration of sulfamethoxazole (SMX) sorption mechanisms onto bentonite clay in the presence of fresh liquid swine manure dissolved organic carbon (DOC) fraction. a) SMX interactions with bentonite (Bt) through acid-base (AB) interactions, van der Waals (vdw) interactions, and cation bridging interactions. b) SMX interactions with fulvic acid-coated bentonite (FA-Bt) through $\pi$ - $\pi$ electron donor-acceptor (EDA) interactions, cation and water bridging, hydrogen bonding, and alkyl- $\pi$ interactions. c) SMX interactions with humic acid-coated bentonite (HA-Bt) through hydrogen bonding, $\pi$ - $\pi$ interactions, water bridging, and cation bridging interactions .....	76
A-1 The calibration curve for High Performance Size-Exclusion chromatography analysis for the polystyrene sulphonate standard .....	94

# 1. GENERAL INTRODUCTION

## 1.1 Occurrence of sulfamethoxazole in the environment

Administration of veterinary antimicrobials in livestock as disease prevention, growth promoters, and reproduction rate enhancers has increased throughout the past decades in the global livestock industry (Sarmah et al. 2006). Sulfamethoxazole (SMX) belongs to the antimicrobial class sulfonamides and is frequently prescribed as co-trimoxazole (i.e., a combined drug of trimethoprim and sulfamethoxazole) to treat livestock urinary tract infections as a bacteriostatic agent to disrupt the biosynthesis of tetrahydrofolate by inhibiting dihydropteroate synthase enzyme in certain microbes (Hanamoto et al. 2021; Thiebault 2020). SMX ranked fourth highest globally consuming human and veterinary medicine, where it is listed as one of the highest-priority antimicrobials in the pharmaceutical industry. Canadian dairy cattle, broiler chicken, turkey, and swine industries also frequently use SMX as a therapeutic drug and a growth promoter (Canadian Pork Council, 2023; Marín-García et al. 2021). Major global and regional organizations emphasize the importance of SMX. The world health organization (WHO) has listed sulfonamides as a highly important human drug, while a European assessment placed sulfamethoxazole as a high-priority class I drug, and Health Canada's veterinary drug directorate classifies it as a class II drug with high importance (Agunos et al. 2019; De Voogt et al. 2009; Scott et al. 2019). Rapid excretion as unmetabolized SMX via livestock urine (i.e., up to 90% of the administered amount) leads to the formation of manure-born antimicrobial contaminants that can frequently be detected in various environmental compartments (Mercer 2022; Soto et al. 2023). Upon metabolism, SMX undergoes nitrosation, methylation, deamination, hydroxylation, or ring cleavage (Xiong et al. 2019). Primary SMX metabolites during human and animal metabolism include N<sub>4</sub>-acetyl-sulfamethoxazole and sulfamethoxazole-N<sub>1</sub>-glucuronide, where these contaminations exhibit the potential to transform

back to the parent compound upon excretion in manure (Martínez-Hernández et al. 2016; Radke et al. 2009).

Examples of environmental input (i.e., to the soil, surface water, and groundwater) of unmetabolized and bio-transformed products of SMX are land application of livestock manure, biosolids from municipal and hospital effluents, partially treated wastewaters used in irrigation practices, and effluents from wastewater treatment plants. In the environment, they can undergo sorption, abiotic or biotic degradation, runoff transport or leaching, and plant uptake entering the food chains (Zheng et al. 2020). Numerous studies quantified environmental SMX inputs and contamination levels. Carballa et al. (2008) showed that the quantity of SMX in raw sewage samples in Spain is  $\sim 0.60 \mu\text{g L}^{-1}$  in the liquid phase, and the result is consistent with reported data from other European countries. Archundia et al. (2019) evaluated concentrations of SMX in the surrounding surface water, groundwater, and soil to determine the effect of outlet discharge from a wastewater treatment plant. The outlet concentration was  $1.31 \mu\text{g L}^{-1}$  and  $0.38 \mu\text{g L}^{-1}$  SMX during wet and dry seasons. Outlet discharge resulted in groundwater concentrations ranging from  $0.048$  to  $0.25 \mu\text{g L}^{-1}$ , along the basin concentrations from  $0.012$  to  $0.013 \mu\text{g L}^{-1}$ , and the soil concentrations up to  $18 \mu\text{g kg}^{-1}$  SMX. In another study, Xiong et al. (2019) observed SMX contaminating downstream of a wastewater treatment plant with a maximum water concentration of  $0.32 \mu\text{g L}^{-1}$  and  $20 \mu\text{g kg}^{-1}$  of water-sediment partition. Because of their mobility, SMX can penetrate deeper depths up to about 1.3 km through saturated porous soil without degrading to reach groundwater (Kim and Carlson 2007). Hamscher et al. (2005) also support the fact as they observed  $55.9 \mu\text{g L}^{-1}$  SMX in groundwater as a result of liquid swine manure amendment in a sandy soil with an average concentration of  $72.3 \mu\text{g kg}^{-1}$  SMX. Some studies show SMX contamination in topsoil resulted from livestock manure amendment. Watanabe et al. (2010)

observed  $6.2 \mu\text{g kg}^{-1}$  SMX in the topsoil after application of lagoon-stored dairy cattle manure containing  $0.43\text{-}4.9 \mu\text{g L}^{-1}$  SMX. Stoob et al. (2007) provide evidence of offsite transport and runoff potential of SMX from manure-applied soils. They detected SMX in surface water ranging from  $0.15$  to  $3.30 \mu\text{g L}^{-1}$  (maximum loss of 50% from the initial load) caused by offsite transportation from SMX-incorporated swine manure applied to grassland. A low level of sulfamethoxazole ( $0.5 \mu\text{g L}^{-1}$ ) contamination in an aquatic system resulted in accumulation in roots of Red Lollo lettuce up to a level higher than  $960 \mu\text{g kg}^{-1}$  (dry weight), indicating their ability to penetrate root cell membranes. Leaves contained  $32.7$  to  $132.6 \mu\text{g kg}^{-1}$  SMX accumulation, indicating their mobility and hydrophilicity to translocate from roots to leaves with water during the transpiration (Zheng et al. 2020). Upon exposure to environmentally relevant concentrations ( $\sim 10 \mu\text{g L}^{-1}$ ), SMX significantly accumulated in tomato fruits at different levels depending on the harvesting time:  $15.6\text{-}86.0 \mu\text{g kg}^{-1}$  for the harvest after 72-78 days,  $119\text{-}2366 \mu\text{g kg}^{-1}$  after 85-92 days, and  $99\text{-}2798 \mu\text{g kg}^{-1}$  after 96-102 days (Christou et al. 2019).

The major environmental threat of antimicrobial contamination is the development of antibiotic-resistance genes in bacteria. SMX reported increasing the antibiotic-resistance genes at their environmentally relevant concentrations, even at  $\text{ng L}^{-1}$  concentrations (Martínez-Hernández et al. 2016; Wu et al. 2022; Zhang et al. 2016). Acute and chronic poisoning and gene mutation are possible with  $\text{mg L}^{-1}$  SMX concentrations (Chen et al. 2017). Other eco-toxicological impacts from SMX contamination include alterations to soil microbial community structure (i.e., a combination of diversity, gene composition, and abundance) by microbial growth inhibition, changes in microbial activity, and influences on their metabolic pathways (Kim and Carlson 2007; Zhang et al. 2016). Bioaccumulation and inhibition of plant growth due to phytotoxic effects resulting from plant uptake are also reported. Liu et al. (2009) found phytotoxic effects on rice at an effective  $0.1$

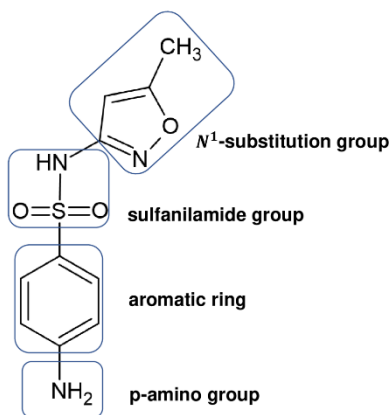
mg L<sup>-1</sup> SMX concentration. Pakchoi and carrots are also reported to be sensitive to SMX exposure (Bhatt and Gauba, 2018; Wang et al. 2016). Environmentally relevant SMX doses (~10 µg L<sup>-1</sup>) are reported to have adverse effects on the nitrogen cycle by altering mineralization, nitrification, and denitrification rates (Gray and Bernhardt, 2022; Li et al. 2023). SMX was also reported to inhibit the growth of several algal species, including *Scenedesmus vacuolatus*, *Scenedesmus obliquus*, *Chlorella vulgaris*, *Cyclotella meneghiniana*, and *Synechococcus leopolensis* (Xiong et al. 2019). The toxicity towards algae by environmental contaminants could negatively impact their numerous ecosystem functions. Besides SMX, their acetylated metabolite N<sub>4</sub>-acetyl-sulfamethoxazole was also reported to create toxicity in algae (García-Galán et al. 2011).

## **1.2 Structure-inherent sorption interactions of sulfamethoxazole**

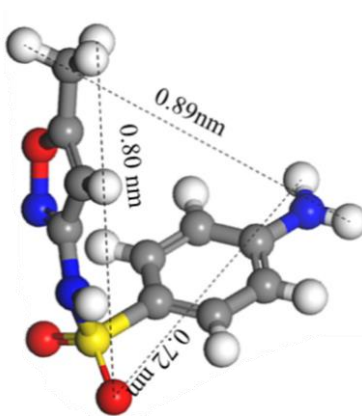
The persistence of SMX in the soil or their transport via leaching and runoff to other ecosystems is determined by their interactions with active adsorptive soil components, including clay colloids, organic colloids, and colloidal oxides. Interaction mechanisms include inter-molecular complexation, ion exchange, cation or water bridging, covalent bonding, hydrogen bonding, and non-polar van der Waals interactions (Kumar et al. 2005). The type and abundance of interactions and sorption reversibility are affected by a variety of physicochemical and environmental factors. Structure-related physicochemical properties (Table 1.1) of SMX affecting the sorption mechanisms include pH speciation, hydrophobicity-

Table 1.1 Physicochemical properties of sulfamethoxazole.

Structure



Structural dimensions <sup>a</sup>



Antimicrobial class

Sulfonamides

Molecular formula

$\text{C}_{10}\text{H}_{11}\text{N}_3\text{O}_3\text{S}$

Molecular weight ( $\text{g mol}^{-1}$ )

253.28

Degradation half-life (Days)

40 (anaerobic and thermophilic conditions)<sup>b</sup>

Dissipation half-life (Days)

74 (in manure slurry)<sup>c</sup>

Water solubility at 25 °C ( $\text{mg L}^{-1}$ )

438<sup>d</sup>

Log  $K_{ow}$

0.89<sup>e</sup>

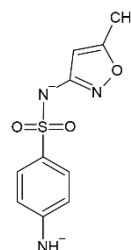
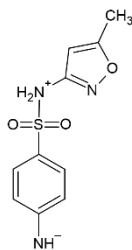
$K_{oc}$  ( $\text{L kg}^{-1}$ )

219<sup>f</sup>

$\text{pK}_a$

$\text{pK}_{a1} = 1.8 \pm 0.03^g$

$\text{pK}_{a2} = 5.6 \pm 0.04^g$



<sup>a</sup> Hernández et al. 2018, <sup>b</sup> Feng et al. 2017, <sup>c</sup> Hou et al. 2015, <sup>d</sup> Fioritto et al. 2007, <sup>e</sup> Lin and Gan 2011, <sup>f</sup> Barron et al. 2009, <sup>g</sup> Lin Ching-Erh et al. 1997

specified partition coefficients, and molecular geometry. The pH, organic carbon forms, clay minerals and their abundance, colloidal oxides, ion exchange capacity, temperature, and moisture content are examples of environmental factors (Archundia et al. 2019; Stoob et al. 2007). A thorough understanding of sorption interactions is viable to assess the potential of contaminating surface and groundwaters adjacent to livestock farms or manure-amended agricultural lands by SMX and their degradation products.

### 1.2.1 Acid dissociation constants

The acid dissociation constants ( $pK_a$ ) of p-amino-N and sulfanilamide-N in the SMX structure are important determinants of their environmental fate. Deprotonation or protonation of the acid functional groups, which depends on the pH of the soil solution, creates charged or zwitterionic species that can impart different soil-antimicrobial interaction mechanisms. Two acid dissociation constants for SMX, (i)  $pK_{a1}$  ranging from 1.39 to 1.97 and (ii)  $pK_{a2}$  ranging from 5.81 to 6.61, determine pH speciation (Straub 2016). Accordingly, SMX being a cation  $[SMX]^+$  when the  $pH < pK_{a1}$  due to protonation of p-amino-N, anionic  $[SMX]^-$  when the  $pH > pK_{a2}$  due to deprotonation of both p-amino-N and sulfanilamide-N and zwitterionic  $[SMX]^\pm$  when the pH ranged in between  $pK_{a1}$  and  $pK_{a2}$  (Rabølle and Spliid 2000; Straub 2016). Therefore, natural aquatic and terrestrial environmental pH conditions (5.5-8.5) allow SMX to exist at 9-50% as  $[SMX]^\pm$  and 50-90% as anionic  $[SMX]^-$  (Srinivasan et al. 2013). The  $[SMX]^\pm$  and  $[SMX]^-$  speciation allowed SMX to exhibit low affinity to soil components, thus, high mobility, hence low soil-liquid partition ( $K_d$ ). Validating the fact, Sarmah et al. (2006) concluded the  $K_d$  range between 0.6 and 7.4 L kg<sup>-1</sup> by reviewing existing data on SMX soil sorption within environmentally relevant pH conditions. Similarly, Park and Huwe (2016) reported  $K_d$  of SMX for soil-water systems as a range between 1.1 and 1.39 L kg<sup>-1</sup> at pH 6.6, while Srinivasan et al. (2013) reported the range as 2-4 L kg<sup>-1</sup> for

pH ranging 4-8. In summary, sorption mechanisms depend on the acid dissociation constants of the antimicrobial. The pH-dependent speciation and specific sorption mechanisms with main soil components are discussed further in section 1.3.

### 1.2.2 Partition coefficients

Veterinary antimicrobials are detected in various environmental matrices (i.e., soils, sediments, and surface- and groundwaters). The spectrum of antimicrobials in a certain environment appears to be definite and predictable from their physicochemical properties. A common approach to assessing the spatiotemporal distribution of these substances within the ecosystem involves the use of their soil-water partition coefficients ( $K_d$ ) and, alternatively, the organic matter normalized partition coefficient ( $K_{oc}$ ) (Zamora et al. 2017). These coefficients reflect the hydrophobicity of the substance. SMX is highly water soluble and, hence, has a low tendency to adsorb onto the soil, resulting in lower  $K_d$  values (ranging from 0.6 to 7.4 L kg<sup>-1</sup>) and  $K_{oc}$  values (ranging from 35 to 610 L kg<sup>-1</sup>) (Sarmah et al. 2006). The octanol-water partition coefficient ( $K_{ow}$ ) is indirectly applied to determine the  $K_d$  to measure the hydrophilicity/hydrophobicity of charge-neutral organic compounds (Wegst-Uhrich et al. 2014). However, one major criticism of using  $K_{ow}$  and  $K_{oc}$  to assess soil sorption of ionizable antimicrobials is their inability to account for electrostatic, H-bonding, ion-exchange, or cation bridging interaction mechanisms. A low  $K_{ow}$  value of SMX ( $\log K_{ow} \leq 0-2.5$ ) indicates they are hydrophilic to inherent low soil sorption and, therefore, low  $K_d$  values.

Runoff or leaching losses of SMX to surface, sub-surface, or groundwater occur during rainfall, irrigation, and spring snowmelt events. Therefore, hydrophilic SMX with low  $K_d$  is relatively mobile and susceptible to off-site migration (Archundia et al. 2019). The  $K_d$  values reflect their environmental occurrence and provide insights into their off-site transportation and degradation

potentials. For example,  $2.3 \text{ L kg}^{-1} K_d$  of sulfadimethoxine for a silt loam soil reflected their low soil sorption to contaminate shallow groundwater ( $0.017\text{-}0.13 \mu\text{g L}^{-1}$ ) near a manure lagoon and shallow water ( $0.005\text{-}0.010 \mu\text{g L}^{-1}$ ) near a manure amended forage field (Watanabe et al. 2010). Variations among  $K_d$  values can occur due to differences between the solid and the liquid phase. For example, the apparent  $K_d$  of sulfamethazine in a swine lagoon water/lagoon sediment system was  $8.3 \text{ L kg}^{-1}$ , which is different from soil-based systems (i.e.,  $0.6\text{-}3.1 \text{ L kg}^{-1}$ ) (Watanabe et al. 2010).

### 1.2.3 Molecular geometry

Molecular geometry is another factor that affects interaction mechanisms, for example, when determining clay intercalation. Molecules with planar geometry can have a greater tendency to enter the interlayers and stabilize through  $\pi$ -complexes with the internal basal oxygen plane of silicon tetrahedrons of smectites. A model study elucidated the intercalation possibilities of SMX because of the planar geometry of the  $-\text{SO}_2-$  group, contrary to the non-planar geometry of sulfamethazine's  $-\text{SO}_2-$  group to hinder their intercalation (Gao and Pedersen 2005). From the molecular dimension perspective (Table 1.1), there would be possible intercalation into smectite interlayers, at least to a partial extent, because of their larger interlayer spacing ( $d_{001} = 1.4\text{-}1.5 \text{ nm}$ ) than that of the SMX molecular dimensions ( $0.80 \times 0.72 \times 0.89 \text{ nm}$ ) (Hernández et al. 2018). In such conditions, functional groups of SMX are favourable to undergo interactions via 'open' surfaces overcoming the confinement obstacles in smectite interlayers. However, several studies conclude that SMX intercalation is unlikely to occur at environmentally relevant pH conditions. Anionic and neutral SMX species in such pH conditions tend to hinder cation-exchange mechanisms with smectite interlayer cations due to unfavourable electrostatic interactions. Thus, surface interactions override interlayer sorption.

## 1.3 Interaction mechanisms with soil components

This section provides background on the effect of the soil colloidal fraction on the movement and retention of SMX, considering silicate clays, organic colloids, and iron/aluminium oxides as sorbates. A thorough understanding of SMX-soil matrix interactions will provide insights to predict their fate and transport in the environment.

### 1.3.1 Soil organic matter

Carbon in soil comprises carbohydrates, proteins, lignin, waxes, phenols, and humic substances (i.e., humic acid, fulvic acid, and humin). The colloidal organic fraction is one of the most active adsorption sites for nutrient ions and contaminants in the soil, including antimicrobial products and their residues (Zhi et al. 2019). Decaying floral and faunal constituents, soil microbiota, sewage, animal manure, and ashes from pyrolyzed organic matter are carbon additions to the soil (Vithanage et al. 2014). Antimicrobial sorption mechanisms on soil organic matter depend on their constituents, structure, composition, and properties (i.e., hydrophobicity, hydrophilicity, aliphaticity, aromaticity, and C/N ratio), functionality, size, and charge. Ion-exchange, complexation, cation bridging, covalent bonding, polar  $\pi$ -interactions, CH- $\pi$  interactions, and van der Waals interactions are possible between organic matter and antimicrobials (Archundia et al. 2019). Cationic  $[\text{SMX}]^+$  and neutral  $[\text{SMX}]^\pm$  species exhibit strong  $\pi$ - $\pi$  donor-acceptor hydrophobic interactions between N-heteroaromatic ring and protonated phenolic groups in organic matter, weaker  $\pi$ - $\pi$  donor-acceptor hydrophobic interactions with benzene rings and protonated carboxyl groups, and H-bonding (De Mastro et al. 2022; Hu et al. 2019). However, electrostatic interactions are unlikely to occur for cationic species with protonated organic matter at acidic pH conditions. When the negative  $[\text{SMX}]^-$  species is dominant, particularly at neutral-

basic pH conditions, the sorption is restricted due to unfavourable electrostatic interactions between negatively charged organic functional groups. Hence, contributions from cation bridging by multivalent metal ions and van der Waals interactions determine the sorption of  $[\text{SMX}]^-$  species (De Mastro et al. 2022).

A high amount of organic carbon usually enhances the sorption of neutral  $[\text{SMX}]^\pm$ , and the dominant mechanism would be a hydrophobic partition with organic matter. Drillia et al. (2005) noted SMX sorption significantly increased from  $K_{oc}$  62.2 L kg<sup>-1</sup> up to 530 L kg<sup>-1</sup> as the soil organic carbon content increased from 0.4% to 7.1%, along with a decreased clay content from 45% to 15%. The ability of neutral  $[\text{SMX}]^\pm$  species in the hydrophobic partition has been proven in many studies (Srinivasan et al. 2013). Small organic matter exhibited a high affinity to SMX. For example, rather small fulvic-like organic matter leached from composted manure exhibited higher SMX sorption compared to more humified humic-like compounds from peat (Chen et al. 2017). According to the functional group perspective, organic matter containing more carboxylic moieties supports the sorption of ionic SMX. However, in the meantime, negative charge in carboxylic acids can electrostatically repel negative  $[\text{SMX}]^-$  at neutral pH conditions, resulting in reduced sorption (Dalkmann et al. 2014). The role of soil organic matter in enhancing the mobility of contaminants is hypothesized in previous studies as saturation of the sorption sites with organic matter, competition for the sorption, and aqueous phase interactions with dissolved organic fractions of the organic matter (Chabauty et al. 2016). The origin of the organic matter and decomposition stage effectively changes the mobility of SMX due to substantial differences in their physicochemical properties. For example, soil organic matter derived from crop straw exhibited different affinities depending on the decomposition stage. Hydrophilic dissolved organic carbon (DOC) at the initial decomposition stages enhanced the SMX sorption due to favourable

interactions with large quantities of amide, polysaccharide, and carbohydrate functional groups. On the contrary, hydrophobic DOC from humification processes at later decomposition stages exhibited low affinity to hydrophilic SMX (Wang et al. 2020).

### 1.3.2 Clay minerals

Understanding SMX sorption to clay constituents is another critical viewpoint to elucidate their mobility in the environment. Antimicrobials tend to form strong sorption interactions with silt and clay fractions. The interactions between clay minerals and antibiotics are dependent on several factors, including the pH-dependent speciation, ionic strength, the surface area of the clay, the permanent and variable charge of the clay, the type of the exchanging cation, and competitive cations (Gao and Pedersen 2005; Wang et al. 2012).

The pH-dependency of SMX speciation in the soil is one of the dominant factors affecting clay-SMX complexation mechanisms. SMX in the soil solution can either be anionic, cationic, or zwitterionic. These forms can exist in the soil solution in different ratios (Table 1.1). Mineral surfaces are negatively charged largely because of the isomorphic substitution of  $\text{Al}^{3+}$  for  $\text{Si}^{4+}$  in surface tetrahedrons. Thus, the cationic  $[\text{SMX}]^+$  species adsorbs majorly onto mineral surfaces via ion-exchange mechanisms driven by electrostatic attractions. Intercalation via the cation-exchange process in smectite clays is affected by interlayer counter cations (i.e.,  $\text{Li}^+$ ,  $\text{Na}^+$ ,  $\text{K}^+$ ,  $\text{Mg}^{2+}$ ,  $\text{Ca}^{2+}$ ) and the ability to displace interlayer cations varies with the antimicrobial's positive charge density. For example, displacement of tightly held strong cations such as  $\text{Ca}^{2+}$  from the negatively charged sites by relatively weak cationic species of antimicrobials is unlikely to occur. Literature suggests that cationic species of sulfonamides, including the  $[\text{SMX}]^+$ , intercalated weakly into smectite interlayers via broken edges (De Mastro et al. 2022; Gao and Pedersen 2005; Hu et al. 2019; Klein

et al. 2021). Electrostatic interactions allowed cationic  $[\text{SMX}]^+$  species to result in high sorption by clay minerals, comparatively to their anionic  $[\text{SMX}]^-$  and neutral  $[\text{SMX}]^\pm$  species. The p-amino group in neutral  $[\text{SMX}]^\pm$  species is capable of forming inner- or outer-sphere bridging complexes with either water molecules or divalent complexing cations (i.e.,  $\text{Ca}^{2+}$ ,  $\text{Mg}^{2+}$ ) on the clay surfaces (De Mastro et al. 2022; Hu et al. 2019). Further, certain sulfonamides can undergo site-specific complexing mechanisms, for example, pyrimidine N and sulfone O sites in neutral sulfamethazine, to form bridging complexes with smectite surfaces (i.e., external and internal basal surfaces) via  $\text{Ca}^{2+}$  ion bridging mechanisms. There is a dearth of literature to explain the contribution from cation bridging,  $\pi$ -interactions, and van der Waals interactions for the sorption of anionic  $[\text{SMX}]^-$  and neutral  $[\text{SMX}]^\pm$  into clay minerals at neutral-basic pH conditions. The pH of the soil solution can also alter the surface charge of clay minerals. Thus, a proper understanding of the pH-driven electrical status of both the adsorbent and the adsorbate is essential to draw proper mechanistic elucidations.

The sorption of antimicrobials by clay minerals is affected by the cation exchange capacity (CEC). CEC of clay varies with isomorphic substitution, the pH of the solution, the number of exchangeable ions on ion-exchange sites, types of exchangeable ions, and the interaction volume. When soil holds CEC greater than  $20 \text{ cmol}_c \text{ kg}^{-1}$ , antimicrobial sorption is through cation exchange mechanisms, and contributions from other mechanisms like surface complexation and multivalent cation bridging become insignificant (Vasudevan et al. 2009). Antimicrobial sorption with pH for such soils exhibits decreased sorption when increasing the pH because of unfavourable electrostatic interactions between neutral and negative antimicrobial species and clay. Ionic strength of the solution determines the thickness of the diffused double layer of clay to affect the sorption. Mono and multivalent cations compress the diffused double layer of negative clay

surfaces to promote the sorption of negative antimicrobial species via electrostatic interactions (Awad et al. 2019).

The limited availability of the exchange sites in soils with CEC less than 20  $\text{cmol}_c \text{ kg}^{-1}$  tends to curb the cation exchange mechanisms; hence, other mechanisms provide more contributions (Vasudevan et al. 2009). These soils exhibit sorption going through a maximum followed by a decline at alkaline pH conditions ( $\text{pH} > 7-8$ ). In general, smectite clays exhibit high CEC (ranging from 54 to 84  $\text{cmol}_c \text{ kg}^{-1}$ ) and larger specific surface areas to facilitate greater antimicrobial sorption via cation exchange mechanisms.

### **1.3.3 Organo-mineral complexes**

Soil organic matter does not exist in soil as a sole fraction but co-exists with other soil components such as clay, silt, and sand. The mineral component itself is insignificant in the sorption of contaminants than the organo-mineral associates derived from organic matter coating on mineral surfaces (Haham et al. 2012; Kleber et al. 2007). Stabilization of soil organic matter (SOM) on clay minerals to form organo-mineral complexes occurs via adsorbing them onto clay colloids. The process is affected by the particle-size and the type of organic matter. For example, Thiele-Bruhn et al. (2004) investigated the composition and quantity of SOM adsorbed by a chernozemic soil with varying particle-size fractions as clay ( $< 2 \mu\text{m}$ ), fine silt (2-6.3  $\mu\text{m}$ ), medium silt (6.3-20  $\mu\text{m}$ ), and coarse silt (20-63  $\mu\text{m}$ ), and sand (63-2000  $\mu\text{m}$ ). They found that the amounts of hydrophilic carbohydrates and peptides adsorbed decreased as particle-size increased from clay to medium silt. However, on the contrary, they reported increased sorption for hydrophobics such as lignin, phenols, lipids, sterols, and alkyl-aromatics with the particle-size. Further, they found a positive correlation between  $K_d$  values for the sulfonamide sorption into organo-mineral

complexes and the mass-to-charge ratio of oxygen-containing polar functional groups in organo-mineral complexes (i.e., alcoholic and phenolic OH-, keto-, enol-, and carboxylic). They suggested that the soil fraction with polar SOM enhanced site-specific sulfonamide sorption, probably due to hydrogen bonding between p-amino NH<sub>2</sub> and oxygen on polar SOM sites (Thiele-Bruhn et al. 2004). Fer et al. (2018) noted polar hydrophilic organic matter coating enhances the hydrophilic SMX sorption. On the contrary, hydrophobic coating reduced the SMX sorption because of electrostatic repulsion. The pH speciation of SMX is somewhat different from other sulfonamides in the class since they dominate anionic and neutral zwitterionic species at environmentally relevant pHs (pH 6-9). Hence, a proper understanding of the ionic status is required when deriving site-specific sorption mechanisms for SMX.

Physical conformation of the structures of humic substances in the aqueous phase undergoes changes as they form organo-mineral complexes during sorption. The formation of micellar structures is one such physical conformation that shields the aromatic portions within the structure and exposes the aliphatic sites to the soil surface (Kleber et al. 2007). Micellular conformations affect the contaminant accessibility to different functional sites in the SOM structure. Hydrophilic and hydrophobic contaminants can adopt interesting mechanistic approaches (e.g., entrapping within the micellular core) and interact with distinct portions of organo-complexes. SOM can retard direct antimicrobial-clay interactions by acting as a surface coating to obscure the sorption process (Charles et al. 2006). However, sorption can enhance in the presence of cations by reducing electrostatic repulsion to facilitate cation bridging for negatively charged contaminant species. On the other hand, SOM can compete with adsorption sites to reduce SMX soil sorption (Dalkmann et al. 2014).

#### **1.4 Physiochemical properties of humic substances originated from animal manure**

Animal manure enhances soil health and productivity by providing soil organic matter. DOC fraction is the most active carbon component of the soil carbon pool. It contains a mixture of aromatic and aliphatic hydrocarbons bearing O-containing functional groups (i.e., carboxylic, phenolic, alcoholic, and enolic). Humic substances, being surfactants, allow interactions with hydrophilic and hydrophobic contaminants (Hansima et al. 2022). Manure amendment adds DOC to the soil, and they play a critical role in various eco-toxicological functions, for example, the fate of pollutants. Humic substances are stable organic matter resulting from a series of biological transformations named humification processes. Solubility defines two types of humic substances: I) fulvic acids, soluble at  $\text{pH} < 1$ , and II) humic acids, insoluble at  $\text{pH} < 1$  (Adusei-Gyamfi et al. 2019). In general, they contain carboxylic, phenolic, aromatic, aliphatic, hetero-aliphatic, acetal, and carbonyl functional groups with varying compositions where their carbon skeleton is crosslinked by O, N heteroatoms (Vasilevich et al. 2018). Fulvic acids contain more surface carboxyl and phenolic functional groups, determining their water solubility. In general, the carbon skeleton of humic acids postures more aromatic structures, while fulvic acids contain more aliphatic structures; however, contrariwise is also reported (Chang Chien et al. 2007). Table 1.2 summarizes the elemental composition and functional group analysis reported in the literature for animal manure-derived humic substances. Elements present in humic substances are C, H, O, N, and S. Literature suggest the elemental composition of humic substances should be within 40-60% of C, 4-5% of H, 30-50% of O, 1-4% of N, and 1-2% of S regardless of the source and humification paths (Gaffney et al. 1996).

The goal of the composting process in manure management practices is to obtain stable organic matter (i.e., organic matter rich in humic substances) (Abdellah et al. 2022; Duan et al. 2019). However, animal manure-derived humic substances from composting processes evolved less in comparison to soil humic substances. Immaturity results in a higher percent of aliphatic carbon, nitrogen-containing compounds, and lower oxidation degree, hence comparatively unstable (Campitelli and Ceppi 2008). The structural composition of a humic substance varies according to the decomposition time. The initial stages of composting processes lead to more hydrophilic functional groups (e.g., amino acids, proteins, carbohydrates, carboxyl, and hydroxyl groups) (Campitelli and Ceppi 2008). Low molecular weight hydrophilic fractions from initial polymerization and condensation reactions undergo non-covalent physical interactions (i.e., aromatic  $\pi$ - $\pi$ , hydrophobic, van der Waals, electrostatic, and hydrogen bonding) to form high molecular weight humic substances (Semenov et al. 2013). Macromolecular humic substances are aromatic and found to be recalcitrant because of their resistance to microbial degradation. Environmental contaminations, including antimicrobials, interact differently with organic matter in different evolutionary stages and different origins. The application of stable organic matter is known to be the best practice in soil organic matter amendment (Campitelli and Ceppi 2008). Therefore, knowing the physicochemical properties of organic matter is important to understand their stability and role in contamination sorption and to adopt manure management practices before their land application.

Table 1.2 Summary of elemental composition and C-functional groups for livestock manure-derived organic matter.

Manure source	Elements (%)					C-functional groups (%)					Reference
	C	H	N	S	O	Aromaticity	Aliphatic	Carbohydrate/O-alkyl	Aromatic	Carboxyl	
Composted cattle-HA	57.8	5.3	3.8	1.1	32.0	42.4	50.4	NA	37.1	10.6	(Chen et al. 1996)
Cow dung-HA	61.1	9.3	4.1	0.7	24.8	NA	NA	NA	NA	NA	(Li et al. 2011)
Vermicompost cow dung-HA	51.5	6.6	5.4	0.9	35.6	NA	NA	NA	NA	NA	(Li et al. 2011)
Fresh cattle-HA	58.9	5.7	3.6	1.0	30.6	56.7	53.6	56.7	35.4	9.5	(Inbar et al. 1990)
Composted cattle-HA	57.7	5.3	3.8	1.1	31.5	42.4	50.4	61.5	37.1	10.6	(Inbar et al. 1990)
Composted swine-HA	54.8	5.7	6.7	1.4	33.0	NA	30.7	27.8	24.2	13.1	(Chang Chien et al. 2007)
Composted swine-FA	45.0	5.0	5.2	1.2	43.5	NA	22.7	41.8	14.6	16.4	(Chang Chien et al. 2007)
Pig slurry	62.7	9.4	5.2	1.3	21.3	NA	NA	NA	NA	NA	Plaza et al. 2002
Fresh swine	30.2	5.4	3.8	0.6	33.8	8.0	34.6	48.5	7.3	9.7	(Wang et al. 2015)

Fresh cow	40.5	5.6	2.3	0.4	36.8	13.5	14.6	64.8	12.4	8.3	(Wang et al. 2015)
Fresh chicken	32.3	5.2	3.9	0.8	38.9	9.1	29.5	52.3	8.2	10.1	(Wang et al. 2015)

---

NA - not assessed

FA - Fulvic acid

HA - Humic acid

## 1.5 Status of animal manure contaminated with sulfamethoxazole

As mentioned in early sections, unmetabolized sulfonamides are excreted through urine and incorporated in livestock manure. A few studies explained the dynamics of SMX and its primary metabolite N<sub>4</sub>-acetyl-sulfamethoxazole in animal manures, during storage, and manure-amended soils (Andriamalala et al. 2018; Goulas et al. 2019; Höltge and Kreuzig 2007; Vieublé Gonod et al. 2022). During the storage, the fate of SMX can be degradation/mineralization, chemical complexation to organic matter or physical sequestration, and offsite transportation. The complexation of SMX into organic matter leads to the formation of non-extractable residues, in other words, stable organic matter-SMX complexes, as a result of irreversible binding via covalent interactions or adsorb or trap within organic matter. Organic matter complexation can also result in extractable residues where SMX is readily desorbed from organic matter-SMX complexes and remobilized. There are some studies to observe the formation of non-extractable SMX residues; however, research is lacking to explain sorption mechanisms, stability, mobility, microbial accessibility, and their environmental impact (Kästner et al. 2014). For example, Holtge and Kreuzig (2007) conducted a study to identify the fate of SMX and N<sub>4</sub>-acetyl-sulfamethoxazole in bovine manure and found that  $\geq 75\%$  of the initial concentration was converted to non-extractable residues where the mineralization occurred only up to 1% during the 72 days of manure incubation period. Further, they have noted an increased amount of non-extractable residues as indicated by increased  $K_d$  upon land application of incubated bovine manure (Höltge and Kreuzig 2007). Andriamalala et al. (2018) also found manure amendment to a farmyard enhanced the formation of non-extractable residues ( $> 50\%$ ). Goulas et al. (2019) found the formation of non-extractable residues up to 37% of the initial amount within 7 days in a manure-applied soil where SMX was resulted from the deacetylation of initial N<sub>4</sub>-acetyl-sulfamethoxazole. Each study noted a decline in the mineralization of SMX because of reduced

microbial accessibility. Some studies observe contradictory sorption behaviours where decreased SMX sorption and enhanced leaching and runoff transported amounts with manure amendment (Wegst-Uhrich et al. 2014). They argue that pH increments resulting from manure amendment decreased SMX sorption as they become anionic to repel negatively charged organic functional groups to become mobile.

## 1.6 Objectives

Most of the literature on contaminant sorption mechanisms, particularly in the presence of organic matter, involved the interpretation of sorption coefficients and indexes based on postulations. There is a dearth of literature on the sorption mechanisms of antimicrobials, including SMX, in combination with exact physicochemical properties and dynamics of intact organic matter. Postulated mechanisms are not sound enough since they do not take into account bulk physical and chemical properties of organic matter (e.g., distribution of functional groups, aromaticity, aliphaticity, hydrophilicity, hydrophobicity, molecular size, and the surface charge) and conformation/orientation of functional groups in their secondary structures in aqueous solutions. It is not informative to apply common interaction mechanisms since organic matter is heterogeneous and inherently variable in physicochemical properties, depending on factors such as the origin, environmental factors, microbial community, humification degree, and many others.

The overall objective of the research was to elucidate the effect of the dissolved organic carbon fraction of fresh liquid swine manure on SMX sorption onto smectite clays to identify the fate and transport of SMX in the environment. Specific objectives were to (i) characterize liquid swine manure humic and fulvic acid fractions using robust spectroscopic techniques, (ii) quantify the sorption of SMX onto bentonite clay in the presence and absence of liquid swine

manure organic matter, (iii) elucidate the impact of humic acid and fulvic acid form fresh liquid swine manure DOC on the SMX sorption mechanisms onto bentonite clay.

## 1.7 Hypotheses

The hypotheses for the specific objectives of the research are as follows:

**Hypothesis I:** Physicochemical properties, including the abundance and orientation of functional groups in humic acid and fulvic acid secondary structures of fresh liquid swine manure DOC are substantially different.

**Hypothesis II:** Organic matter coating on mineral surfaces by fresh liquid swine manure DOC, humic acid, and fulvic acid increases the amount of SMX sorption sites to facilitate increased sorption.

**Hypothesis III:** Subtle differences in physicochemical properties among humic substances inherent variations in functional group-specific SMX binding mechanisms.

## 1.8 Thesis outline

The thesis contains three chapters and follows the layout in the guidelines of the Department of Soil Science, Faculty of Agricultural and Food Sciences, University of Manitoba. Chapter 1 provides an overview of the literature on the fate of livestock-administered SMX in the environment and the role of clay minerals and organic matter in determining the environmental fate of SMX. Chapter 2 presents the thesis research prepared in manuscript style formatted to the journal of Environmental Science and Technology, titled “Physicochemical properties of humic and fulvic acid in fresh liquid swine manure and their effect on sulfamethoxazole sorption onto bentonite clay.” Chapter 3 is the overall synthesis of the project, including a summary of findings and contributions to knowledge, implications of the research, and knowledge gaps and research recommendations.

## 1.9 References

- Abdellah, Y. A. Y., Z. J. Shi, S. S. Sun, Y. Sen Luo, X. Yang, W. T. Hou and R. L. Wang. 2022.** An assessment of composting conditions, humic matter formation and product maturity in response to different additives: A meta-analysis. *J. Clean. Prod.* **366**: 132953. doi: 10.1016/j.jclepro.2022.132953
- Adusei-Gyamfi, J., B. Ouddane, L. Rietveld, J. P. Cornard, and J. Criquet. 2019.** Natural organic matter-cations complexation and its impact on water treatment: A critical review. *Water Res.* **160**: 130-147. doi: 10.1016/j.watres.2019.05.064.
- Agunos, A., S. P. Gow, D. F. Léger, C. A. Carson, A. E. Deckert, A. L. Bosman, D. Loest, R. J. Irwin, and R. J. Reid-Smith. 2019.** Antimicrobial use and antimicrobial resistance indicators-integration of farm-level surveillance data from broiler chickens and turkeys in British Columbia, Canada. *Front. Vet. Sci.* **6**: 131. doi: 10.3389/fvets.2019.00131.
- Andriamalala, A., L. Vieublé-Gonod, V. Dumeny and P. Cambier. 2018.** Fate of sulfamethoxazole, its main metabolite N-ac-sulfamethoxazole and ciprofloxacin in agricultural soils amended or not by organic waste products. *Chemosphere*, **191**: 607-615. doi: 10.1016/j.chemosphere.2017.10.093.
- Archundia, D., C. Duwig, L. Spadini, M. C. Morel, B. Prado, M. P. Perez, V. Orsag and J. M. F. Martins. 2019.** Assessment of the Sulfamethoxazole mobility in natural soils and of the risk of contamination of water resources at the catchment scale. *Environ. Int.* **130**: 104905. doi: 10.1016/j.envint.2019.104905.
- Awad, A. M., S. M. R. Shaikh, R. Jalab, M. H. Gulied, M. S. Nasser, A. Benamor and S. Adham. 2019.** Adsorption of organic pollutants by natural and modified clays: a comprehensive review. *Sep. Purif. Technol.* **228**; 115719. doi:10.1016/j.seppur.2019.115719
- Barron, L., J. Havel, M. Purcell, M. Szpak, B. Kelleher and B. Paull. 2009.** Predicting sorption of pharmaceuticals and personal care products onto soil and digested sludge using artificial neural networks. *Analyst.* **134**(4). doi: 10.1039/b817822d.
- Campitelli, P. and S. Ceppi. 2008.** Effects of composting technologies on the chemical and physicochemical properties of humic acids. *Geoderma.* **144**(1): 325-333. doi: 10.1016/j.geoderma.2007.12.003.
- Canadian Pork Council. 2023.** New rules for the access and use of veterinary drugs. Medically Important Antimicrobials. Retrieved from: <https://www.cpc-ccp.com/mia#:~:text=Commonly%20used%20medically%20important%20antimicrobial,Erythromycin> (accessed May 2023).
- Carballa, M., F. Omil and J. M. Lema. 2008.** Comparison of predicted and measured concentrations of selected pharmaceuticals, fragrances and hormones in Spanish sewage. *Chemosphere.* **72**(8): 1118-1123. doi: 10.1016/j.chemosphere.2008.04.034.
- Chabauty, F., V. Pot, M. Bourdat-Deschamps, N. Bernet, C. Labat and P. Benoit. 2016.** Transport of organic contaminants in subsoil horizons and effects of dissolved organic matter related to organic waste recycling practices. *Environ. Sci. Pollut. Res.* **23**(7): 6907-6918. doi: 10.1007/s11356-015-5938-9.

- Chang Chien, S. W., M. C. Wang, C. C. Huang and K. Seshaiiah. 2007.** Characterization of humic substances derived from swine manure-based compost and correlation of their characteristics with reactivities with heavy metals. *J. Agric. Food Chem.* **55**(12): 4820-4827. doi: 10.1021/jf070021d.
- Charles, S. M., H. Li, B. J. Teppen and S. A. Boyd. 2006.** Quantifying the availability of clay surfaces in soils for adsorption of nitrocyano benzene and diuron. *Environ. Sci. Technol.* **40**(24): 7751-7756. doi: 10.1021/es0611700.
- Chen, K.-L., L.-C. Liu and W.-R. Chen. 2017.** Adsorption of sulfamethoxazole and sulfapyridine antibiotics in high organic content soils. *Environ. Pollut.* **231**: 1163-1171. doi: 10.1016/j.envpol.2017.08.011.
- Chen, Y., B. Chefetz and Y. Hadar. 1996.** Formation and properties of humic substance originating from composts. In M. de Bertoldi, P. Sequi, B. Lemmes, and T. Papi (Eds.), *Sci. of Compost.* 382-393. doi: 10.1007/978-94-009-1569-5\_36.
- Christou, A., M. C. Kyriacou, E. C. Georgiadou, R. Papamarkou, E. Hapeshi, P. Karaolia, C. Michael, V. Fotopoulos and D. Fatta-Kassinou. 2019.** Uptake and bioaccumulation of three widely prescribed pharmaceutically active compounds in tomato fruits and mediated effects on fruit quality attributes. *Sci. Total Environ.* **647**: 1169-1178. doi: 10.1016/j.scitotenv.2018.08.053.
- Dalkmann, P., C. Siebe, W. Amelung, M. Schloter and J. Siemens. 2014.** Does long-term irrigation with untreated wastewater accelerate the dissipation of pharmaceuticals in soil? *Environ. Sci. Technol.* **48**(9): 4963-4970. doi: 10.1021/es501180x.
- De Mastro, F., C. Cacace, A. Traversa, M. Pallara, C. Cocozza, F. Mottola and G. Brunetti. 2022.** Influence of chemical and mineralogical soil properties on the adsorption of sulfamethoxazole and diclofenac in Mediterranean soils. *Chem. Biol. Technol. Agric.* **9**(1): 34. doi: 10.1186/s40538-022-00300-8.
- De Voogt, P., M. L. Janex-Habibi, F. Sacher, L. Puijker and M. Mons. 2009.** Development of a common priority list of pharmaceuticals relevant for the water cycle. *Water Sci. Technol.* **59**(1):39-46. doi: 10.2166/wst.2009.764.
- Drillia, P., K. Stamatelidou and G. Lyberatos. 2005.** Fate and mobility of pharmaceuticals in solid matrices. *Chemosphere.* **60**(8): 1034-1044. doi:10.1016/j.chemosphere.2005.01.032.
- Duan, Y., S. K. Awasthi, T. Liu, Z. Zhang and M. K. Awasthi. 2019.** Response of bamboo biochar amendment on volatile fatty acids accumulation reduction and humification during chicken manure composting. *Bioresour. Technol.* **291**: 121845. doi:10.1016/j.biortech.2019.121845.
- Bhatt, E. and P. Gauba. 2018.** Impact of antibiotics on plants. *Int. J. Pharm. Sci. Rev. Res.* **52**(1): 49-53.
- Feng, L., M. E. Casas, L. D. M. Ottosen, H., Møller, B., and Bester, K. 2017.** Removal of antibiotics during the anaerobic digestion of pig manure. *Sci. Total Environ.*, **603–604**: 219-225. doi: 10.1016/j.scitotenv.2017.05.280.
- Fer, M., R. Kodešová, O. Golovko, Z. Schmidtová, A. Klement, A. Nikodem, M. Kočárek and R. Grabic. 2018.** Sorption of atenolol, sulfamethoxazole and carbamazepine onto

- soil aggregates from the illuvial horizon of the haplic luvisol on loess. *Soil Water Res.* **13**(3): 177-183. doi: 10.17221/82/2018-SWR.
- Fioritto, A. F., S. N. Bhattachar and J. A. Wesley. 2007.** Solubility measurement of polymorphic compounds via the pH-metric titration technique. *Int. J. Pharm.* **330**(1-2): 105-113. doi: 10.1016/j.ijpharm.2006.09.003.
- Gaffney, J. S., N. A. Marley and S. B. Clark. 1996.** Humic and fulvic acids and organic colloidal materials in the environment. ACS Symposium Series. **651**. doi: 10.1021/bk-1996-0651.ch001.
- Gao, J. and J. A. Pedersen. 2005.** Adsorption of sulfonamide antimicrobial agents to clay minerals. *Environ. Sci. Technol.* **39**(24): 9509-9516. doi: 10.1021/es050644c.
- García-Galán, M. J., M. S. Díaz-Cruz and D. Barceló. 2011.** Occurrence of sulfonamide residues along the Ebro river basin. Removal in wastewater treatment plants and environmental impact assessment. *Environ. Int.* **37**(2): 462-473. doi:10.1016/j.envint.2010.11.011.
- Goulas, A., N. Sertillanges, K. Brimo, P. Garnier, V. Bergheaud, V. Dumény, P. Benoit and C.-S. Haudin. 2019.** Environmental availability of sulfamethoxazole and its acetylated metabolite added to soils via sludge compost or bovine manure. *Sci. Total Environ.* **651**: 506-515. doi: 10.1016/j.scitotenv.2018.09.100.
- Gray, A. D. and E. Bernhardt. 2022.** Are nitrogen and carbon cycle processes impacted by common stream antibiotics? A comparative assessment of single vs. mixture exposures. *PLoS ONE.* **17**(1). doi: 10.1371/journal.pone.0261714.
- Haham, H., A. Oren and B. Chefetz. 2012.** Insight into the role of dissolved organic matter in sorption of sulfapyridine by semiarid soils. *Environ. Sci. Technol.* **46**(21): 11870-11877. doi: 10.1021/es303189f.
- Hamscher, G., H. T. Pawelzick, H. Höper and H. Nau. 2005.** Different behavior of tetracyclines and sulfonamides in sandy soils after repeated fertilization with liquid manure. *Environ. Toxicol. Chem.* **24**(4): 861-868. doi: 10.1897/04-182R.1.
- Hanamoto, S., R. Yamamoto-Ikemoto and H. Tanaka. 2021.** Predicting mass loadings of sulfamonomethoxine, sulfamethoxazole, and lincomycin discharged into surface waters in Japanese river catchments. *Sci. Total Environ.* **776**: 146032. doi: 10.1016/j.scitotenv.2021.146032.
- Hansima, M. A. C. K., A. T. Jayaweera, J. Ketharani, T. Ritigala, L. Zheng, D. R. Samarajeewa, K. G. N. Nanayakkara, A. C. Herath, M. Makehelwala, K. B. S. N. Jinadasa, S. K. Weragoda, Y. Wei and R. Weerasooriya. 2022.** Characterization of humic substances isolated from a tropical zone and their role in membrane fouling. *J. Environ. Chem. Eng.* **10**(3): 107456. doi: 10.1016/j.jece.2022.107456.
- Hernández, D., L. Lazo, L. Valdés, L. C. de Ménorval, Z. Rozynek and A. Rivera. 2018.** Synthetic clay mineral as nanocarrier of sulfamethoxazole and trimethoprim. *Appl. Clay Sci.* **161**. doi: 10.1016/j.clay.2018.03.016.
- Höltge, S. and R. Kreuzig. 2007.** Laboratory testing of sulfamethoxazole and its metabolite acetyl-sulfamethoxazole in soil. *Clean-Soil, Air, Water.* **35**(1): 104-110. doi: 10.1002/clen.200600019.

- Hou, J., Wan, W., Mao, D., Wang, C., Mu, Q., Qin, S., & Luo, Y. 2015.** Occurrence and distribution of sulfonamides, tetracyclines, quinolones, macrolides, and nitrofurans in livestock manure and amended soils of Northern China. *Environ. Sci. Pollut. Res.*, **22**(6): 4545–4554. doi: 10.1007/s11356-014-3632-y.
- Hu, S., Y. Zhang, G. Shen, H. Zhang, Z. Yuan and W. Zhang. 2019.** Adsorption/desorption behavior and mechanisms of sulfadiazine and sulfamethoxazole in agricultural soil systems. *Soil Tillage Res.* **186**: 233-241. doi: 10.1016/j.still.2018.10.026.
- Inbar, Y., Chen, Y., and Hadar, Y. 1990.** Humic substances formed during the composting of organic matter. *Soil Sci. Soc. Am. J.* **54**(5): 1316-1323. doi:10.2136/sssaj1990.03615995005400050019x.
- Kästner, M., Nowak, K. M., Miltner, A., Trapp, S., and Schäffer, A. 2014.** Classification and modelling of nonextractable residue (NER) formation of xenobiotics in soil - A synthesis. *Crit. Rev. Environ. Sci. Technol.* **44**(19): 2107-2171. doi:10.1080/10643389.2013.828270.
- Kim, S.-C. and K. Carlson. 2007.** Temporal and spatial trends in the occurrence of human and veterinary antibiotics in aqueous and river sediment matrices. *Environ. Sci. Technol.* **41**(1): 50-57. doi: 10.1021/es060737+.
- Kleber, M., P. Sollins and R. Sutton. 2007.** A conceptual model of organo-mineral interactions in soils: self-assembly of organic molecular fragments into zonal structures on mineral surfaces. *Biogeochemistry.* **85**(1): 9-24. doi: 10.1007/s10533-007-9103-5.
- Klein, A. R., E. Sarri, S. E. Kelch, J. J. Basinski, S. Vaidya, and L. Aristilde. 2021.** Probing the fate of different structures of beta-lactam antibiotics: hydrolysis, mineral capture, and influence of organic matter. *ACS Earth and Space Chem.* **5**(6): 1511-1524. doi: 10.1021/acsearthspacechem.1c00064.
- Kumar, K., S. C. Gupta, Y. Chander, and A. K. Singh. 2005.** Antibiotic use in agriculture and its impact on the terrestrial environment. *Adv. Agron.* **87**: 1-54. doi: 10.1016/S0065-2113(05)87001-4.
- Li, T., Y. Li, M. Li, N. Wang, Z. Sun, X. Li and B. Li. 2023.** Effects of sulfamethoxazole on nitrogen transformation and antibiotic resistance genes in short-cut nitrification and denitrification process treating mariculture wastewater. *J. Chem. Eng.* **454**: 140517. doi: 10.1016/j.ccej.2022.140517.
- Li, X., M. Xing, J. Yang and Z. Huang. 2011.** Compositional and functional features of humic acid-like fractions from vermicomposting of sewage sludge and cow dung. *J. Hazard. Mater.* **185**(2). 740-748. doi: 10.1016/j.jhazmat.2010.09.081.
- Lin Ching-Erh, C. C. Chang and W. C. Lin. 1997.** Migration behavior and separation of sulfonamides in capillary zone electrophoresis III. Citrate buffer as a background electrolyte. *J. Chromatogr. A.* **768**(1): 105-112. doi: 10.1016/S0021-9673(97)00010-1.
- Lin, K. and J. Gan. 2011.** Sorption and degradation of wastewater-associated non-steroidal anti-inflammatory drugs and antibiotics in soils. *Chemosphere.* **83**(3): 240-246. doi: 10.1016/j.chemosphere.2010.12.083
- Liu, F., G.-G. Ying, R. Tao, J.-L. Zhao, J.-F. Yang and L.-F. Zhao. 2009.** Effects of six selected antibiotics on plant growth and soil microbial and enzymatic activities. *Environ. Pollut.* **157**(5): 1636-1642. doi: 10.1016/j.envpol.2008.12.021.

- Marín-García, M., M. de Luca, G. Ragno and R. Tauler. 2021.** Coupling of spectrometric, chromatographic, and chemometric analysis in the investigation of the photodegradation of sulfamethoxazole. *Talanta*. **235**: 122953. doi: 10.1016/j.talanta.2021.122953.
- Martínez-Hernández, V., R. Meffe, S. H. López and I. de Bustamante. 2016.** The role of sorption and biodegradation in the removal of acetaminophen, carbamazepine, caffeine, naproxen and sulfamethoxazole during soil contact: a kinetics study. *Sci. Total Environ.* **559**: 232-241. doi: 10.1016/j.scitotenv.2016.03.131.
- Mercer, M. A. 2022.** Sulfonamides and sulfonamide combinations use in animals. MERCK manual. Retrieved from: <https://www.merckvetmanual.com/pharmacology/antibacterial-agents/sulfonamides-and-sulfonamide-combinations-use-in-animals> (accessed May 2023).
- Park, J. Y. and B. Huwe. 2016.** Effect of pH and soil structure on transport of sulfonamide antibiotics in agricultural soils. *Environ. Pollut.* **213**: 561-570. doi: 10.1016/j.envpol.2016.01.089.
- Rabølle, M. and N. H. Spliid. 2000.** Sorption and mobility of metronidazole, olaquinox, oxytetracycline and tylosin in soil. *Chemosphere*. **40**(7): 715-722. doi: 10.1016/S0045-6535(99)00442-7.
- Radke, M., C. Lauwigi, G. Heinkele, T. E. Múrdter and M. Letzel. 2009.** Fate of the antibiotic sulfamethoxazole and its two major human metabolites in a water sediment test. *Environ. Sci. Technol. Lett.* **43**(9): 3135-3141. doi: 10.1021/es900300u.
- Sarmah, A. K., M. T. Meyer and A. B. A. Boxall. 2006.** A global perspective on the use, sales, exposure pathways, occurrence, fate and effects of veterinary antibiotics (VAs) in the environment. *Chemosphere*. **65**(5): 725-759. doi: 10.1016/j.chemosphere.2006.03.026.
- Scott, H. M., G. Acuff, G. Bergeron, M. W. Bourassa, J. Gill, D. W. Graham, L. H. Kahn, P. S. Morley, M. J. Salois, S. Simjee, R. S. Singer, T. C. Smith, C. Storrs and T. E. Wittum. 2019.** Critically important antibiotics: criteria and approaches for measuring and reducing their use in food animal agriculture. *Ann. N. Y. Acad. Sci.* **1441**(1): 8-16. doi: 10.1111/nyas.14058.
- Semenov, V. M., A. S. Tulina, N. A. Semenova and L. A. Ivannikova. 2013.** Humification and nonhumification pathways of the organic matter stabilization in soil: A review. *Eurasian Soil Sci.* **46**(4): 355-368. doi: 10.1134/S106422931304011X.
- Srinivasan, P., A. K. Sarmah and M. Manley-Harris. 2013.** Co-contaminants and factors affecting the sorption behaviour of two sulfonamides in pasture soils. *Environ. Pollut.* **180**: 165-172. doi: 10.1016/j.envpol.2013.05.022.
- Stoob, K., H. P. Singer, S. R. Mueller, R. P. Schwarzenbach and C. H. Stamm. 2007.** Dissipation and transport of veterinary sulfonamide antibiotics after manure application to grassland in a small catchment. *Environ. Sci. Technol.* **41**(21): 7349-7355. doi: 10.1021/es070840e.
- Straub, J. O. 2016.** Aquatic environmental risk assessment for human use of the old antibiotic sulfamethoxazole in Europe. *Environ. Toxicol. Chem.* **35**(4): 767-779. doi: 10.1002/etc.2945.

- Thiebault, T. 2020.** Sulfamethoxazole/Trimethoprim ratio as a new marker in raw wastewaters: A critical review. *Sci. Total Environ.* **715**: 136916. doi: 10.1016/j.scitotenv.2020.136916.
- Thiele-Bruhn, S., T. Seibicke, H.-R. Schulten and P. Leinweber. 2004.** Sorption of sulfonamide pharmaceutical antibiotics on whole soils and particle-size fractions. *J. Environ. Qual.* **33**(4). doi: 10.2134/jeq2004.1331.
- Vasilevich, R., E. Lodygin, V. Beznosikov and E. Abakumov. 2018.** Molecular composition of raw peat and humic substances from permafrost peat soils of European Northeast Russia as climate change markers. *Sci. Total Environ.* **615**: 1229-1238. doi: 10.1016/j.scitotenv.2017.10.053.
- Vasudevan, D., G. L. Bruland, B. S. Torrance, V. G. Upchurch and A. A. MacKay. 2009.** pH-dependent ciprofloxacin sorption to soils: Interaction mechanisms and soil factors influencing sorption. *Geoderma.* **151**(3): 68-76. doi: 10.1016/j.geoderma.2009.03.007.
- Vieublé Gonod, L., L. P. Y. Dellouh, A. Andriamalala, V. Dumény, V. Bergheaud and P. Cambier. 2022.** Fate of sulfamethoxazole in compost, manure and soil amended with previously stored organic wastes. *Sci. Total Environ.* **803**: 150023. doi: 10.1016/j.scitotenv.2021.150023.
- Vithanage, M., A. U. Rajapaksha, X. Tang, S. Thiele-Bruhn, K. H. Kim, S. E. Lee and Y. S. Ok. 2014.** Sorption and transport of sulfamethazine in agricultural soils amended with invasive-plant-derived biochar. *J. Environ. Manage.* **141**: 95-103. doi: 10.1016/j.jenvman.2014.02.030.
- Wang, B., M. Li, H. Zhang, J. Zhu, S. Chen and D. Ren. 2020.** Effect of straw-derived dissolved organic matter on the adsorption of sulfamethoxazole to purple paddy soils. *Ecotoxicol. Environ. Saf.* **203**: 110990. doi: 10.1016/j.ecoenv.2020.110990.
- Wang, C., B. J. Teppen, S. A. Boyd and H. Li. 2012.** sorption of lincomycin at low concentrations from water by soils. *Soil Sci. Soc. Am. J.* **76**(4): 1222-1228. doi: 10.2136/sssaj2011.0408.
- Wang, J., H. Lin, W. Sun, Y. Xia, J. Ma, J. Fu, Z. Zhang, H. Wu and M. Qian. 2016.** Variations in the fate and biological effects of sulfamethoxazole, norfloxacin and doxycycline in different vegetable-soil systems following manure application. *J. Hazard. Mater.* **304**: 49–57. doi: 10.1016/j.jhazmat.2015.10.038.
- Wang, K., C. He, S. You, W. Liu, W. Wang, R. Zhang, H. Qi and N. Ren. 2015.** Transformation of organic matters in animal wastes during composting. *J. Hazard. Mater.* **300**: 745-753. doi: 10.1016/j.jhazmat.2015.08.016.
- Watanabe, N., B. A. Bergamaschi, K. A. Loftin, M. T. Meyer and T. Harter. 2010.** Use and environmental occurrence of antibiotics in freestall dairy farms with manured forage fields. *Environ. Sci. Technol.* **44**(17): 6591-6600. doi: 10.1021/es100834s.
- Wegst-Uhrich, S. R., D. A. G. Navarro, L. Zimmerman and D. S. Aga. 2014.** Assessing antibiotic sorption in soil: a literature review and new case studies on sulfonamides and macrolides. *Chem. Cent. J.* **8**(1): 5. doi: 10.1186/1752-153X-8-5.
- Wu, Y., Q. Wen, Z. Chen, Q. Fu and H. Bao. 2022.** Response of antibiotic resistance to the co-exposure of sulfamethoxazole and copper during swine manure composting. *Sci. Total Environ.* **805**: 150086. doi: 10.1016/j.scitotenv.2021.150086.

- Xiong, J.-Q., S.-J. Kim, M. B. Kurade, S. Govindwar, R. A. I. Abou-Shanab, J.-R. Kim, H.-S. Roh, M. A. Khan and B.-H. Jeon. 2019.** Combined effects of sulfamethazine and sulfamethoxazole on a freshwater microalga, *Scenedesmus obliquus*: toxicity, biodegradation, and metabolic fate. *J. Hazard. Mater.* **370**: 138-146. doi: 10.1016/j.jhazmat.2018.07.049.
- Zamora, W. J., C. Curutchet, J. M. Campanera and F. J. Luque. 2017.** prediction of pH-dependent hydrophobic profiles of small molecules from miertus–scrocco–tomasi continuum solvation calculations. *J. Phys. Chem. B.* **121**(42): 9868-9880. doi: 10.1021/acs.jpcc.7b08311.
- Zhang, Y., J. Geng, H. Ma, H. Ren, K. Xu and L. Ding. 2016.** Characterization of microbial community and antibiotic resistance genes in activated sludge under tetracycline and sulfamethoxazole selection pressure. *Sci. Total Environ.* **571**: 479-486. doi: 10.1016/j.scitotenv.2016.07.014.
- Zheng, W., M., Guo and G. Czapar. 2020.** Environmental fate and transport of veterinary antibiotics derived from animal manure. *Anim. Manure.* **67**: 409-430. doi: 10.2134/asaspecpub67.c15.
- Zhi, D., D. Yang, Y. Zheng, Y. Yang, Y. He, L. Luo and Y. Zhou. 2019.** Current progress in the adsorption, transport and biodegradation of antibiotics in soil. *J. Environ. Manage.* **251**: 109598. doi: 10.1016/j.jenvman.2019.109598.

## **2. PHYSICOCHEMICAL PROPERTIES OF HUMIC AND FULVIC ACID IN FRESH LIQUID SWINE MANURE AND THEIR EFFECT ON SULFAMETHOXAZOLE SORPTION ONTO BENTONITE CLAY**

### **2.1 Abstract**

The widespread use of sulfamethoxazole (SMX) as a veterinary drug in the swine industry increases its occurrence in manure and dispersal in the environment. Humic substances deriving from dissolved organic carbon (DOC) in swine manure influence the sorption of SMX onto smectite clays, hence the environmental fate. The objective of the study was to elucidate the effect of fresh liquid swine manure DOC fraction on SMX sorption mechanisms onto smectite clay to understand the fate and transport in the environment. Humic acid (HA) and fulvic acid (FA) were isolated from the DOC fraction of fresh liquid swine manure using the alkaline extraction method and characterized spectroscopically. A batch sorption study with a randomized complete block design was used to quantify the sorption, and the equilibrated aqueous phase and the clay-mineral fraction were further analyzed for surface and interlayer SMX sorption. Fluorescence spectroscopy was used to capture fluorescence quenching in humic substances by SMX. Sorption data fitted the Freundlich isotherm except for SMX sorption by aqueous FA. Subtle physicochemical differences in the core and the surface of HA and FA secondary structures resulted in different sorption mechanisms. SMX interactions with FA-coated bentonite involved fluorophore quencher  $\pi$ - $\pi$  electron-donor-acceptor interactions, cation and water bridging, and H-bonding with phenolic groups. HA-coated bentonite allowed non-fluorophore quencher H-bonding and cation and water bridging with amide groups. The abundance of FA in the DOC fraction (10 FA: 1 HA) dominated the organic matter coating on the clay mineral surface. SMX complexed to free FA in the aqueous phase can be transported via runoff or leaching and released to the environment. We suggest the oxidation of FA-phenolic functional groups under aerobic conditions in lagoon storage or by composting and

allowing the transformation of FA to HA through humification under long-term storage before land application to reduce the environmental dispersion of SMX.

## **2.2 Introduction**

Manure application is among the indispensable practices in sustainable agriculture that enhances soil fertility and soil health. Poultry litter, beef or dairy cattle manure, and swine manure are the most common manure amendments (Amorim et al. 2022; Antoneli et al. 2019; Nyiraneza et al. 2009). They can be pre-stored solid/liquid, lagoon stored, composted, anaerobically digested, or deposited directly on pasture, range, or paddock by grazing animals (Marinier 2004). Manure addition improves soil chemical properties by increasing inorganic nutrients (e.g., N, P, K, Ca, Mg, P, K, Fe, Cu, Zn, and B), organic matter (e.g., humic acid, fulvic acid, soluble organic compounds, hemicellulose, cellulose, lignin), and C/N ratio (Nyiraneza et al. 2009; Rees et al. 2014; Samson et al. 2020). It also enhances soil physical properties such as aggregation size and stability, soil pH, cation exchange capacity, bulk density, water infiltration, and porosity (Antoneli et al. 2019; Assefa et al. 2004; Nyiraneza et al. 2009).

Livestock excretory products can contain harmful contaminants, including toxic heavy metals, pathogenic microorganisms, antimicrobial residues and their metabolites, and natural and synthetic steroidal hormones. Contaminating the ecosystem with these substances is a great risk associated with manure management (Hanselman et al. 2003; Kumar et al. 2013; Soto et al. 2023). Veterinary antimicrobials are one of the major groups of contaminants in livestock manure. Sulfamethoxazole (SMX), which belongs to the sulfonamides class of antimicrobials, is frequently used in the Canadian swine industry as a therapeutic or disease-prevention drug (Kahle and Stamm 2007). Application of stored/non-stored liquid swine manure in Canadian prairies causes ubiquitous detection of SMX in soils, groundwater, surface water, and crops in

substantial amounts (Awosile et al. 2017; Miao et al. 2004; Topp et al. 2013). The World Health Organization has identified antimicrobial resistance in bacteria due to environmental accumulation and prolonged exposure as one of the top 10 global health threats to the human population (WHO, 2020).

The environmental fate of SMX in manured soil is affected by many factors, including soil pH, ionic strength, type of manure, method of application, rate and time of application, microbiota, and hydro-geological conditions (Mina et al. 2017). Manure adds dissolved organic carbon (DOC) to the total soil organic carbon pool, enhancing the most mobile carbon fraction of the soil (Leenheer and Croué 2003). Mobile DOC fraction facilitates the adsorption of contaminants to the DOC fraction, including antimicrobials. As a result, higher DOC reduces contaminant interactions with other soil components, thus increasing the runoff transportation and leaching as DOC-bound forms (Briceño et al. 2008).

Some studies explain sorption potentials and transport dynamics of veterinary antimicrobials in contact with manure-derived organic matter. Most of the studies used distribution coefficient ( $K_d$ ) or organic matter normalized distribution constant ( $K_{oc}$ ) to account for the sorption strengths and transport potentials (Loke et al. 2002; Wang et al. 2015). Different indexes were used by other authors, for example, antimicrobial losses/mass balances, isotherm coefficients, and dissipation half-lives (Arikan et al. 2016; Aust et al. 2008; Briceño et al. 2008; Song and Guo 2014; Stoob et al. 2007; Wu et al. 2012). Mechanistic interpretations were mostly postulated using these constants and indexes. There is a dearth of literature to explain antimicrobial sorption mechanisms parallel to the explanations of exact physicochemical properties and dynamics of the organic matter fraction, specifically the humic substances. Postulated mechanisms are not sound enough since they lack the knowledge of bulk physical and chemical properties (e.g., distribution of functional groups, aromaticity, aliphaticity, hydrophilicity, hydrophobicity, molecular size, the surface charge) and

conformation/orientation of functional groups in secondary structures in aqueous solutions. It is not precise to apply common interaction mechanisms since humic substances are heterogeneous and have various chemical and physicochemical properties according to the origin, environmental factors, microbial community, humification degree, and many others.

The objective of the research was to elucidate the effect of fresh liquid swine manure DOC on SMX sorption onto smectite clay to understand the fate and transport in the environment. Specific objectives were to (i) characterize HA and FA in fresh liquid swine manure DOC; (ii) quantify the sorption of SMX onto bentonite clay in the presence and absence of organic matter, i.e., HA, FA, and DOC; (iii) elucidate SMX sorption mechanisms onto bentonite clay in the presence of fresh liquid swine manure DOC. We hypothesized subtle differences in the physicochemical properties of fresh liquid swine manure humic acid (HA) and fulvic acid (FA) in the DOC to facilitate functional group-specific SMX binding mechanisms.

## **2.3 Materials and Methods**

### **2.3.1 Isolation and purification of humic and fulvic acid from fresh liquid swine manure dissolved organic carbon fraction**

**Manure:** A sample of fresh semi-solid swine manure slurry (39.82% solids) was collected into a 20-L pail in June 2022 from a wet manure well at Glenlea Research Station University of Manitoba (49°38'57.4" N, 97°7'5.0" W), Winnipeg, MB, Canada, where no SMX was administered. The capacity of the facility is 130, which includes breeding animals, piglets, and weanlings. In the facility, manure is stored beneath the slats in pits as a slurry. Manure slurry in the pits is emptied into the wet manure well within six weeks once they are 90% full. In addition, the pens are flushed thoroughly, and the grey water follows the same path as the manure slurry to reach the wet well.

**Chemicals:** Methanol (HPLC grade), HCl (ACS grade), NaOH pellets (ACS grade), Supelite DAX-8 resin, and AmBerlite+ IR-120(H) cation exchange resin were from Fisher Scientific, CA. Hydrophilic polyvinylidene difluoride 0.45  $\mu\text{m}$  (50 mm) filter papers were from Millipore sigma, CA. Nalgene Oak Ridge Teflon 50 mL centrifuge tubes were from Thermo Scientific, CA.

**Extraction procedure:** The DOC fraction from the fresh semi-solid manure sample was obtained after centrifugation at 10,000 rpm for 10 min to obtain the liquid fraction and vacuum filtration through 0.45  $\mu\text{m}$  polyvinylidene difluoride membrane filters. The semi-solid fresh swine manure and the DOC fraction were analyzed from Farmers Edge Laboratories (Winnipeg, MB, CA) and summarized in Table A-1 in appendices. Isolation and fractionation of HA and FA were carried out by an alkaline extraction using hydrophilic-hydrophobic DAX-8 resin following a modification to the procedure described by Thurman and Malcolm (1985) at particular steps. The steps of the extraction procedure are as follows:

**Resin cleaning:** The resin was washed with DI water ( $3 \times$  bed volume (BV) = 720 mL) in a beaker, followed by soaking overnight in 95% methanol (2BV = 480 mL). Resin beads were packed as a methanol slurry in a glass column (BV = 240 mL). The resin inside the column was sequentially washed with 95% methanol (2BV), DI water (2BV), 4% (w/v) NaOH (1BV), DI water (2BV), and 4% (v/v) HCl (1BV). Finally, the resin was washed with DI water until the effluent's pH became neutral.

**Separation of humic substances:** A 1-L from the filtered manure DOC fraction was acidified by concentrated HCl to pH 2.00 and subjected to flow through the resin column under gravity at a flow rate ranging from 2.0-4.0 mL  $\text{min}^{-1}$ . Column effluent contained microbial by-products and aromatic proteins, whereas high molecular weight humic substances were retained in the column stationary phase. Elution of the retained humic substances was carried out using 0.1

mg L<sup>-1</sup> NaOH ( $3 \times$  void volume ( $V_0$ ) = 470 mL) at a flow rate of 2.0 mL min<sup>-1</sup> under gravity. The last 45 mL of the eluent NaOH was recycled through the column to ensure the elution of most of the humic substances attached to the stationary phase. Eluted humic substances were reconcentrated in a second DAX-8 column (BV = 50 mL) at a flow rate of 1 mL min<sup>-1</sup> under gravity after adjusting the pH back to 2.00. Elution from the second column was carried by 0.1 mg L<sup>-1</sup> NaOH ( $3V_0$  = 100 mL). The total effluent volume collected was 90 mL.

**Fractionation of humic substances:** Concentrated humic substances in NaOH were acidified to pH 1.00 with conc. HCl to fractionate HA and FA and allowed to settle for 24 h in Oak Ridge centrifuge tubes. The settled precipitates were centrifuged at 10,000 rpm for 10 min at 14 °C, and FA in the supernatant was decanted. HA precipitate was washed several times with DI water to ensure the removal of NaCl formed during the acidification. FA supernatant was passed through a small DAX-8 column (BV = 15 mL) to remove the NaCl after adjusting the pH back to 2.00, followed by the elution with 0.1 mg L<sup>-1</sup> NaOH ( $3V_0$  = 30 mL) and a rinse with DI water (5 mL).

**Hydrogen saturation:** Fractionated humic substances as their sodium salts; hence, a hydrogen saturation step was carried out using a strong cation exchange resin. The resin (20 g in 200 mL of DI water) was packed in a glass column (BV = 6 mL), treated with 5% (v/v) HCl (50 mL) for 10 min, washed with DI water until the effluent pH becomes neutral, and dried at room temperature for 24 h. Sodium humate precipitate was dissolved in a minimum amount of 0.1 mg L<sup>-1</sup> NaOH, raised the volume to 25 mL with DI water, and passed immediately through the cation exchange resin. A 1BV of DI water was added to the column to ensure the elution of total HA volume. The sodium form of FA was passed into another activated cation exchange resin, followed by the DI water rinse to obtain FA in H form. Finally, the H forms of HA and FA were freeze-dried to get the solids.

### 2.3.2 Analytical methods for characterization of swine manure humic substance

**Solid state  $^{13}\text{C}$ -Nuclear Magnetic Resonance spectroscopy:** To identify C functionalities,  $^{13}\text{C}$ -Cross Polarization Magic-Angle-Spinning Nuclear Magnetic Resonance ( $^{13}\text{C}$ -CPMAS-NMR) was performed for freeze-dried, isolated humic substances using Bruker Avance III 400 Widebore instrument with a 4 mm magic-angle spinning (MAS) probe head. The  $^1\text{H}$  transmitter frequency was 400.142 MHz, while the  $^{13}\text{C}$  transmitter frequency was 100.625 MHz.  $^{13}\text{C}$  chemical shift referencing was calibrated versus an adamantane standard. Approximately 60-100 mg of freeze-dried solid HA/FA were placed in a 4 mm zirconium rotor (Bruker Biospin) and sealed using a KeLF cap. Number of transients was 32000 transients with a recycle delay of 2s. Spectra were recorded with a window from 302.5 to -102.6 ppm for  $^{13}\text{C}$  and plotted using Origin Pro 2018 software. Numerical integration of peak areas was used to calculate aromaticity, aliphaticity, hydrophobicity, and the hydrophilicity of the humic substances by following Eq. 1, 2, 3, and 4, respectively (Al-Faiyz 2017).

$$\text{Aromaticity (\%)} = \frac{\text{Sum of peak areas of aromatic C}}{\text{Sum peak area (aliphatic C + aromatic C)}} \times 100 \quad [1]$$

$$\text{Aliphaticity (\%)} = \frac{\text{Sum of peak area of aliphatic C}}{\text{Peak area (aliphatic C + aromatic C)}} \times 100 \quad [2]$$

$$\text{Hydrophobicity (\%)} = \frac{\text{Sum of peak areas of hydrophobic C}}{\text{Total area}} \times 100 \quad [3]$$

$$\text{Hydrophilicity (\%)} = \frac{\text{Sum of peak areas of hydrophilic C}}{\text{Total area}} \times 100 \quad [4]$$

**Fourier-Transformed Infrared Spectroscopy:** Freeze-dried samples were compressed with KBr to make pellets. Nicolet 6000 FTIR (Thermo Scientific, US) was used to obtain the IR spectra of the humic substances. Transmittance was recorded for 32 scans from 400 to 4000

cm<sup>-1</sup> wavenumbers with 4 cm<sup>-1</sup> spectral resolution, and the spectra were obtained using Origin Pro 2018 software.

**X-ray Photoelectron Spectroscopy:** Powdered samples were mounted and spread evenly on a double-sided copper tape pasted on the sample holder using a clean spatula. X-ray photoelectron spectra were collected from Karto Axis Ultra X-ray photoelectron spectrophotometer using Al K $\alpha$  (1486.7 eV) X-ray source. The base pressure of the analytical chamber was  $1 \times 10^{-9}$  Torr. The fixed pass energy was 160 eV with 1.0 eV step size while obtaining the survey spectra, and it was 20 eV with 0.1 eV step size for high-resolution scans. Data were processed using CasaXPS software. The spectra were calibrated using a binding energy correction to the apex of the C1s peak by applying 285 eV to the measured value. The high-resolution C1s, O1s, and N1s spectra were fitted using the Gaussian-Lorentzian mixed function after Shirley background subtraction. Peak areas and positions were compared to quantify the percent C, O, and N functionalities in swine manure humic substances.

**Zeta potential:** Concentrations of 0.01, 0.1, and 1 g L<sup>-1</sup> of HA solutions were prepared in 0.01 mg L<sup>-1</sup> NaOH to overcome difficulties in the dissolution, while FA solutions were in DI water, followed by standing overnight (Klučáková 2018). Zeta potentials were measured using Anton Paar Litesizer 500 particle size analyzer, where samples were loaded in disposable Omega cuvettes (Anton Paar Canada Inc.). Water was chosen as the reference solvent, and the target temperature reached 25 °C. The mean zeta potential and the particle sizes were recorded.

**High-Pressure Size-Exclusion Chromatography:** High-Pressure Size-Exclusion Chromatography (HPSEC) was performed using Waters e2696 HPLC module (Waters Associates, Milford, MA) equipped with a photodiode array detector (range: 190-400 nm) to acquire average molecular weight distribution of the swine manure DOC fraction. The DOC fraction was 100 $\times$  diluted, filtered through polyvinylidene difluoride syringe filters (17 mm,

0.45  $\mu\text{m}$ ), and adjusted for pH at 7.00 using 25 mM  $\text{Na}_2\text{HPO}_4 \cdot 7\text{H}_2\text{O}$  buffer and adjusted for ionic strength (IS) at 0.1 mS/cm using 75 mM KCl. Separation was carried out using a BioSep-SEC-S2000 column obtained from Phenomenex, Terrance CA (silica stationary phase, 300 x 7.8 mm, SE range 1-75 kDa). The injection volume was 100  $\mu\text{L}$  at a constant flow elution rate (1.0 mL  $\text{min}^{-1}$ ). A 100 mM phosphate buffer solution at pH 7.00 (0.0016 M  $\text{Na}_2\text{HPO}_4$  and 0.0024 M  $\text{NaH}_2\text{PO}_4$ ) was used as the mobile phase, where its ionic strength was adjusted to 0.1 mS  $\text{cm}^{-1}$  using 75 mM KCl. A molecular weight standard solution series at 1.6, 5, 7, and 16 kDa ( $M=1 \text{ g L}^{-1}$ ,  $\text{pH}=7.00$ ,  $\text{IS}=0.1 \text{ mS cm}^{-1}$ ) was prepared using polystyrene sulphonate (Scientific Polymer Products Inc., Ontario NY) and syringe filtered using 0.45  $\mu\text{m}$  polyvinylidene difluoride filters. The calibration solutions and sample were degasified overnight with  $\text{N}_2$  to overcome bubble formation in the column. HPSEC for the standards and the sample was carried out within the same day to prevent drift in instrument and column conditions. HPSEC for the standards was carried out at UV absorbance 230 nm, whereas for the sample from 200 to 400 nm. Absorbances at UV 254 nm of the sample were plotted against the time (min), and overlapped peaks were resolved using the Fit peaks (pro) function in Origin Pro 2018 software by fitting the data in the Gaussian function. Time data in the x-axis was converted to average molecular weight using Eq. 5, where  $m$  is the slope,  $c$  is the intercept of the calibration curve, and  $t$  is the time in min (Brezinski 2018).

$$\text{Average Molecular Weight} = 10^{(-mt+c)} \quad [5]$$

### 2.3.3 Sorption study

**Materials:** Analytical grade SMX and isotopically labeled standard sulfamethoxazole- $\text{d}_4$  (SMX- $\text{d}_4$ ) were from Toronto Research Chemicals, ON, CA. Sodium-Bentonite was from Sigma-Aldrich. KCl (ACS grade), *iso*-propanol (for sterilization), and Decon Contrad (detergent) were from Fisher Scientific, CA. HyperSep Retain PEP cartridges (60 mg bed

weight, 3 mL capacity) were from Thermo Scientific, CA, for solid-phase extraction. BRAND special laboratory tubing to pass SPE liquids was from Millipore Sigma, CA, and Bond Elute adaptors for mounting tubing on the cartridges were from Agilent, CA. Hydrophilic Polytetrafluoroethylene syringe filters (17 mm, 0.45  $\mu\text{m}$ ) were from Millipore Sigma, CA. Hydrophilic polyvinylidene difluoride Uniflo luer-lock syringe filters (13 mm, 0.22  $\mu\text{m}$ ) were from Cytiva, CA, and 1.0 mL Agilent glass syringe was used to attach the syringe filters. Amber Boston glass bottles (100 mL) were from Fisher Scientific, CA. Screw top polystyrene-divinylbenzene LC vials (2 mL) were from Merck Emd Millipore. Milli-Q water was obtained from the Milli-Q Direct water purification system (Millipore SAS, France). Glassware was pre-cleaned by immersing them in a 5% Contrad bath for 24 h, followed by RO water rinse, and immersing in 10% (v/v) HCl bath for 24 h, followed by RO and Milli-Q water rinse prior to air drying.

**Batch equilibrium experiments:** A stock solution of 1000  $\mu\text{g L}^{-1}$  analytical grade SMX was prepared in methanol and used to prepare sorption solutions. A stock standard solution of 10,000  $\mu\text{g L}^{-1}$  SMX-d<sub>4</sub> was prepared in methanol and stored at -20 °C for internal standard spiking. Removal of organic matter from Na-bentonite was carried out by heating at 450 °C for 3 h. A randomized complete block design with a 2  $\times$  2  $\times$  5 factorial treatment structure was used to perform three sets of batch sorption experiments by varying the type of manure-derived organic matter as DOC, HA, and FA. Factor 1 was bentonite, with 2 levels (0 and 0.005 kg L<sup>-1</sup>); factor 2 was organic matter, with 2 levels (0 and 25 mg L<sup>-1</sup>); and factor 3 was SMX, with 5 levels (0, 20, 40, 60, and 100  $\mu\text{g L}^{-1}$ ). Sorption solutions were prepared in 0.01 mg L<sup>-1</sup> KCl (100 mL), and the pH was maintained at neutral by adding 0.01 mg L<sup>-1</sup> HCl or 0.01 mg L<sup>-1</sup> NaOH as needed. The solution was transferred into an amber glass bottle and placed in an end-to-end shaker (120 rpm) for 17 h at room temperature. After the equilibration, the treatment solution was centrifuged (4,000 rpm) for 10 min, and the supernatant was vacuum filtered

through 0.45  $\mu\text{m}$  polyvinylidene difluoride membrane filter. Solid bentonite was freeze-dried for further characterization. All treatments were replicated three times.

**Solid-phase extraction and elution:** Vacuum-filtered equilibrium solutions ( $\sim 100$  mL and the exact volume was noted) were subjected to solid-phase extraction following the method described by Amarakoon et al. (2016) with added modifications. Tubing, adaptors, and ports of the vacuum manifold were pre-cleaned sequentially with milli-Q water (10 mL) and methanol (10 mL), whereas the manifold was sterilized with *iso*-propanol. Hypersep Retain PEP cartridges were placed on top of the ports and conditioned sequentially with methanol (10 mL, flow rate  $1 \text{ mL min}^{-1}$ ) and milli-Q water (10 mL, flow rate  $0.5 \text{ mL min}^{-1}$ ). Extraction of SMX was carried by passing the equilibrium filtrates ( $\sim 100$  mL) through the solid-phase extraction setup, followed by milli-Q water rinse (3 mL) and air-drying for 30 min under vacuum pressure. The cartridges were stored at  $4 \text{ }^\circ\text{C}$  until elution.

Elution of the cartridges was carried out using methanol (3 mL, at the flow rate of  $0.5 \text{ mL min}^{-1}$  under gravity) to pre-cleaned glass test tubes. The eluents were then spiked with standard SMX- $\text{d}_4$  (50  $\mu\text{L}$ ) and vortexed, followed by concentration to dryness using an  $\text{N}_2$ -evaporator (OA-SYS Heating system and N-Evap 111, Organomation Associates, Inc.) at  $42 \text{ }^\circ\text{C}$  with ultra-pure  $\text{N}_2$  (Praxiar Canada Inc.), followed by reconstitution with 50:50 (v/v) methanol: milli-Q water (1.0 mL), and vortex. The extracts were then syringe filtered to 2 mL LC vials through  $0.22 \text{ } \mu\text{m}$  microfilters fitted to a luer-locked glass syringe and stored at  $-20 \text{ }^\circ\text{C}$  until analysis by liquid chromatography-tandem mass spectrometry (LC-MS/MS).

**Chromatographic analysis:** Analysis of SMX in equilibrated solutions was performed by Agilent 1260 Infinity II UHPLC (Agilent Technologies) LC-MS/MS instrument. An Agilent Eclipse Plus  $\text{C}_{18}$  column (2.1 mm ID x 50 mm,  $1.8 \text{ } \mu\text{m}$  particle size) was used as the analytical column, where it was coupled to an Agilent Eclipse Plus  $\text{C}_{18}$  guard column (2.1 mm ID x 5

mm). Gradient elution was performed using two mobile phases, milli-Q water (Solvent A) and methanol (Solvent B), and programmed as a linear ramp to increase B from 5% (5:95 (v/v), methanol/milli-Q) to 95% (95:5 (v/v), methanol/milli-Q) during the first 2 min, followed by a hold for next 2 min with 95% B, followed by a linear ramp from 95% B to 5% B to reach initial concentration within 2 min, and re-equilibration with 5% B for another 3 min for the next injection. The injection volume was 10  $\mu\text{L}$ , the mobile phase flow rate was 300  $\mu\text{L min}^{-1}$ , and the column temperature was 42  $^{\circ}\text{C}$  during the analyte separation. Sulfamethoxazole was quantified by Agilent 6740 triple quadrupole mass spectrometer using multiple reaction monitoring (MRM) mode. The electrospray ionization interface was set in positive mode (i.e., ESI+).

**Method relative percent recovery (R%):** Method recovery was tested by spiking the 0.01 mg  $\text{L}^{-1}$  KCl matrix after pH adjustment to neutral, followed by end-to-end shaking (120 epm) for 17 h at room temperature followed by vacuum filtration (0.45  $\mu\text{m}$ ) with 20, 50, and 100  $\mu\text{g L}^{-1}$  analytical SMX. Matrix was then extracted for antimicrobial quantification as described before. Percent recovery was 100.6% at 20  $\mu\text{g L}^{-1}$  SMX, 101.7% at 50  $\mu\text{g L}^{-1}$  SMX, and 96.4% at 100  $\mu\text{g L}^{-1}$  SMX ( $n = 3$  at each concentration).

**Method limit of detection (LOD) and limit of quantification (LOQ):** Method limit of detection (LOD) was tested by spiking 0.01 mg  $\text{L}^{-1}$  KCl matrix ( $n = 7$ ) with 2.5  $\mu\text{g L}^{-1}$  analytical SMX, followed by pH adjustment to neutral, end-to-end shaking (120 epm), vacuum filtration (0.45  $\mu\text{m}$ ) and extraction for antimicrobials as described above. LOD and LOQ were 0.224  $\mu\text{g L}^{-1}$  and 2.24  $\mu\text{g L}^{-1}$ , respectively.

**Statistical analysis:** Sorption data followed the Freundlich sorption isotherm (Eq. 6):

$$C_{ads} = K_f C_e^{1/n} \quad [6]$$

$$C_{ads} = C_0 - C_e \quad [7]$$

Where  $C_e$  is the equilibrium SMX concentration ( $\mu\text{g L}^{-1}$ ),  $C_{ads}$  is the amount of sulfamethoxazole adsorbed ( $\mu\text{g L}^{-1}$ ) and calculated using Eq.7, where  $C_0$  is the initial SMX concentration in ( $\mu\text{g L}^{-1}$ ). Mass balance was implemented in calculations  $C_{ads}$ , assuming there was no degradation or loss during the batch experiment.  $K_f$  ( $(\mu\text{g L}^{-1}/((\mu\text{g L}^{-1})^{1/n}))$ ) and  $n$  are empirical constants for sorption capacity and adsorption strength, respectively (Amarakoon et al. 2019). Freundlich parameters were estimated by fitting sorption data using PROC NLIN in SAS 9.4 (SAS Institute, 2013), and the difference in Freundlich parameters between treatments was determined using 95% confidence levels.

Analysis of variance (ANOVA) was conducted for FTIR and X-ray diffraction data generated during the characterization of the solid phase equilibrated with SMX with and without DOC/FA/HA from the sorption study. The full width at half maximum (FWHM) of  $d_{001}$  peak of diffractograms and changes to the positions of Si-O and SiO<sub>4</sub> vibrational peaks of FTIR spectra were statistically analyzed using R software (version 4.2.2) for ANOVA after checking for the normality using ‘Shapiro.test’ followed by applying ‘aov’ function for the linear model fitted for randomized complete block design by setting organic matter and SMX level as fixed effects/factors and block as the random effect.

### 2.3.3.1 Characterization of the solid phase

**X-ray Diffraction:** Freeze-dried solid fractions from the batch sorption experiments were analyzed for interlayer SMX sorption by Powder X-ray Diffraction (PXRD) using a Siemens D5000 powder diffractometer consisting of a Cu X-ray tube. Finely ground samples were top-loaded into a shallow well of a zero-background sample holder to obtain random powders and scanned from  $3^{\circ}$  to  $30^{\circ}$   $2\theta$  with a step size of  $0.02^{\circ}$   $2\theta$  and dwell time was 1 s per step with Cu-

K $\alpha$  radiation ( $\lambda$ , 1.54 Å). The X-ray tube was operated at 40 kV and 35 mA during the analysis. Diffraction patterns were obtained by using Origin Pro 2018 software.

**Fourier-Transformed Infrared Spectroscopy:** FTIR spectra of the solid phase were used to capture alterations in vibration frequencies of surface groups in bentonite to elucidate molecular interactions. Acquisition of the spectra and sample preparation was carried out as the same procedure for humic substances. Spectra were obtained, and Si-O and SiO<sub>4</sub> vibrational peaks were fitted in Gaussian function in the Origin Pro 2018 software.

**Scanning Electron Microscopic Images:** Scanning electron microscopic images were used to visualize bentonite surfaces to aid adsorption mechanisms. A small amount of a powdered sample was mounted and spread evenly using a toothpick on carbon tape pasted on the sample holder. A thin layer (~20 nm) of Au: Pd (60: 40) was coated using a Denton Vacuum Desk II coater ( $5 \times 10^{-2}$  Torr, 45 A current for 60 s) to make non-conducting bentonite samples to conducting. Everhart-Thornley Detector (ETD) in FEI Quanta 650 environmental Scanning Electron Microscope was used to image humic substances. The operating voltage was kept at 5 kV while the vacuum pressure was  $10^{-4}$  pa.

### 2.3.3.2 Characterization of the liquid phase

Equilibrium sorption solutions were subjected to 3D-fluorescence spectra from Agilent Cary Eclipse fluorescence spectrophotometer equipped with a Xenon excitation source. A 4-mL aliquot from each solution was poured into a quartz cell (1 cm path length). XPS were recorded by increasing the excitation (Ex) wavelength from 200 to 600 nm with 10 nm increments and measuring the emission (Em) intensities from 200 to 600 nm for each Ex-step with 2.00 nm data intervals. The slit width for Em and Ex was 5 nm, whereas PMT (Photo Multiplier Tube) voltage was set to medium mode and scan mode was set to fast during the spectra recording.

The Ex and Em regions for HA and FA-like substances were defined according to the supporting literature (Chen et al. 2003). 3D-EEM matrices for FA-like substances (Ex 200-250 nm/Em 380-680 nm) and FA-like substances (Ex 250-500 nm/Em 380-500 nm) were separated and drawn using Origin Pro 2018 software. Rayleigh scattering was removed manually by zeroing the respective intensities in the matrices. Quantification of EEM spectral regions was performed by using the 2D volume integrate function (Origin Pro 2018) to account for the volume beneath each peak. Data was used to capture fluorophore-quencher complex formation mechanisms in the aqueous phase.

## **2.4 Results and Discussion**

### **2.4.1 Constituents of fresh liquid swine manure DOC fraction**

High-Pressure Size-Exclusion Chromatography (HPSEC) at UV absorbance 254 nm ( $UV_{254}$ ), energy for  $\pi \rightarrow \pi^*$  electronic transitions in benzene rings, was used to measure molecular weight fractions in swine manure DOC fraction. Figure 2.1a represents the entire spectrum of molecular weights ranging from 10-400,000 Da. High molecular weight (HMW) molecules appear first in the spectra since they were excluded from HPSEC column pores to facilitate a fast elution. Low molecular weight (LMW) ones appear last. Several components lie in the LMW range, representing humic substances, whereas the HMW fraction for biopolymers (i.e., polysaccharides and proteins) shows low abundance. In the literature, molecular weights between 100 and 70,000 Da are for hydrophobic bases, including proteins and amino acids (Brezinski 2018). Therefore, hydrophobic bases contribute to the swine manure DOC fraction (Figure 2.1c and d). The molecular weight fraction between 600 and 2100 Da is reported to represent LMW fulvic acids (600-1100 Da) and humic-like substances (1600-2100 Da). Hence, a higher proportion of the swine manure DOC is enriched with FAs (Brezinski 2018). The LMW components are identified as the major DOC fraction contributing to the organic carbon

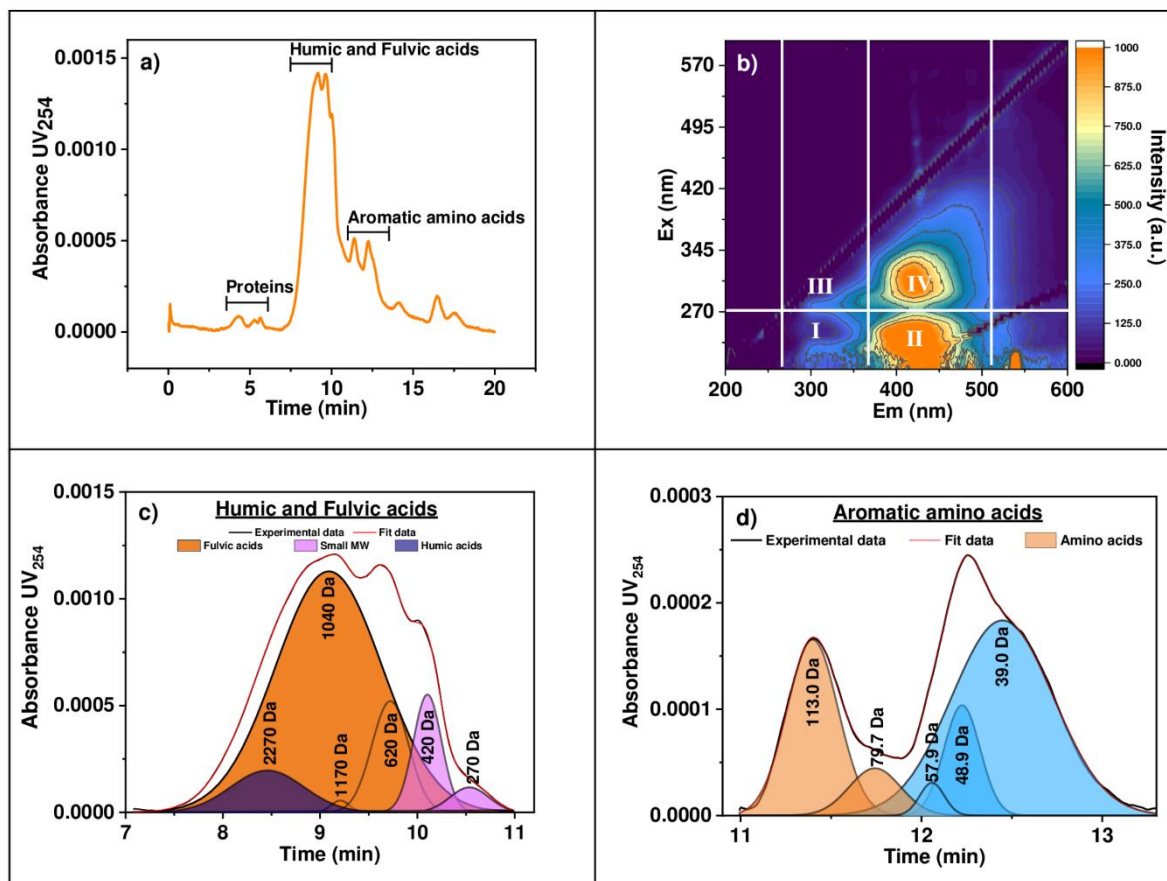


Figure 2.1 Characterization of swine manure DOC fraction for a) molecular weight distribution by High-Performance Size-Exclusion Chromatography (HPSEC) at  $UV_{254}$ , b) identification of their components by Excitation-Emission Matrix spectroscopy and deconvoluted HPSEC spectra for c) humic and fulvic acids, and d) aromatic amino acids. Region I) of b) is for protein-like fluorophores, II) is for fulvic-like fluorophores, III) is for soluble microbial byproduct fluorophores, and IV) is for humic-like fluorophores.

pool in soils and aquatic environments (85%) (particularly < 1 kDa fraction) and ingredients for refractory organic matter (Liu et al. 2014; Makehelwala et al. 2019).

3D Excitation-Emission Matrix (3D-EEM) data were used to map fluorophores in swine manure DOC fraction. Specific regions in a 3D-EEM spectrum are I) protein-like fluorophores ( $\lambda_{ex}$ = 200-250 nm,  $\lambda_{em}$ = 280-380 nm), II) fulvic-like fluorophores ( $\lambda_{ex}$ = 200-250 nm,  $\lambda_{em}$ = 380-600 nm), III) soluble microbial byproduct fluorophores ( $\lambda_{ex}$ = 250-350 nm,  $\lambda_{em}$ = 280-380 nm), and IV) humic-like fluorophores ( $\lambda_{ex}$ = 250-500 nm,  $\lambda_{em}$ = 380-500 nm) (Jacquin et al. 2017).

The fluorescence spectrum in Figure 2.1b shows higher fluorophore intensities in fulvic and humic-like regions, with the highest intensity for the fulvic region. There is a less intense peak

for protein-like fluorophores where the soluble microbial byproduct peak is overlapped with humic peaks. The results observed for 3D-EEM data are compatible with the HPSEC data.

## **2.4.2 Structural characteristics of fresh liquid swine manure humic substances**

### **2.4.2.1 Solid-state $^{13}\text{C}$ -CPMAS-NMR spectroscopy**

High-resolved solid state  $^{13}\text{C}$ -Cross Polarization Magic-Angle-Spinning Nuclear Magnetic Resonance ( $^{13}\text{C}$ -CPMAS-NMR) spectra of fractionated humic substances are presented in Figures 2.2a and b. These spectra show four well-resolved resonance regions for carbon functionalities, namely, aliphatic region in 0 to 50, carbohydrate region in 51 to 110, aromatic region in 111 to 160, and carboxyl region in 161 to 190 ppm (Al-Faiyz 2017; Zheng et al. 2021). Both humic substances show common peaks in each region with slight variations in the position (Table 2.1) and the relative intensity (Figure 2.2c).

Aliphaticity of the humic substances was calculated by summing the integrated areas of 0-110 and 161-190 ppm ranges. Higher relative intensities for aliphatic and carbohydrate regions are responsible for rather higher aliphaticity observed for humic acid (66.0%). Fulvic acid also shows a comparable aliphaticity (62.7%), which is attributed to higher carboxyl content despite the low contribution from the carbohydrate region. Aliphatic nature of humic acid comes mostly from the intense peak at 25.81 ppm for methyl ( $-\text{CH}_3$ ) and methylene ( $-(\text{CH}_2)_n$ ) and at 39.07 ppm for carbons bonded to carbons (C-alkyl C). HA shows a peak at 15.11 ppm for aliphatic  $-\text{CH}-$  and  $-\text{CH}_2-$ , whereas a slightly shifted peak at 17.04 ppm of fulvic acid is for terminal  $-\text{CH}_3$  groups (Al-Faiyz 2017). Contributions from the carbohydrate region are a combined result of carbons bonded to a single oxygen atom as for  $\text{C}_6$  atoms and carbon atoms bonded to two oxygen atoms as anomeric  $\text{C}_1$  atoms of hexose monomers in polysachcharides (Abakumov et al. 2015; Chen et al. 1989). Swine manure HA shows higher intensities in both  $\text{C}_6$  peak at 71.11 ppm and the shoulder peak of  $\text{C}_1$  carbons at 82.78 ppm in comparison to the

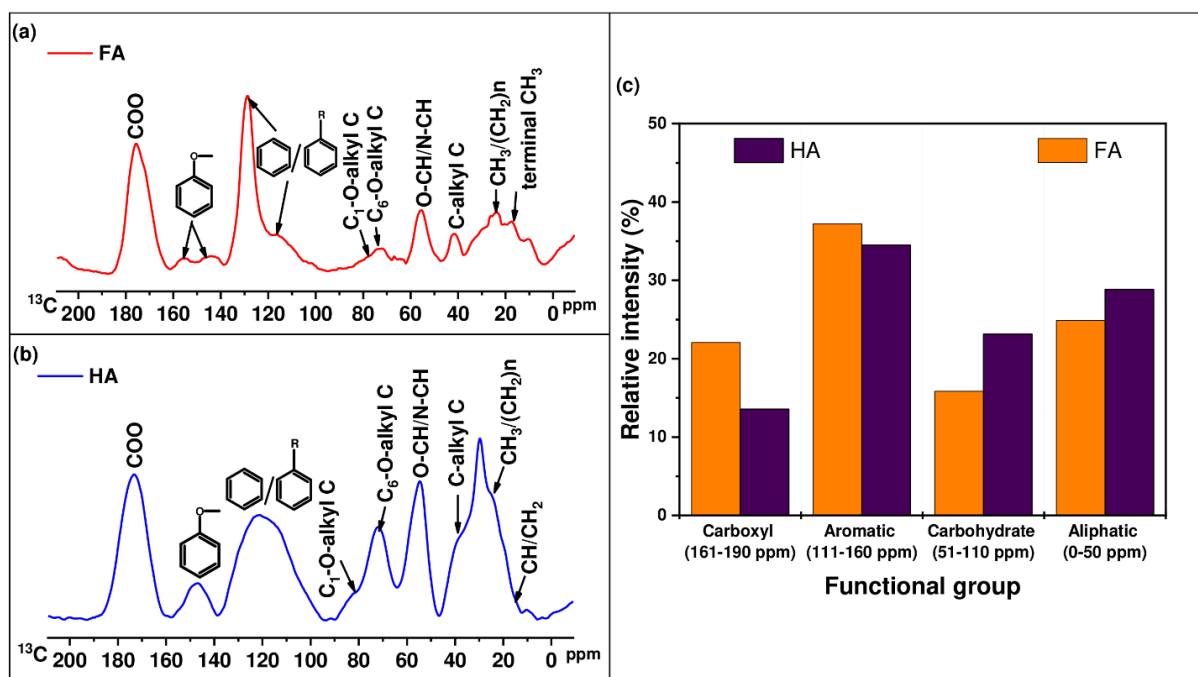


Figure 2.2  $^{13}\text{C}$ -Cross Polarization Magic-Angle-Spinning Nuclear Magnetic Resonance spectra of a) fulvic acid (FA) and b) humic acid (HA) isolated from fresh liquid swine manure dissolved organic carbon fraction with c) a comparison of relative intensities of carbon functionalities of carboxyl, aromatic, carbohydrate, and aliphatic region.

FA counterparts at 64.98 and 72.69 ppm, respectively. These carbohydrate carbon atoms are believed to arise from swine diet and indicate a lower degree of decomposition as the manure is less matured, collected from the manure well at the Glenlea Research Farm before reaching the wastewater lagoon.

The aromaticity of the swine manure humic substances was calculated by summing the integrated areas for unsubstituted or alkyl substituted aromatic rings (Ar/Ar-R) in 105-144 ppm region and oxygen substituted aromatic rings (Ar-O) in 144-155 ppm region. The most intense peak in the fulvic spectrum (31.63%) appeared at 129.26 ppm resonance frequency and was assigned to Ar/Ar-R carbons (Figure 2.2-a). The Ar/Ar-R peak of HA only accounted for 24.66% of the total spectrum, indicating its decreased contributions to the aromaticity, whereas a rather higher contribution from the Ar-O region of HA (10.77%) compared to FA (7.45%). The Ar/Ar-R in the aromatic region further contributes to the hydrophobicity in addition to the

Table 2.1 A summary of chemical shifts of major carbon functional groups obtained from  $^{13}\text{C}$ -Cross Polarization Magic-Angle-Spinning Nuclear Magnetic Resonance spectra of fresh liquid swine manure humic acid and fulvic acid and a comparison of their bulk chemical properties.

	Peak position (ppm)			
	Aliphatic (0-50 ppm)	Carbohydrate (51-110 ppm)	Aromatic (111-160 ppm)	Carboxyl (161-190 ppm)
Fulvic acid	41.04, 24.63	72.69, 64.98, 55.88	155.57, 145.8, 133.42, 129.26, 117.99	176.34, 173.97
Humic acid	39.07, 29.77, 25.81	82.78, 71.11, 54.30	142.12, 124.32	172.78
	Bulk chemical property (%)			
	Hydrophilicity	Hydrophobicity	Aliphaticity	Aromaticity
Fulvic acid	35.1	56.5	62.7	37.2
Humic acid	34.0	53.0	66.0	34.0

unoxidized C-alkyl carbons. Swine manure-derived HA and FA in the current study exhibit similar hydrophobicity among each other except for the slightly higher hydrophobicity of FA (Table 2.1). However, in general, the aromaticity index and hydrophobicity are higher for HAs than their FA equivalents because of their condensed, recalcitrant, and aromatized structures due to their higher humification degree. This observation is prominent for HAs derived from plant residues (Abakumov et al. 2015).

In the carboxylic range, humic substances exhibit a sharp, intense peak for carboxyl carbon (Figure 2.2a and b) with a notably higher relative intensity for FA (Table 2.1). This property contributes to the hydrophilic nature of the fulvic structure, which can increase the interaction between hydrophilic contaminants and migration in the aqueous phase. However, both humic substances exhibit similar hydrophilicity despite the variation in contributions from polar functional groups. Displaying both hydrophilic and hydrophobic properties suggests that fresh liquid swine manure humic substances are amphiphilic in nature, which facilitates the sorption of hydrophilic, hydrophobic, and amphiphilic contaminants.

#### 2.4.2.2 Fourier Transformed Infrared Spectroscopy

Infrared spectra of fresh liquid swine manure humic substances are illustrated in Figure 2.3. Absorption bands in IR spectra are divided into three major regions: high-frequency (3600-2600  $\text{cm}^{-1}$ ), mid-frequency (1800-1500  $\text{cm}^{-1}$ ), and low-frequency (1400-400  $\text{cm}^{-1}$ ) (Hansima et al. 2022). The first peak at the high-frequency region exhibits a narrow strong absorption band around 3410  $\text{cm}^{-1}$  (Figure 2.3a and d) for H-bonded O–H or N–H groups. Narrower adsorption bands in this area denote less aggregation and hence can interpret the less humified nature of these humic substances from fresh liquid swine manure (Machado et al. 2020). A series of three slight shoulders at 3080-3030  $\text{cm}^{-1}$  is for aromatic C–H stretching vibrations, whereas the peak at 2935  $\text{cm}^{-1}$  is for aliphatic stretching vibrations. A shoulder band at 2545  $\text{cm}^{-1}$  for H-bonded O–H of carboxyl groups in the FA spectrum designates an abundance of carboxyl functionality where there is no evidence for these vibrations in the HA spectrum.

Three distinct peaks in the mid-frequency region of FA are for the C=O stretch of COOH (1705  $\text{cm}^{-1}$ ), C=C stretch aromatic groups, H-bonded C=O stretch or NH<sub>2</sub> deformations (1635  $\text{cm}^{-1}$ ), and NH<sub>2</sub> deformation of amides (1504  $\text{cm}^{-1}$ ). The absence of the C=O stretch of COOH in the HA spectrum resulted in only two distinct peaks at 1636  $\text{cm}^{-1}$  for aromatics and 1510  $\text{cm}^{-1}$  for amides.

Infrared vibrations in the low-frequency region comprise absorption bands responsible for a single bond in the chemical structure. The peak at 1447  $\text{cm}^{-1}$  in HA and 1460  $\text{cm}^{-1}$  in FA and the peak cluster at 1420-1385  $\text{cm}^{-1}$  is assigned for aliphatic C–H deformations. The broad band around 1240  $\text{cm}^{-1}$  is a result of a combination of ester -C–O- in carbohydrates and -C–N- stretching vibrations and O–H bending vibrations. Peaks around 1160-1120  $\text{cm}^{-1}$  for aromatic ring bending, C–O or O–H stretching while the peaks around 1100-1020  $\text{cm}^{-1}$  for C–O

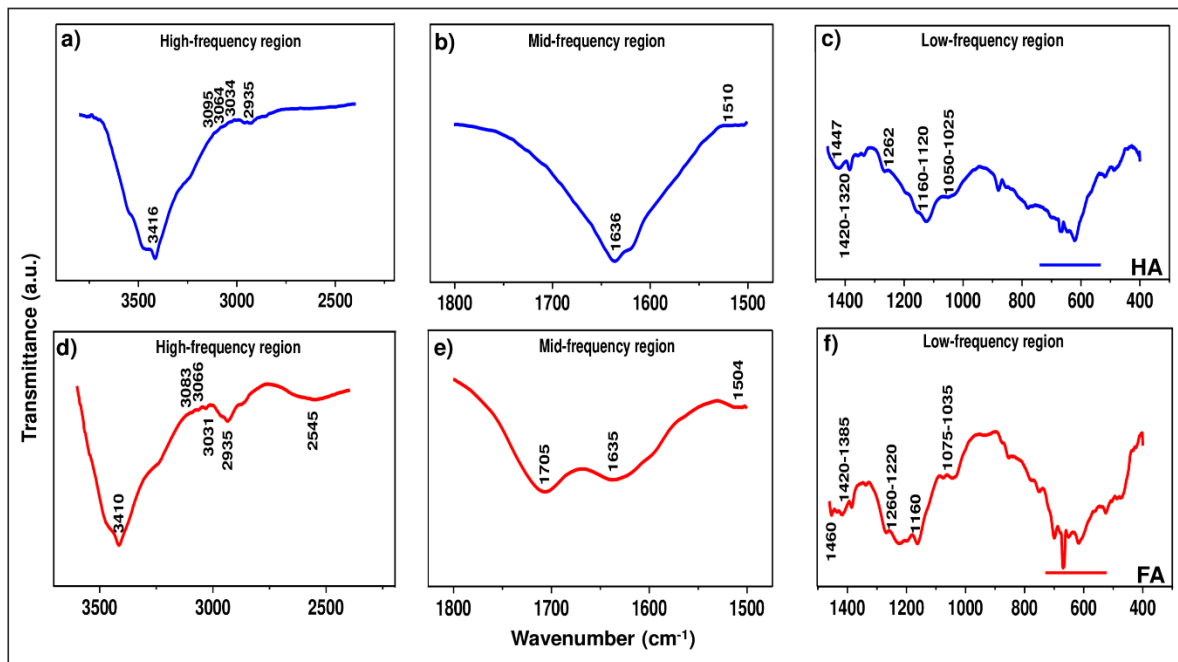


Figure 2.3 Splits of FTIR spectra obtained for fresh liquid swine manure humic substances. High-frequency region of a) humic acid (HA) and d) fulvic acid (FA) to capture O-H and C-H vibrations, mid-frequency region of b) HA and e) FA to capture C=C and C=O vibrations, and low-frequency region of c) HA and f) FA to capture single bond vibrations in their chemical structures.

stretching vibrations of carbohydrates. Infrared spectra were interpreted based on the work by Piccolo et al. (1992).

Infrared spectral environs observed for swine manure in the study are concomitant with the humic substances isolated and characterized from manure and sludge in previous studies (Gerasimowicz and Byler 1985; Piccolo et al. 1992). The presence of pronounce bands for polysaccharide (broad band around  $1240\text{ cm}^{-1}$  and the broad peak cluster in between  $1100\text{--}1020\text{ cm}^{-1}$ ) and peptide structural vibrations (sharp peak at  $1636\text{ cm}^{-1}$  of FA and broad band of HA) are indications of their lower decomposition levels.

### 2.4.2.3 X-ray Photoelectron Spectroscopy

X-ray Photoelectron Spectroscopy was used in the study to probe surface elemental composition and the chemical status of solid HA and FA derived from liquid swine manure.

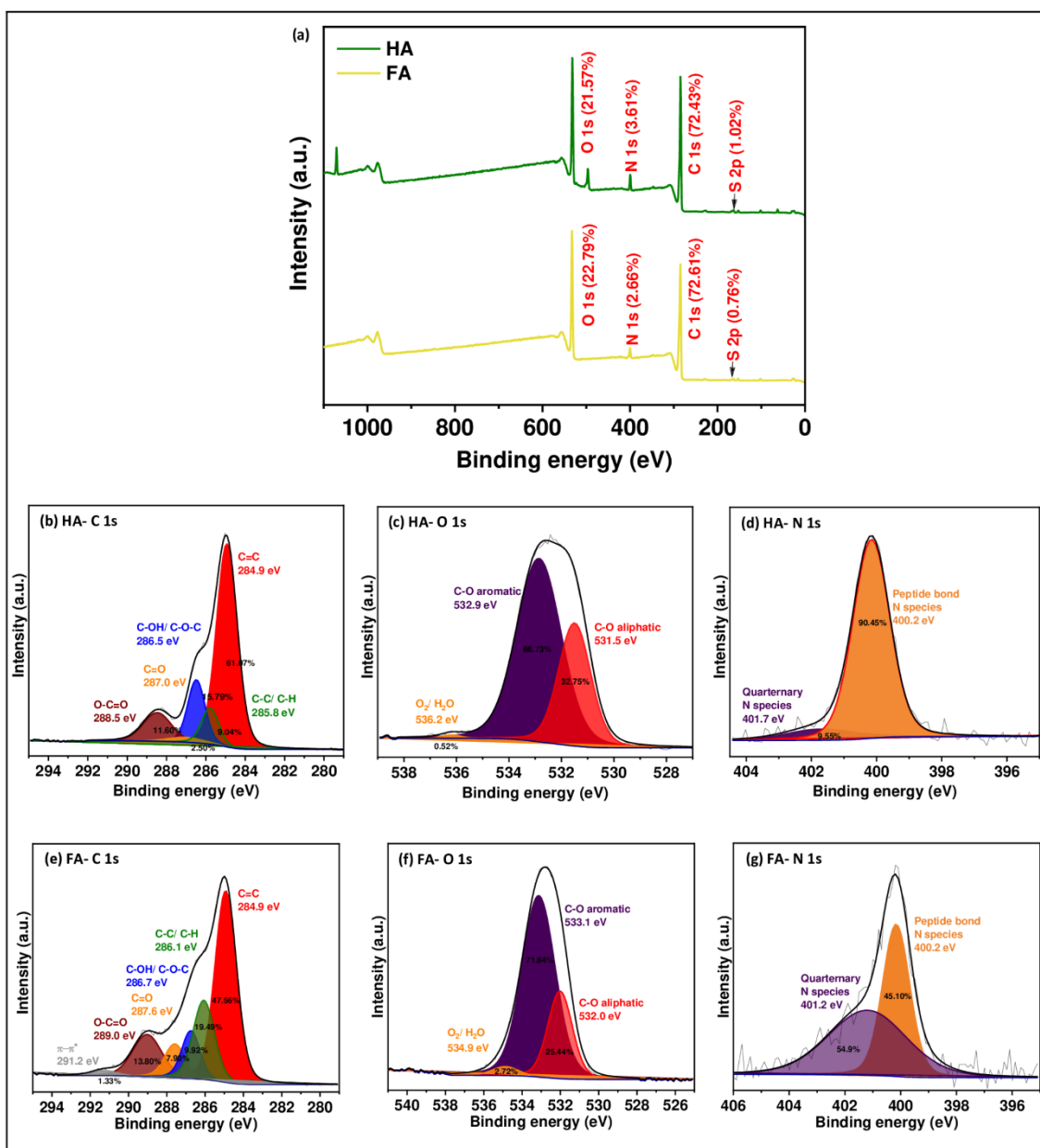


Figure 2.4 a) Survey X-ray Photoelectron spectra illustrating the surface elemental composition of humic acid (HA) and fulvic acid (FA) with high resolution Gaussian-Lorentzian fitted curves for C-1s status of b) HA and e) FA, O-1s status of c) HA and f) FA, and N-1s status of d) HA and g) FA.

Survey spectra illustrated in Figure 2.4a showed peaks for C, N, O, and S as major elements, and there is no notable difference for quantities among humic substances. The abundance of the elements followed the order, C-1s (72.43%) > O-1s (21.57%) > N-1s (3.61%) > S-2p (1.02%) for HA and similarly, C-1s (72.61%) > O-1s (22.79%) > N-1s (2.66%) > S-2p (0.76%) for FA.

There were five Gaussian-Lorentzian (G-L) fitted curves identified for humic C-1s status with the primary CC peak (PI) for unsubstituted aromatic SP<sup>2</sup> C=C or C-H appearing at 284.9 eV (Figure 2.4b). Next, CC peaks appear successively at 285.8 eV (PI + 0.9) for aliphatic SP<sup>3</sup> C-C or C-H, 286.5 eV (PI + 1.6) for alcohol C-OH or ether C-O-C, 287.0 eV (PI + 2.1) for ketonic C=O, and 288.5 eV (PI + 3.6) for carboxyl O-C=O. The peaks were assigned according to the binding energy added to the primary peak as defined by Smith et al. (2016). Fulvic C-1s status exhibits six G-L fitted curves starting with the PI peak for aromatic carbon at 284.9 eV (Figure 2.4e) followed by peaks for aliphatic carbon at 286.1 eV (PI + 1.0), alcohol carbon at 286.74 eV (PI + 1.8), ketone carbon at 287.6 eV (PI + 2.7), carboxyl carbon at 289.0 eV (PI + 4.1), and  $\pi \rightarrow \pi^*$  aromatic shake-up satellite at 291.3 eV, respectively. Even though they had similar surface carbon content, the carbon speciation was quite different. The percentage of HA carbon functional groups decreased in the order aromatic (61.07%) > alcohol/ether (15.79%) > carboxyl (13.80%) > aliphatic (9.04%) > ketone (2.50%) order. With some changes, FA carbon functionalities follow aromatic (47.56%) > aliphatic (19.47%) > carboxyl (11.60%) > alcohol/ether (9.92%) > ketone (7.90%) order. These observations vary from NMR data for carbon functionalities among the two substances, implying their surface chemical composition is substantially different from their bulk chemical composition to indicate heterogeneity (Monteil-Rivera et al. 2000). Inter-molecular interactions during aggregation caused different orientations that resulted in heterogeneity. For example, the higher unsubstituted aromatic carbon content observed in NMR of FA in compared to HA decreased in XPS data probably because inter-molecular  $\pi \rightarrow \pi$  interactions during the aggregation masked them from surface exposure. Similarly, the higher alkyl carbon content of HA might have been excluded from the surface during the aggregation process. In brief, the core of humic aggregates contains a comparatively higher amount of unsubstituted aliphatic chains, whereas the fulvic core contains a comparatively higher amount of unsubstituted/alkyl-substituted aromatic carbon.

Therefore, comparing NMR data with XPS data for solid humic substances is useful to deduce the orientation of functional groups during the aggregation. However, the secondary structures of humic substances in aqueous solutions are susceptible to dynamic changes and are discussed in detail in the latter sections.

The G-L fitting resulted in two major peaks for the O-1s region, with an insignificant peak assigned for oxygen in water for both humic substances (Figure 2.4-c and f). HA exhibits an aliphatic C–O peak at 531.5 eV where its abundance is 32.75%. The peak at 532.9 eV of HA is for aromatic oxygen, with a percent abundance of 66.73%. Aliphatic C–O of FA appeared at 532.0 eV with an abundance of 25.44%, while the aromatic C–O appeared at 533.1 eV with a notably higher percent of 71.84%. Results suggest oxygen-containing functionalities are likely to be surface-orientated for both the humic substances, which play the major role in their surface charge (Hansima et al. 2022).

High-resolution N-1s spectra of HA and FA resulted in an asymmetrical peak fitted into two components. The major contributor to the humic N-1s peak from peptide bond nitrogen (90.45%) species (i.e., amides) at 400.2 eV, where the rest 9.55% is from quaternary ammonium N species at 401.7 eV (Beamson and Briggs 1993). For fulvic, the amide-N peak at 400.2 eV is less intense (45.10%) than the ammonium-N peak at 401.2 eV (54.90%). The amide genesis mechanism includes the nucleophilic addition of aromatic amino acids (i.e., tyrosine and tryptophane in the current study) following elimination during the humification processes (Gulkowska et al. 2012). These amide groups are surface oriented and play a role in contaminant binding mechanisms by facilitating H-bonding.

#### **2.4.2.4 Particle size distribution and Zeta potential**

Secondary structures of humic substances in aqueous solution vary in size and shape. They are very dynamic and can be affected by concentration, pH, and ionic strength (Durge et al. 2016;

Klučáková 2018). Particle sizes of humic substances are quite often categorized into three different splits considering their mean diameter: smaller nanoparticles ( $< 0.1$  nm), sub-microparticles (500-12,000 nm), and larger macroparticles ( $> 1\mu\text{m}$ ) (Esfahani et al. 2015; Klučáková 2018). HA isolated from swine waste exhibits a mono-model particle size distribution in the sub-microparticle region for  $0.1 \text{ g L}^{-1}$  and  $0.01 \text{ g L}^{-1}$  concentrations (Figure 2.5a). FA also shows a mono-model distribution in the sub-microparticle region for its lowest concentration,  $0.01 \text{ g L}^{-1}$  (Figure 2.5b). Higher fulvic concentrations allowed particles to exhibit a poly-model distribution (in macro- and sub-micro- regions) for the  $0.1 \text{ g L}^{-1}$  solution, where the distribution extended to the higher end of macroparticles for  $1 \text{ g L}^{-1}$  solution.  $1 \text{ g L}^{-1}$  of HA also falls in a poly-model distribution where their particles lie in macro- and sub-micro-regions. Overall, FA exhibited larger aggregates, particularly for medium to higher concentrations than for humic ones. This observation is contradictory to traditional definitions of humic substances, where HAs have larger aggregates than FAs (Chen et al. 2017). However, mean particle sizes observed in previous studies suggest FAs formed larger aggregates as they can form aggregates in aqueous solutions due to inter-molecular interactions with active functional sites (Klučáková 2018). We used alkaline solutions to overcome the difficulties in the dissolution of HA in aqueous solutions. Alkaline solutions typically suppress aggregation by expanding the coiled structures by deprotonating acid functional groups. This could be another factor explaining the smaller aggregate sizes observed for HA. Besides the aggregate size in aqueous solutions, solid phase SEM images of humic substances (Figure 2.5c and e) further revealed substantially larger aggregates with rigid cuboid shape fulvic structure versus small spherical nanoparticles/sphere colloids for humic structure. The increased surface area of HA due to the smaller size can facilitate a higher number of sorption sites. However, the spherical and cuboidal structures of HA and FA aggregates in the current study were transformed into a linear/elongated form as a result of the pH of the aqueous solutions during

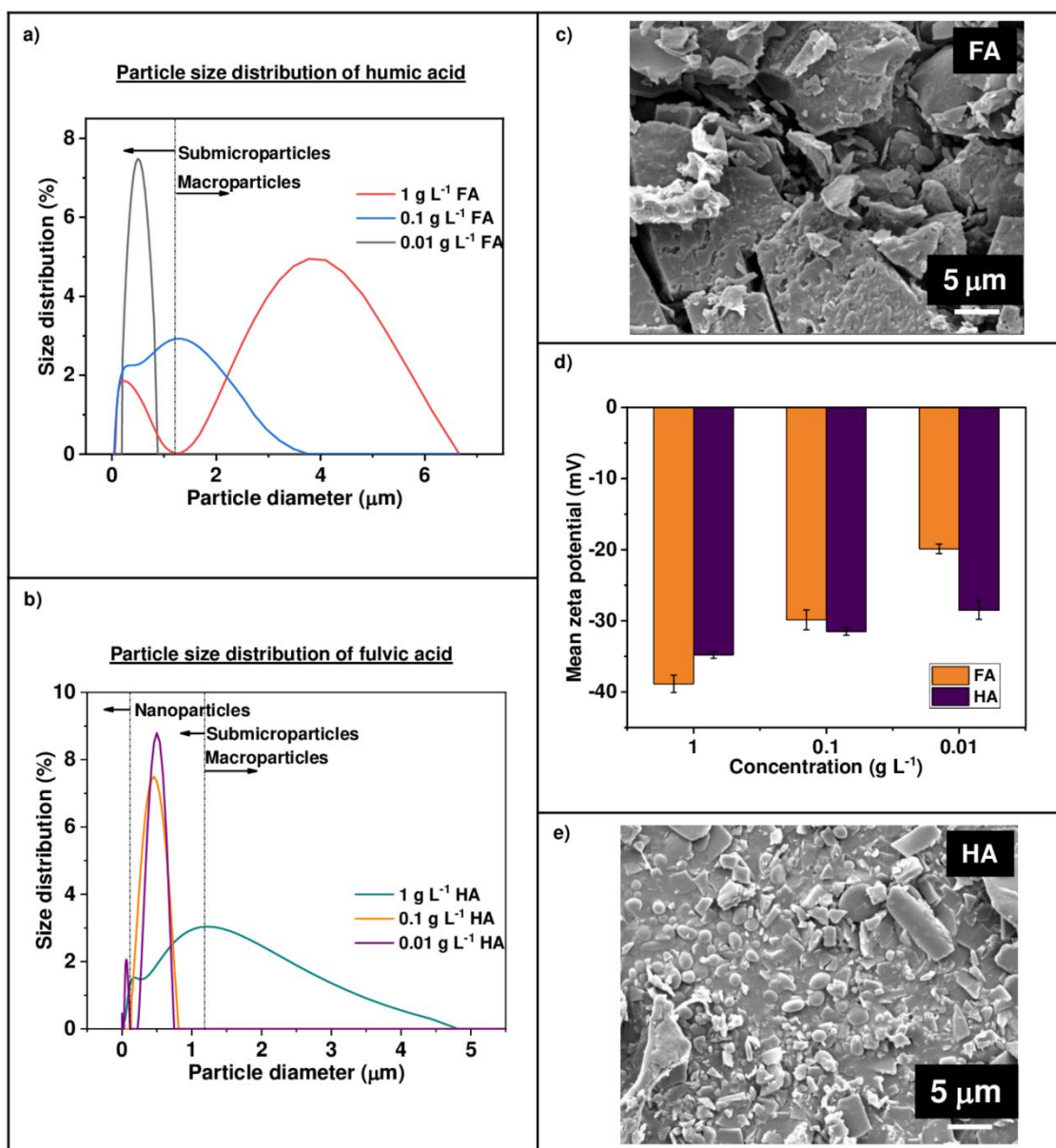


Figure 2.5 Variation of intensity weighted particle size distribution with the concentration of a) humic acid (HA) dissolved in 0.01 mg L<sup>-1</sup> NaOH, b) fulvic acid (FA) dissolved in water. Solid phase Scanning Electron Microscopic surface imaging to illustrate c) the rigid-cuboid structure of fulvic acid and e) spherical humic acid colloids. d) A comparison of mean zeta potentials of humic substances with the concentration to indicate colloidal stability.

the sorption process. This was evident from the SEM images of organic matter sorbed clay surfaces (Figure 2.7) and previous studies by Joo and Antal (1998) and Peng et al. (2005).

Determination of the zeta potential of humic substances is useful to deduce the colloidal stability and to understand their dynamics in aqueous environments. These substances periodically undergo dynamic changes in aqueous solutions. Aggregation, precipitation, and

resolubilization are examples (Klučáková 2018). Greater negative zeta potentials ( $> -30$  mV) observed for fresh liquid swine manure HA compared to FA indicate their stability in aqueous solutions, particularly at moderate to low ( $0.1-0.01$  g L<sup>-1</sup>) concentrations (Figure 2.5d) (Klučáková 2018). The reason behind the colloidal stability of HA is due to its lower amount of carboxylic functional groups. FA is vulnerable to change dynamically because of its higher dissociation of carboxylic constituents, resulting in less stable colloids. Understanding the colloidal fraction in the current study was applied to predict the stability of HA or FA-associated environmental contaminants and their environmental fate, as summarized in section 2.6.

#### **2.4.3 Sorption mechanisms from Freundlich parameters combined with the physicochemical characteristics of the dissolved organic carbon fraction and characteristics of mineral bentonite**

We used isotherm parameters to probe partial sorption mechanisms and ultimately to elucidate the SMX sorption mechanisms onto smectite clays in the presence of fresh liquid swine manure DOC fraction. Partial sorption mechanisms will aid in understanding all probable interactions for a system containing fresh liquid swine manure DOC fraction (i.e., a combination of FA, HA, aromatic amino acids, and multivalent metal ions), smectite clay, and SMX residues. Adsorption was well-fitted with the non-linear Freundlich model except for the SMX sorption onto FA. Empirical constants in Freundlich isotherm describe the sorption of substances on heterogeneous surfaces where the value of the Freundlich constant  $K_f$  is the partitioning constant while linearity constant  $n$  represents the sorption strength (Walter 1998). As presented in Table 2.2, the  $K_f$  is not significantly varied among the adsorbents as they have overlapped confidence limits.

Table 2.2 Non-linear Freundlich parameters  $K_f$  and  $n$  for sulfamethoxazole sorption for 20, 40, 60, and 100  $\mu\text{g L}^{-1}$  levels of concentration onto bentonite clay in the presence of dissolved organic carbon (DOC) fraction, fulvic acid (FA), and humic acid (HA) derived from fresh liquid swine manure.

	$K_f$ ( $\mu\text{g L}^{-1}$ ) <sup>1-1/n</sup>	Std. Err.	95% CL	$n$	Std. Err.	95% CL	Model <i>p</i> -value
<u>Sorption study 1</u>							
Bentonite	0.576	0.531	(- 0.607) - 1.759	1.010	0.203	0.559 - 1.461	< 0.0001
DOC	0.168	0.136	(- 0.135) - 0.471	1.240	0.176	0.848 - 1.632	< 0.0001
Bentonite + DOC	0.586	0.092	0.382 - 0.790	1.079	0.034	1.003 - 1.156	< 0.0001
<u>Sorption study 2</u>							
Bentonite	1.275	1.093	(- 1.160) - 3.709	0.850	0.186	0.435 - 1.265	< 0.0001
FA	-	-	-	-	-	-	0.6204
Bentonite + FA	0.422	0.277	(- 0.195) - 1.039	1.109	0.140	0.798 - 1.420	< 0.0001
<u>Sorption study 3</u>							
Bentonite	0.535	0.332	(- 0.205) - 1.274	1.065	0.141	0.750- 1.379	< 0.0001
HA	0.634	0.957	(- 1.500) - 2.767	0.731	0.354	(- 0.057) - 1.518	0.0009
Bentonite + HA	0.427	0.121	0.157 - 0.697	1.140	0.064	0.997 - 1.283	< 0.0001

$K_f$  - Freundlich Partition constant  
 $n$  - Freundlich Linearity constant  
 CL - Confidence limits

### 2.4.3.1 Mechanism I - Sorption of sulfamethoxazole to bentonite

The permanent negative charge of smectite clays results from isomorphic substitution. Also, broken Si-O-Si(Al) bonds in tetrahedral or octahedral sheets provide reactive Lewis/negative surface sites. Protonation or deprotonation of surface-OH sites cause variable charge upon the solution pH. Theoretically, the sorption of anionic [SMX]<sup>-</sup> species at environmentally relevant pH conditions (pH 6.5-9) is restricted by electrostatic repulsion facilitated by the permanent negative charge (De Mastro et al. 2022; Hu et al. 2019). However, in the contrary, the sorption data in the current study suggest SMX sorption onto bentonite clay; hence, a variable charge-driven sorption mechanism is proposed (Table 2.2). Literature suggests the protonation of surface-OH groups results in positive bentonite clay surface charge when the solution pH < 7.5 (Wieland et al. 1994). The current sorption study was conducted at pH 7. Hence, the positive variable charge is viable. Thus, the sorption of SMX onto smectite clays is possible via Lewis acid-base interactions between deprotonated -NH- sites of [SMX]<sup>-</sup> and protonated surface -OH<sub>2</sub><sup>+</sup> sites at ~ pH 7. Further, formation of inner- and outer-sphere complexes facilitated by water or divalent cation bridging between the surface-OH sites and the deprotonated -NH- sites of [SMX]<sup>-</sup>, van der Waals  $\pi$ -interactions between basal oxygen plane of the outer/surface tetrahedron layer and aminobenzene portion of the antibiotic, intercalation via broken edges are other possible mechanisms (Adams 1987; De Mastro et al. 2022; Hu et al. 2019). Freundlich model is used to explain the adsorption of substances on heterogeneous surfaces (Sposito 1980). Surface heterogeneity of the bentonite on SMX adsorption may have resulted from the uneven distribution of the active sites on the surface. The linearity constant  $n$  exhibits values closer to 1, indicating the sorption is linear and increasing with the SMX concentration. However, the extent of the linearity is probably up to a certain level

of SMX concentrations; higher concentrations beyond the experimental conditions could reach a plateau.

#### **2.4.3.2 Mechanism II - Sorption of sulfamethoxazole to organic matter**

SMX adsorption depends on bulk physicochemical properties of the organic matter (distribution of functional groups, aromaticity, aliphaticity, hydrophilicity, hydrophobicity, average molecular size, the surface charge) and surface chemical properties like molecular conformation/orientation of functional groups in aqueous solutions (Murphy et al. 1990). Sorption of SMX onto organic matter adsorbents was not the same as we noted differences in isotherm data for DOC, HA, and FA. We observed well-fitted Freundlich sorption for DOC ( $p < 0.0001$ ) and HA ( $p < 0.0009$ ) but not for FA (Table 2.2). Characteristics of the swine manure humic substances suggested quite similar aromaticity, aliphaticity, hydrophobicity, and hydrophilicity, but variations among the percentage of functional groups, particle size, zeta potential, and the orientation of functional groups in secondary structures might have resulted in different sorption behaviours.

SMX sorption on FA did not follow the Freundlich isotherm, and that can be because of the instability of formed FA-SMX complexes. FAs are vulnerable to changing their colloidal structure in aqueous solutions as they contain more carboxylic functional groups. As discussed, less negative values for the zeta potential for FA also suggest the instability of fulvic colloids in aqueous solutions compared to humic colloids (section 2.4.2.4). Therefore, SMX bound to FA can easily be desorbed (i.e., extractable residue) during the initial filtering and the rest of the solid phase extraction process and can be quantified as un-sorbed. XPS data suggested (section 2.4.2.3) more surface-oriented O-containing aromatic groups for FA, which can act as a  $\pi$ -electron donor to electron deficit aminobenzene ring (due to sulfano group) in SMX to facilitate  $\pi$ - $\pi$  electron donor-

accepter (EDA) interactions. Direct H-bonding or water bridging mechanisms between phenolic-OH and  $-\bar{N}H-$  in SMX is another possible binding mechanism (Li et al. 2018). A reasonably higher percent of surface-oriented C-alkyl chains can also contribute to the SMX complexation mechanisms via alkyl- $\pi$  interactions. We used fluorescence spectroscopy of the DOC fraction obtained from equilibrated batch sorption solutions to capture the changes to the fluorophore functional groups in humic substances during the antimicrobial complexation. 3D-EEM spectra in Figure 2.6 suggest the formation of FA-SMX fluorophore-quencher complexes as indicated by reduced fluorophore intensity in the fulvic-like region at  $\lambda_{ex}= 200-250$  nm,  $\lambda_{em}= 380-600$  nm. More importantly, the observation was only for the fulvic-like region, not for the humic-like region, indicating no involvement of fluorophore functional groups for SMX binding mechanisms with swine manure HA. Previous studies were keen on the importance of carboxyl groups in antimicrobial complexation mechanisms (Ou et al. 2007; Ou et al. 2009; Wang et al. 2017). Fluorescence of humic substances quenched by  $\pi$ -stacked complexation is also reported (Wang et al. 2018). The current study revealed phenolic fluorophores in FA over carboxyl fluorophores played the dominant role in complexation mechanisms due to their high surface abundance (Figure 2.10 in section 2.5). Carboxyl groups oriented in the core of fulvic colloids seem out of reach by SMX molecules due to the steric hindrance. We highlight the importance of knowing the orientation of functional groups/molecular conformation of humic substances in aqueous environments to probe exact contaminant sorption mechanisms.

SMX sorption to HA shows an  $n < 1$  for the linearity constant. When  $n < 1$ , there is enhanced sorption due to increased adsorption sites by the first layer of adsorbate molecules. The observation was reported majorly among hydrophobic substances (Giles et al. 1974). Despite the hydrophilicity, monolayer SMX can facilitate hydrophobic interactions via the aminobenzene ring.

We noted from the fluorescence data that there is no involvement of fluorophores, i.e., phenolic groups, for the HA-SMX complexation mechanism. XPS data suggest a significantly higher amount of surface amide groups in the HA structure than FA to facilitate H-bonding with SMX (Li et al. 2021). Hydrophobic  $\pi$ - $\pi$  interactions between surface-oriented un-substituted aromatic portions and the benzene ring of SMX can also be possible. The stable electronic status of HA in an aqueous solution, as indicated by the zeta potential, allowed stable HA-SMX complexes. Hence, desorption of SMX during the SPE procedure is unlikely to occur, and they can be considered non-extractable residues (Andriamalala et al. 2018). The differences observed in the stability of HA-SMX and FA-SMX complexes affect the environmental fate of the antimicrobial.

An  $n > 1$  value for the linearity constant indicates the SMX sorption to DOC is non-linear, where sorption increases sharply with the SMX concentration, even for the elevated levels. Characterization by HPSEC and 3D-EEM spectroscopy revealed the presence of HA, FA, and aromatic amino acids in the swine manure DOC fraction (Figure 2.1). The combined effects of these constituents can provide an adequate amount of complexation sites for sulfamethoxazole, even for elevated concentrations. Moreover, the multivalent cations ( $M^{2+}/M^{3+}$ ) in the DOC fraction can participate in cation-bridging mechanisms to facilitate  $OM-M^{2+/3+}-SMX$  complexation. As discussed earlier and revealed by 3D-EEM spectra, SMX binds on FA via fluorescence quencher mechanisms and HA via non-fluorescence quencher mechanisms. The binding of SMX to aromatic amino acids is out of scope in the current study. However, we can see a significant intercalation in the X-ray Diffraction patterns for the DOC treatment (Table 2.4), indicating organic cations formed by the complexation of metal ions and amino acids could reach the bentonite interlayer; further discussions are in section 2.4.3.5. As mentioned before, HA is the dominant contributor in

the fresh liquid swine manure DOC to establish stable HA-SMX complexes, considering the instability of FA-SMX in aqueous solutions.

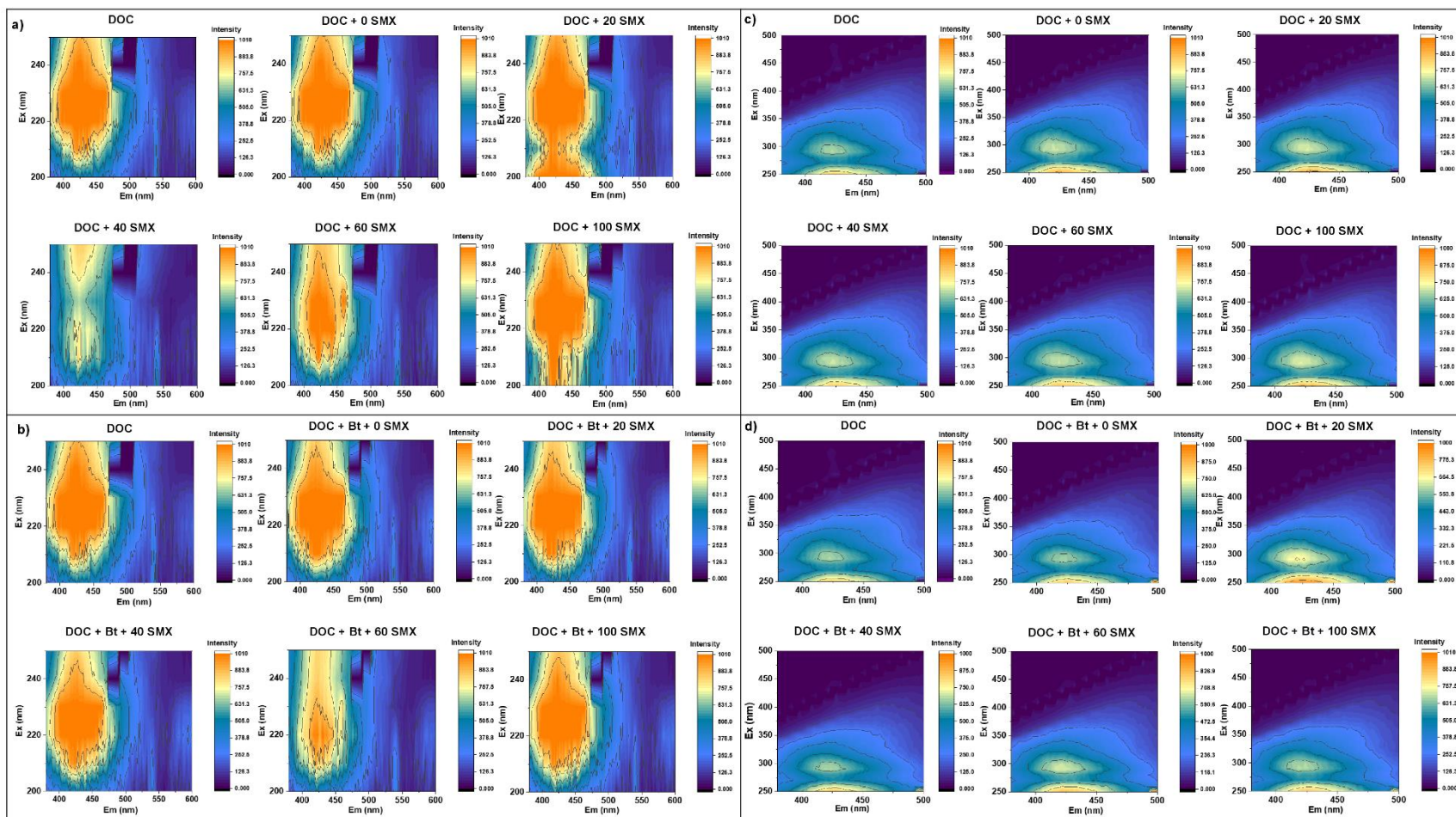


Figure 2.6a 3D-Excitation Emission spectra of fulvic acid (FA) region in a) and b) and humic acid (HA) region in c) and d) to visualize fluorescence reduction when sulfamethoxazole (SMX) concentration varied from 0-100  $\mu\text{g L}^{-1}$  for the treatments obtained from equilibrated batch sorption solutions. Treatments consisted of fresh liquid swine manure dissolved organic carbon (DOC) fraction with and without bentonite (Bt) to capture fulvic-like fluorescence quenching by FA-SMX complexes and non-fluorescence quencher HA-SMX complexes in the aqueous phase.

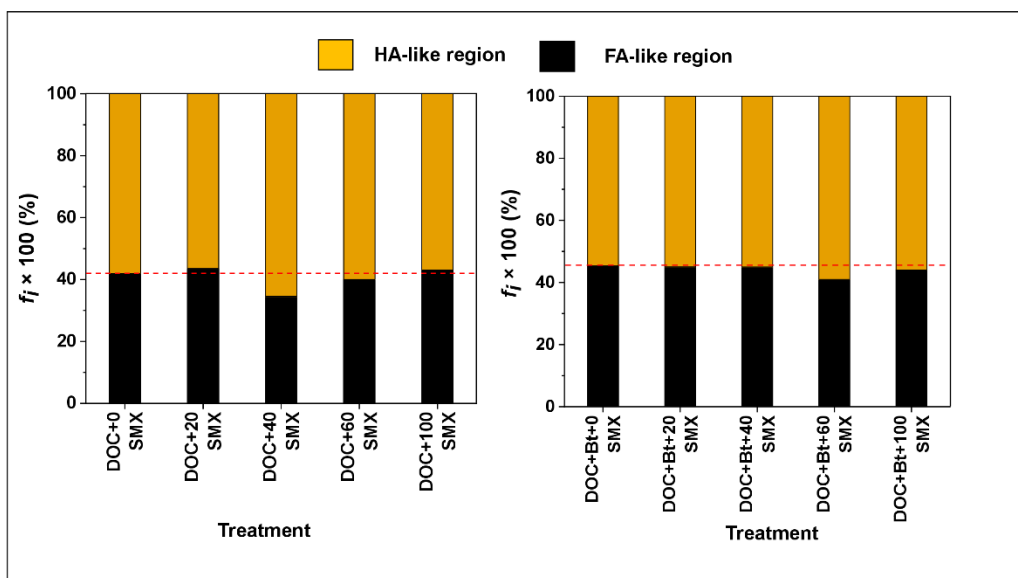
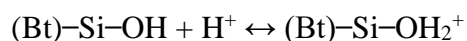


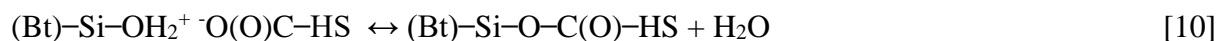
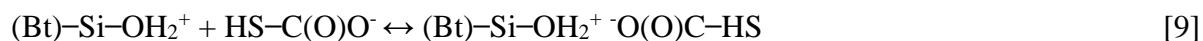
Figure 2.6b Cont. Percent fluorescence intensities calculated by 2D volume integrate ( $f_i$  in %) for humic acid (HA)-like and fulvic acid (FA)-like regions.

### 2.4.3.3 Mechanism III - Formation of organic matter-bound bentonite

Organic matter bound to mineral surfaces is known to enhance the complexation of contaminants because of the increased quantity of adsorption sites and the active surface area (Murphy and Zachara 1995). The binding of humic substances on 2:1 mineral surfaces is credited to be via a ligand exchange mechanism and depends on the solution pH (Murphy et al. 1990; Zhang et al. 2012). Similarly, sorption of humic substances on bentonite surface at  $\text{pH}_{\text{PZC}} < 7.5$  (Kim 2003) follows (1) protonation of the surface-OH groups (Eq. 8), (2) outer-sphere complexation of humic substances (HS) via carboxylate groups (Eq. 9), and (3) ligand exchange reaction to yield inner-sphere mineral-HS complexes (Eq. 10). When the pH of the solution  $< 7.5$ , electrostatic repulsion from the permanent negative sites in the bentonite is compensated by the positive charge gained from the pH-dependent variable charge.



[8]



Mineral-HS complexes resulting in step 3 (Eq. 10) allow the retardation of intrinsic hydrophilic properties of the mineral surface to become more hydrophobic. Infrared spectra of organic matter sorbed bentonite surfaces were used to capture the alterations that occurred to the Si-O vibrations and O-H vibrations during the complexation. Vibrational peaks of bentonite were assigned by referring to the work by Reddy et al. 2017. In Figure 2.7, we observed a weakening in the transmittance/intensity to the maximum adsorption peak of the bentonite IR spectrum at  $1056 \text{ cm}^{-1}$  for Si-O in-plane stretching vibration of  $\text{SiO}_4$  tetrahedrons indicating the organic matter coating covering the mineral surface for HA and DOC. A marked reduction in the  $\text{SiO}_4$  peak and the appearance of organic matter features in the spectra for DOC indicate their intense accumulation via cation bridging by the multivalent metal ions (Zhang et al. 2012). A reduction in the intensity is observed for the sharp IR peak at  $3623 \text{ cm}^{-1}$  and the following broadband at  $3433 \text{ cm}^{-1}$  for structural-OH stretching and water absorbed in the mineral for HA complexation. A similar observation was for the sharp peak at  $1630 \text{ cm}^{-1}$  for asymmetric O-H stretching vibrations. This implies some of the mineral (Bt)-Si-OH surfaces had been converted to inner-sphere (Bt)-Si-O-C(O)-HS complexes formed from the ligand exchange reactions by HA. However, no observed structural changes in the IR spectrum indicate a poor sorption of FA. Literature suggests that molecules with more aliphatic structures preferentially adsorb onto 2:1 minerals (Weishaar et al. 2003). The percent aliphaticity of the HA is higher than the FA; however, they are mostly core-oriented in HA secondary structures. Fractionation of dissolved humic substances on the mineral surfaces tends to expose core-oriented alkyl functional groups and might have facilitated the sorption, similar to the study by Zhang et al. 2012. According to Murphy et al. (1990), the strength

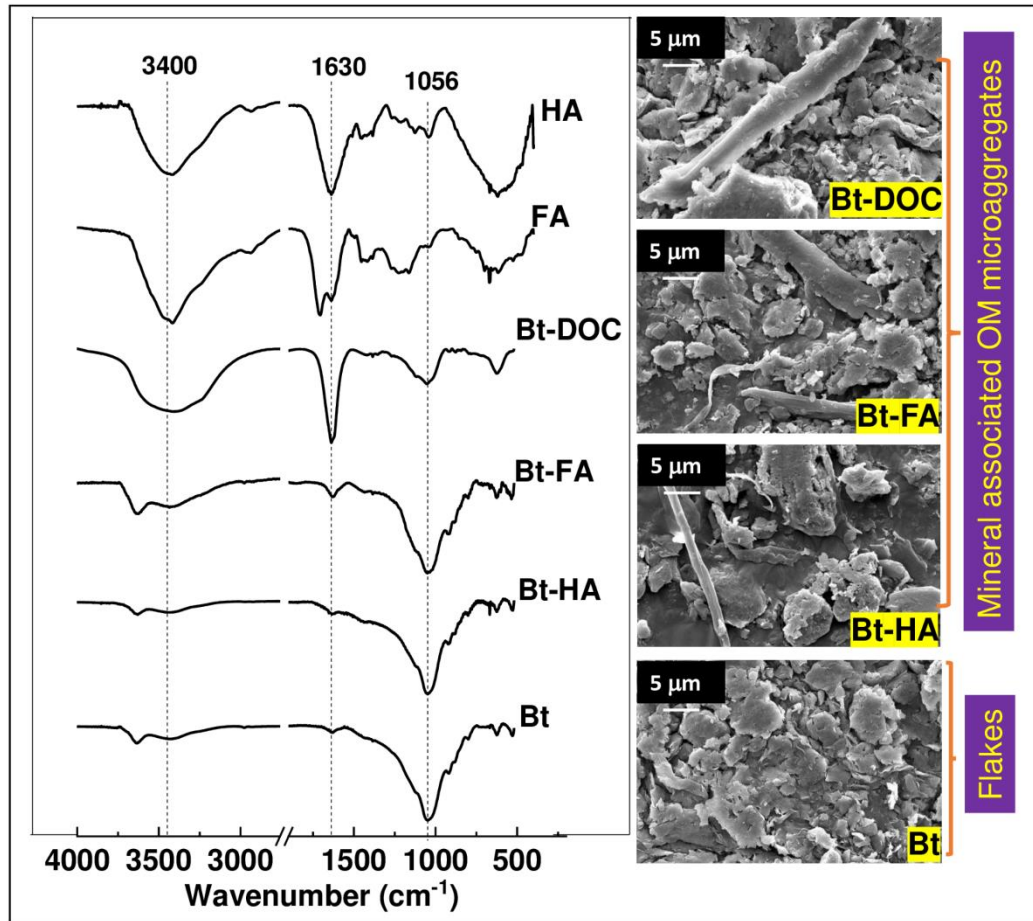


Figure 2.7 A comparison of Fourier-Transformed Infrared spectra of potassium saturate bentonite (Bt), humic acid (HA) and fulvic acid (FA), the organic matter (OM) sorbed bentonite to understand the OM-mineral complexation mechanisms. Bt-DOC is fresh liquid swine manure dissolved organic carbon fraction as the OM; Bt-FA is fulvic acid as the OM; and Bt-HA is humic acid as the OM. Scanning Electron Microscopic images of the pure mineral and OM-mineral surfaces to visualize the microstructural changes that arose from the OM complexation.

of organic matter-mineral complexes is proportional to the hydrophobicity of the humic substance. As we noted from the NMR spectroscopy (Table 2.1), both the humic substances had reasonably similar hydrophobicities, whereas different orientations of the hydrophobic functional groups (i.e., un-substituted aliphatic and aromatic groups) in the colloidal surfaces. Therefore, the strength of the organic matter complexes for the current study is hard to deduce, even though the rather strong sorption of HA was suggested from IR data.

Scanning Electron Microscopic images were used to visualize the microstructure of non-sorbed and organic matter-sorbed mineral surfaces. They suggest the formation of micro aggregates due to organic matter complexation with the mineral where the flaky layered surface structure of pure bentonite has been disturbed (Figure 2.7). Enhanced hydrophobicity might have facilitated inter-molecular interactions for the aggregation process.

#### **2.4.3.4 Mechanism IV - Sorption of sulfamethoxazole to organic matter-bound bentonite**

Previous studies suggested combining contributions from mineral surfaces plus organic matter partition to decide the overall contaminant sorption (Karickhoff 1984; McCarty et al. 1981). Thus, the number of active sites could double for organo-mineral complexes compared to organic matter colloids in aqueous solutions. Hence, increased SMX sorption for bentonite + DOC/HA/FA treatments was expected. Non-linear Freundlich isotherm provided a good fit to the sorption data, except FA. However, there were no significant differences between the  $K_f$  values obtained for SMX sorption to pure bentonite and organic matter-bound bentonite. Further, there is no significant strength difference for the adsorption, as there is no significant difference between  $n$  values (Table 2.2). Infrared data and SEM images suggested organic matter covered most of the bentonite surfaces, with no evidence of uncoated mineral surfaces. The flake-like platy structure of pure K sat. Bt turned into a more porous structure because of micro aggregation resulting from organic matter coating (Figure 2.7) (Gu et al. 2011). Organic matter association might have overridden the SMX-bentonite interactions that occurred when there was no organic matter association, resulting in similar net sorption. Moreover, SMX-bound organic matter in the aqueous phase followed similar fluorophore quencher complexation mechanisms with non-sorbed FA and non-fluorophore quencher complexation mechanisms with non-sorbed HA as revealed from the 3D-EEM data for bentonite + DOC + SMX treatments (Figures 2.6a-b,d and 2.6b). The amount of

SMX adsorbed on organo-mineral complexes is affected by the affinity of SMX with organic matter on the mineral surface, the strength of organic matter and mineral interactions, and the affinity to non-sorbed organic matter in the aqueous phase, resulting in different affinities with respect to the type of the organic matter. In addition to the bulk properties, the structure of the sorbed humic substances on the mineral surface can also affect the sorption (Murphy et al. 1990). The number of active sorption sites, ionization degree, colloidal conformation in aqueous solutions, and distribution of surface-OH groups in mineral surface affect the structure and orientation of sorbed organic matter.

The sorption of SMX onto these organic matter-bound mineral complexes exhibits a heterogeneous non-linear behaviour. The non-linear behaviour of the sorption observed for  $n$  values  $> 1$  indicates that the dominant interaction between SMX and organic matter-bound minerals is hydrophobic interaction. Humic-bound mineral surfaces contain more surface-oriented un-substituted aromatic rings that can facilitate hydrophobic interactions with the aminobenzene portion of SMX. On the other hand, surface-oriented phenolic groups in fulvic-bound mineral surfaces can facilitate  $\pi$ - $\pi$  electron donor-acceptor interactions, where they act as the  $\pi$ -electron donor while slightly positive (due to sulfano group) aminobenzene rings of SMX act as the  $\pi$ -electron acceptor. The strength and the abundance of these mechanisms seem similar for both humic substances as they exhibit closer  $n$  and  $K_f$  values (Table 2.2).

#### **2.4.3.5 Surface and interlayer sulfamethoxazole sorption onto mineral bentonite**

**Adsorption of sulfamethoxazole on bentonite surface via Infrared spectroscopy:** Five Infrared peaks in the bentonite spectra were chosen to capture spectral changes (i.e., peak position) due to interactions between SMX and bentonite with and without the organic matter component

Table 2.3 Statistical significance from Analysis of Variance (ANOVA) for the changes occurred to the Infrared peak position of bentonite (Bt) Si-O vibrations when changing the sulfamethoxazole (SMX) concentration as 0, 20, 40, 60, and 100  $\mu\text{g L}^{-1}$  in the presence of fresh liquid swine manure derived organic matter (dissolved organic carbon fraction (DOC)/fulvic acid (FA)/humic acid (HA)) obtained from equilibrated sorption solids.

	<u>P value for the peak position</u>		
	DOC	FA	HA
<i>Si-O in-plane stretching at 1050 <math>\text{cm}^{-1}</math></i>			
Organic matter (0 and 25 $\text{mg L}^{-1}$ )	<b>0.033</b>	0.425	<b>0.064</b>
SMX level	0.374	0.280	0.263
Block	0.214	<b>&lt; 0.001</b>	0.200
Organic matter $\times$ SMX level	0.626	0.987	0.100
<i>Si-O in-plane stretching at 1119 <math>\text{cm}^{-1}</math></i>			
Organic matter (0 and 25 $\text{mg L}^{-1}$ )	<b>0.027</b>	<b>0.001</b>	<b>0.087</b>
SMX level	0.172	<b>0.0003</b>	0.442
Block	<b>0.001</b>	<b>&lt; 0.001</b>	<b>0.029</b>
Organic matter $\times$ SMX level	0.257	<b>0.006</b>	0.732
<i>Overtone (<math>\nu_4</math>) of <math>\text{SiO}_4</math> vibration at 618 <math>\text{cm}^{-1}</math></i>			
Organic matter (0 and 25 $\text{mg L}^{-1}$ )	0.944	0.479	0.929
SMX level	0.528	0.416	0.928
Block	<b>0.001</b>	<b>0.022</b>	0.278
Organic matter $\times$ SMX level	0.625	0.465	0.915
<i>Combination band of <math>\text{SiO}_4</math> vibrations at 2850 <math>\text{cm}^{-1}</math></i>			
Organic matter (0 and 25 $\text{mg L}^{-1}$ )	0.658	0.734	0.191
SMX level	0.355	0.949	0.636
Block	<b>&lt; 0.001</b>	0.177	0.315
Organic matter $\times$ SMX level	0.787	0.997	0.139
<i>Combination band of <math>\text{SiO}_4</math> vibrations 2925 <math>\text{cm}^{-1}</math></i>			
Organic matter (0 and 25 $\text{mg L}^{-1}$ )	0.141	0.678	<b>0.046</b>
SMX level	0.344	0.550	0.717
Block	<b>0.027</b>	0.560	<b>0.086</b>
Organic matter $\times$ SMX level	0.397	0.715	0.754

(DOC/FA/HA). Changes in peak position were analyzed by ANOVA. The significance of the results is summarized in Table 2.3, and the peak positions extracted from vibrational spectra are

summarized in Table A-2. We hypothesized chemical bonds in silicon tetrahedrons are susceptible to changing their strengths as a result of inter-molecular interactions with sorbent molecules. Main adsorption peak for Si–O in-plane stretching at  $1050\text{ cm}^{-1}$  and shoulder peak at  $1119\text{ cm}^{-1}$  significantly red-shifted ( $p < 0.05$ ) when SMX sorption to DOC bound mineral surfaces indicating inter-molecular interactions arose between DOC and bentonite following the mechanisms explained earlier (Eq. 8-10). Red-shift can be explained as the reduction occurred to the strength of the Si–O bond in  $(\text{Bt})\text{--Si--OH}_2^+$  after the ligand exchange mechanism to result in covalent  $(\text{Bt})\text{--Si--O--C(O)--HS}$  complexes. These peaks were slightly red-shifted ( $p < 0.1$ ) for humic acid-binding. Significant red-shift occurred to the peak at  $1119\text{ cm}^{-1}$  for fulvic acid binding ( $p < 0.01$ ). However, there is no significant change in the peak position with increasing the level of SMX, implying no direct interactions between SMX and mineral surface due to the organic matter coating. Other peaks in the Si–O domain (i.e., overtones and combined bands) exhibit no significant peak shifts, probably because of the less abundance as indicated by low intensities in the vibrational spectra. There is no significant interaction between with or without organic matter and SMX concentration. This observation indicates the presence of enough sorption sites in both  $(\text{Bt})\text{--Si--OH}_2^+$  and  $(\text{Bt})\text{--Si--O--C(O)--HS}$ , allowing the adsorption of SMX at high concentrations. If the sorption at higher concentrations was facilitated by the adsorbed SMX in the first layer, the electronic status of the Si–O bond would have changed. Overall, Infrared data suggests that organic matter binding hindered the direct SMX interactions with the mineral surfaces, whereas mineral surfaces and organic matter-bound mineral surfaces provide sufficient adsorption sites for the entire range of SMX concentrations considered in the current study.

**Interlayer adsorption via Powder X-ray Diffraction:** Simultaneous changes occurring to the shape of the basal reflection peak ( $d_{001}$  plane) in the PXRD pattern of bentonite have been used to

probe interlayer sorption (Ou et al. 2009). Hence, the full width at half maximum (FWHM) of the  $d_{001}$  peak (Table A-3) was used in the current study. Ion-exchange reaction with interlayer exchangeable cations is the dominant mechanism for interlayer sorption (Janek et al. 2014). Molecular dimensions of SMX ( $0.80 \times 0.72 \times 0.89$  nm) are compatible with the interlayer incorporation, at least to a partial extent, because of the greater  $d$ -spacing of bentonite ( $d_{001} = 1.07$  nm). However, according to the previous research, surface adsorption is more favourable rather than intercalation (Hernández et al. 2018). As summarized in Table 2.4 and illustrated in Figure 2.8, the FWHM of swine manure DOC treatment exhibits a significant reduction ( $p < \sim 0.05$ ), implying expansion to the bentonite interlayer spacing. However, no significant changes occurred to the FWHM for HA and FA treatments. Further, no significant difference occurred in the FWHM when increasing the SMX concentration, indicating no direct intercalation by the antimicrobial. Swine manure DOC fraction contained reasonably high quantities of multivalent cations such as  $Mg^{2+}$ ,  $Ca^{2+}$ ,  $Fe^{3+}$ , and  $Zn^{2+}$ , and the extraction procedure managed to remove them from humic substances (Table A-1). The higher increased interlayer spacing is expected if there is any intercalation of organo-cationic species (Chikkamath et al. 2022; Huang et al. 2016; Kabadagi et al. 2018). For instance, we can hypothesize the formation of organic cations (M(II)/M(III)-DOC, where M = Mg/Fe/Ca/Zn and DOC = Trp/Tyr) by multivalent metal ion complexation to amino acids present in the swine manure DOC fraction. These organo-cations can successfully exchange with Na or K ions in bentonite interlayers to facilitate enhanced  $d$ -spacing. However, further studies are warranted to understand SMX interlayer migration with the aid of organo-cations. Migration of SMX ions to the interlayers is not evident from the results as there is no significant change in the FWHM when changing the SMX concentration.

Table 2.4 Statistical significance from Analysis of Variance (ANOVA) for the changes that occurred to the full width at half maximum (FAHM) of the basal reflection peak ( $d_{001}$ ) of bentonite X-ray diffraction pattern when changing the sulfamethoxazole (SMX) concentration from 0, 20, 40, 60, to 100  $\mu\text{g L}^{-1}$  in the presence of fresh liquid swine manure derived organic matter (dissolved organic carbon fraction (DOC)/fulvic acid (FA)/humic acid (HA)) obtained from equilibrated sorption solids.

	FWHM of $d_{001}$ peak		
	DOC	<i>P</i> value	
		FA	HA
Organic matter (0 and 25 mg L <sup>-1</sup> )	<b>0.056</b>	0.934	0.735
SMX level	0.436	0.920	0.471
Block	<b>0.009</b>	0.130	<b>0.010</b>
Organic matter $\times$ SMX level	0.844	0.889	0.832

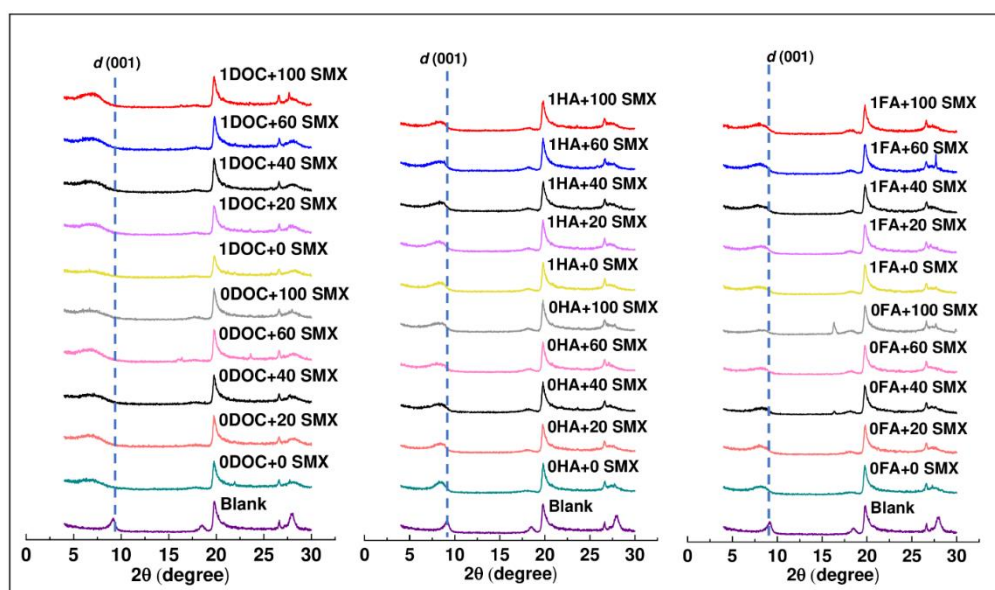


Figure 2.8 X-ray Diffraction patterns of mineral bentonite obtained from the sorption equilibrium to illustrate changes to the basal reflection  $d_{001}$  peak when changing the sulfamethoxazole (SMX) concentration as 0, 20, 40, 60, and 100  $\mu\text{g L}^{-1}$  in the presence or absence of fresh liquid swine manure derived organic matter (dissolved organic carbon fraction (DOC)/fulvic acid (FA)/humic acid (HA)).

**Surface morphology via Scanning Electron Microscopy:** Bentonite undergoes changes in its surface properties and microstructure when in contact with humic substances. SEM images for SMX treatments without organic matter resulted in no morphological changes to the crystalline structure of bentonite (Figure 2.9a). However, organic matter coating on mineral surfaces disrupted the flaky crystalline mineral surface into an amorphous rough surface. Linear ridges of the

uncoated bentonite structure are lost, resulting in a coiled configuration. This observation is more prominent with HA-coated surfaces compared to FA- and DOC-coated surfaces (Figure 2.9b). Previous studies reported that when the humic substances in the solution exceed critical micelle concentration (CMC), they can deposit and dry on the surface to form visible films (Joo and Antal 1998). We observe the same phenomenon for the current experimental organic matter concentrations. The colloidal shape of the HA and FA changed from rigid cuboidal or spherical (Figure 2.5) to flexible linear elongated/uncoiled, generally because of the pH of the sorption solution (i.e., pH 7) due to surface ionization (Joo and Antal 1998). Further, the physical conformation of humic substances changes upon mineral complexation (Charles et al. 2006). HA allowed the formation of a hydrogel to plug the mineral macropores, as observed from the SEM images in Figure 2.9a. However, the microporous structure is still visible for FA and DOC treatments. This observation indicates FA in the DOC plays the leading role when forming organo-mineral complexes over the HA. A comparatively higher quantity of FA in swine manure DOC fraction (section 2.4.1) might have presumed their role in mineral complexation.

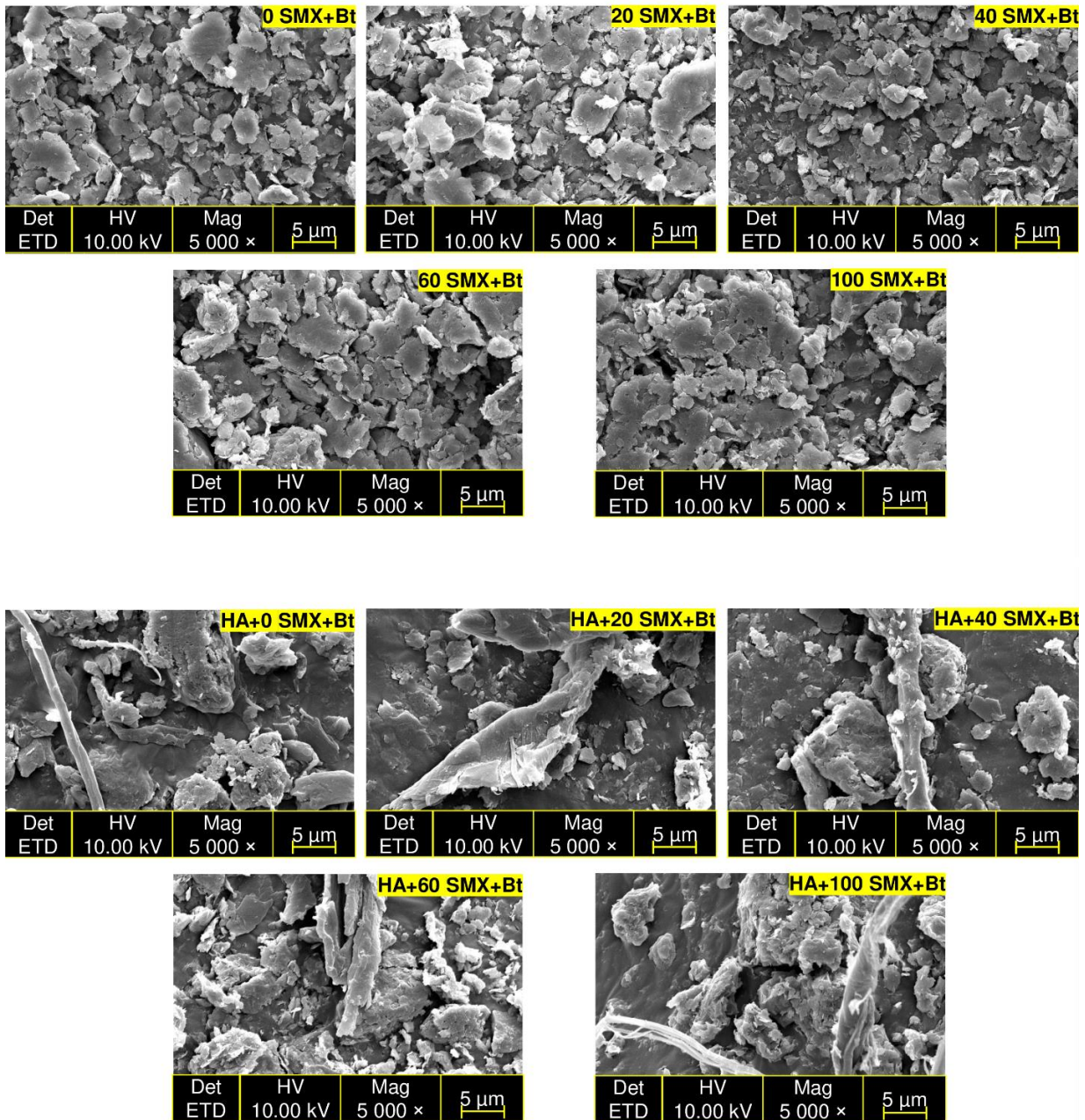


Figure 2.9a Scanning Electron Microscopic images of mineral bentonite (Bt) obtained from sorption equilibrium to visualize unaffected flaky crystalline structure with increased sulfamethoxazole (SMX) concentration and effect of swine manure humic acid (HA) to alter their surface morphology and mineral microstructure.

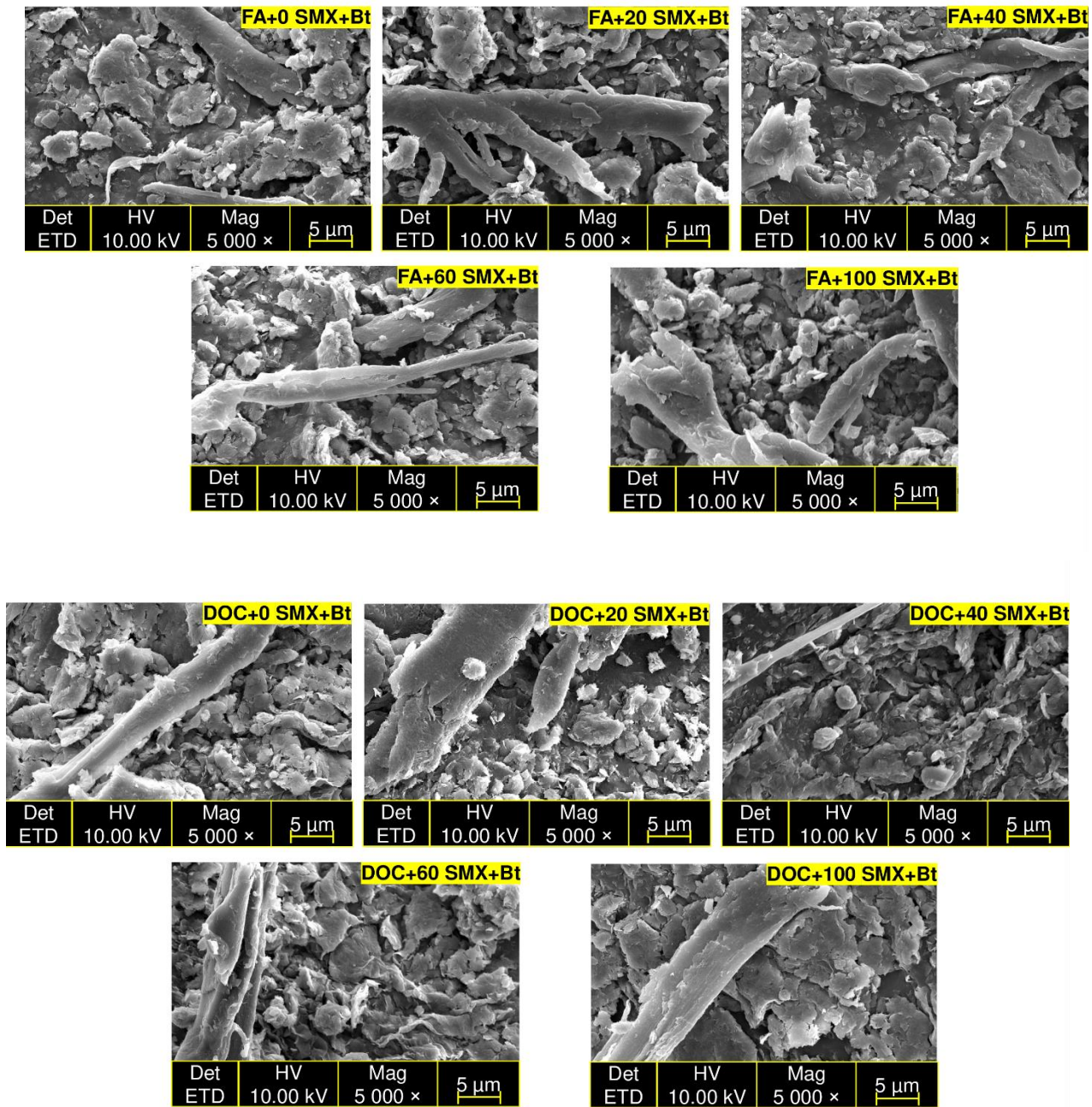


Figure 2.9b Cont. Effect of swine manure fulvic acid (FA) and swine manure dissolved organic carbon (DOC) fraction to alter the surface morphology and mineral microstructure.

## 2.5 Mechanism highlights to illustrate sulfamethoxazole sorption onto bentonite in the presence of fresh liquid swine manure dissolved organic carbon fraction

Humic substances are the main constituents of fresh liquid swine manure DOC fraction, where aromatic amino acids (i.e., Tyr and Trp) and multivalent metal ions ( $Mg^{2+}$ ,  $Ca^{2+}$ ,  $Fe^{3+}$ ,  $Zn^{2+}$ ) are other constituents. The abundance of FA to HA in fresh liquid swine manure DOC is approximately 10:1 by weight. Fresh liquid swine manure humic substances display similar bulk chemical properties such as hydrophobicity, hydrophilicity, aromaticity, and aliphaticity, as revealed by NMR data (Table 2.1). However, their secondary structures in the aqueous phase are different. Bentonite surfaces undergo ligand exchange reactions at pH 7 (i.e., environmentally relevant pH conditions) to form Bt-HA or Bt-FA organo-mineral complexes. Humic substances cover the entire mineral surface and tend to disrupt the linear ridges in flaky crystalline structures to form coiled Bt-FA/HA micro aggregates. Organo-coated Bt-HS surfaces provide novel sorption sites for SMX. However, it does not override the number of sorption sites in the uncoated mineral surface where both exhibit non-linear Freundlich-type isotherm. Subtle differences among the percent functional groups, particle size and shape, zeta potential, and the orientation of functional groups (Figures 2.2, 2.4, and 2.5) in the secondary structures allowed humic substances to orient differently on mineral surfaces. SMX complexation on FA undergoes a fluorophore quencher mechanism, whereas non-fluorophore quencher mechanisms dominate on HA (Figures 2.6a and b). Figure 2.10 illustrates the main SMX sorption mechanisms identified in the current study for a system containing bentonite and swine manure DOC (humic substances, aromatic amino acids, and multivalent metal ions as the constituents). FA-SMX complexation mechanisms (Figure 2.10b) include  $\pi$ - $\pi$  EDA interactions and water/metal ion bridging, H-bonding where contributions from fluorophore phenol groups, and alkyl- $\pi$  interactions. HA-SMX complexation mechanisms lead by amide groups via H-bonding and water/metal ion bridging with contributions from  $\pi$ - $\pi$

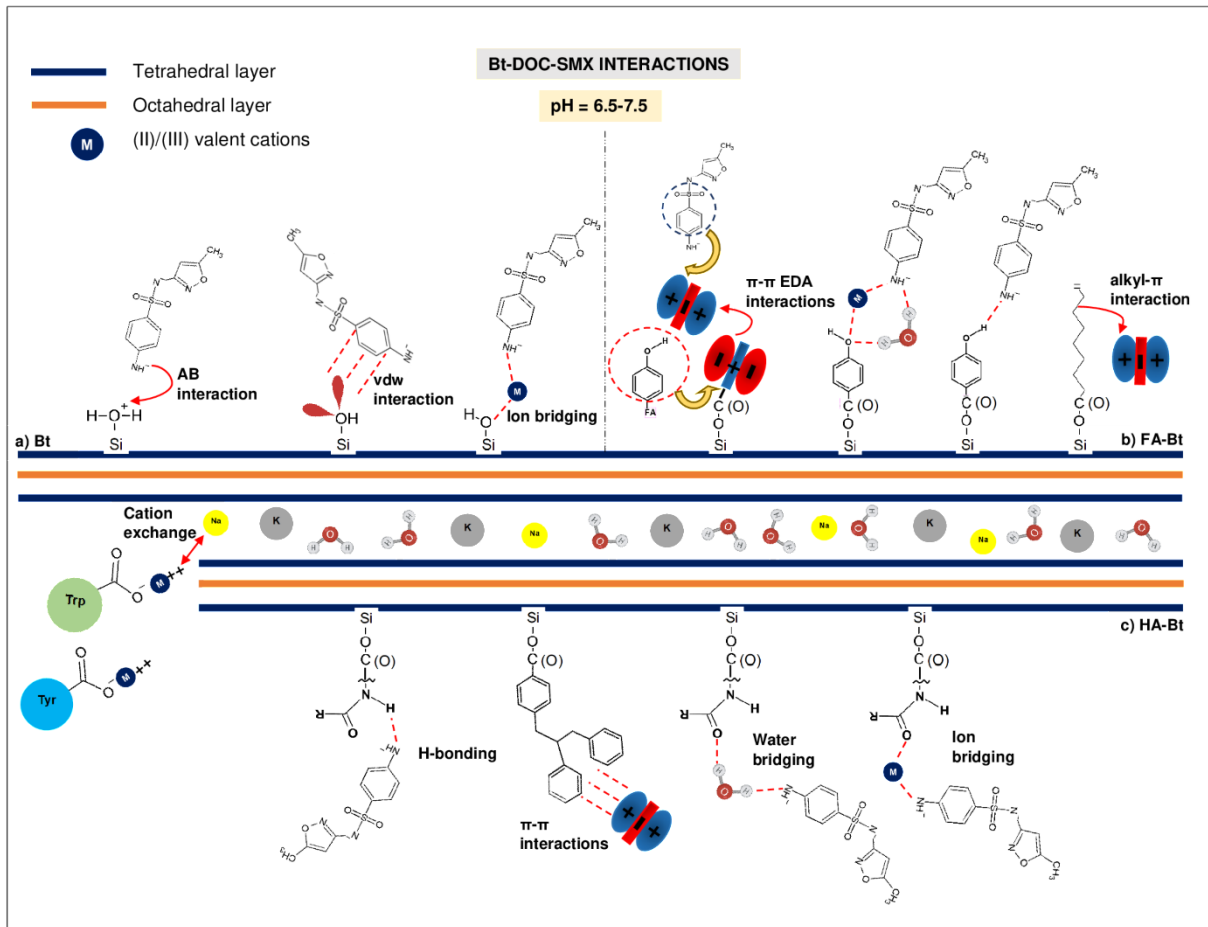


Figure 2.10 Schematic illustration of sulfamethoxazole (SMX) sorption mechanisms onto bentonite clay in the presence of fresh liquid swine manure dissolved organic carbon (DOC) fraction. a) SMX interactions with bentonite (Bt) through acid-base (AB) interactions, van der Waals (vdw) interactions, and cation bridging interactions. b) SMX interactions with fulvic acid-coated bentonite (FA-Bt) through  $\pi$ - $\pi$  electron donor-acceptor (EDA) interactions, cation and water bridging, hydrogen bonding, and alkyl- $\pi$  interactions. c) SMX interactions with humic acid-coated bentonite (HA-Bt) through hydrogen bonding,  $\pi$ - $\pi$  interactions, water bridging, and cation bridging interactions.

interactions. Further, H-bonding is possible with surface-oriented O-containing alkyl groups for both the humic substances (Figure 2.10-c). Organic matter coating hinders the direct interactions between bentonite and sulfamethoxazole. Multivalent metal ions in DOC fraction play a vital role in sulfamethoxazole bridging mechanisms. Interlayer exchangeable cationic species can be a result of metal ion complexation with aromatic amino acids (i.e., Tyr and Trp). Identifying the role of these cationic species in the sulfamethoxazole intercalation requires future research.

Our results suggest that isotherm coefficients alone are insufficient to interpret precise binding mechanisms when heterogeneous humic substances are involved. Thus, understanding the characteristics of the DOC fraction and their components (i.e., humic substances) is critical. We successfully used spectroscopy to reveal chemical and physicochemical characteristics of swine manure humic substances. These techniques can be applied to characterize any humic substance from any origin to interpret sorption coefficients/observations for contaminants such as heavy metals, natural estrogens, and other veterinary antimicrobials.

## **2.6 Conclusions and environmental implications**

Our research was to elucidate the sorption mechanisms of SMX in fresh liquid swine manure onto smectite clay minerals to predict the environmental fate of SMX of manure origin. We conducted a comprehensive mechanistic study that probes molecular interactions between SMX and smectite clay bentonite in the presence of swine manure DOC fraction when HA and FA are the major constituents.

Physicochemical properties revealed that the inner and outer parts of swine manure FA and HA secondary structures are substantially different, and they are

- i- The amount of carboxylic in swine manure FA is higher than that of swine manure HA, and the amount of amides in HA is higher than in FA.
- ii- Surface-oriented unsubstituted aliphatic groups determine the hydrophobicity of the FA, whereas surface-oriented unsubstituted aromatic groups in HA determine their hydrophobicity.
- iii- FA made larger aggregates (even for small concentrations such as  $0.01 \text{ g L}^{-1}$ ) and exhibited poly-modal distribution in the aqueous phase because of inter-molecular interactions

facilitated by carboxyl groups. However, they are unstable and susceptible to breakdown in the aqueous phase.

- iv- HA aggregates in solutions are comparatively smaller and fall in the sub-microparticle region/closer to the nanoparticle region and showed a mono-modal distribution (at  $0.1 \text{ g L}^{-1}$  and  $0.01 \text{ g L}^{-1}$ ), providing a larger surface area for the sorption.
- v- Solid FA aggregates exhibit a rigid cuboid shape, while solid humic acid aggregates are spherical.
- vi- The relatively high negative zeta potential of HA secondary structures makes them stable in aqueous solutions compared to FA.

Differences in the secondary structures resulted in different polar and non-polar SMX binding mechanisms and FA and HA coating on mineral surfaces and provided multiple novel adsorption sites for SMX sorption, and they are

- i- Polar interactions including  $\pi$ - $\pi$  electron-donor-acceptor interactions, multivalent cation and water bridging, and H-bonding with surface-oriented fluorophore phenolic groups of FA, whereas non-polar interactions include alkyl- $\pi$  hydrophobic interactions with surface-oriented alkyl groups of FA.
- ii- Polar interactions, including H-bonding, multivalent cations, and water bridging with surface-oriented amide groups of HA, whereas non-polar interactions include  $\pi$ - $\pi$  hydrophobic interactions with surface-oriented unsubstituted aromatic groups of HA.

The binding of SMX to FA dominates fluorophore quencher mechanisms for both mineral-bound and free FA in the aqueous phase, and they are extractable. The binding of SMX to mineral-bound and free HA is via non-fluorophore quencher mechanisms, and they are non-extractable.

We found that the aqueous HA-SMX is stable and non-extractable compared to aqueous FA-SMX due to the stability of the colloidal fraction, where FA-bound SMX is susceptible to desorb/extractable and likely to release back to the environment. Swine manure DOC contains a high amount of FA, approximately 10 FA:1 HA ratio. Hence, FA dominates organo-mineral complex formation and SMX binding. The aqueous complexes formed by DOC with contaminants are believed to be mobile in the environment and liable to runoff transport and leach to the nearby surface and groundwaters (Briceño et al. 2008). This way, FA-SMX complexes in the aqueous phase can be transported in runoff and leaching water to reach aquatic environments, contaminating the receiving ecosystem. To reduce the environmental impact of unstable FA-SMX complexes, we suggest facilitating the oxidation of phenolic groups (active adsorption sites for SMX) through practices such as composting and aerated lagoon storage before land application. Further, allowing the humification to transform unstable FA to stable HA with extended storage will reduce the formation of unstable FA-SMX. Care should be taken to reduce the transport of unstable FA-SMX complexes to surface and groundwaters when liquid swine manure is stored in lagoons under direct soil contact. SMX bound to aqueous HA is stable/non-extractable and can be preserved in aqueous systems due to reduced accessibility to microbial degradation. Further, soils with poor physical properties, including poor aggregation and structure, can increase the loss of clay components and might allow the transport of SMX as clay-FA-SMX or clay-HA-SMX with gravity and water to reach waters and other sensitive environments (Lado et al. 2004).

The detection of antibiotics in receiving environmental compartments (i.e., soil, surface water, groundwater) can develop antimicrobial resistance in bacteria. However, the role of humic-bound non-extractable SMX in antimicrobial resistance development in environmental bacteria and SMX persistence in the environment needs further research.

## 2.7 References

- Abakumov, E., E. Lodygin and V. Tomashunas. 2015.**  $^{13}\text{C}$  NMR and ESR characterization of Humic substances isolated from soils of two Siberian Arctic islands. *Int. J. Environ.* **2015**. doi: 10.1155/2015/390591.
- Adams, J. M. 1987.** Synthetic organic chemistry using pillared, cation-exchanged and acid-treated montmorillonite catalysts-A review. *Appl. Clay Sci.* **2**(4): 309-342. doi: 10.1016/0169-1317(87)90039-1.
- Al-Faiyz, Y. S. S. 2017.** CPMAS  $^{13}\text{C}$  NMR characterization of humic acids from composted agricultural Saudi waste. *Arab. J. Chem.* **10**: S839-S853. doi: 10.1016/j.arabjc.2012.12.018.
- Amarakoon, I. D., F. Zvomuya, S. Sura, F. J. Larney, A. J. Cessna, S. Xu and T. A. McAllister. (2016).** Dissipation of antimicrobials in feedlot manure compost after oral administration versus fortification after excretion. *J. Environ. Qual.* **45**(2): 503-510. doi: 10.2134/jeq2015.07.0408.
- Andriamalala, A., L. Vieubl e-Gonod, V. Dumeny and P. Cambier. 2018.** Fate of sulfamethoxazole, its main metabolite N-ac-sulfamethoxazole and ciprofloxacin in agricultural soils amended or not by organic waste products. *Chemosphere*, **191**: 607-615. doi: 10.1016/j.chemosphere.2017.10.093.
- Antoneli, V., A.C. Mosele, J.A. Bednarz, M. Pulido-Fern andez, J. Lozano-Parra, S.D. Keesstra, J. Rodrigo-Comino. 2019.** Effects of applying liquid swine manure on soil quality and yield production in tropical soybean crops (Paran , Brazil). *Sustainability*, **11**: 3898. doi: 10.3390/su11143898.
- Assefa, B. A., J. J. Schoenau and M. C. J. Grevers. 2004.** Effects of four annual applications of manure on Black Chernozemic soils. *Can. Biosyst. Eng. Canada*, **46**, [Online]. Retrieved from: <https://library.csbe-scgab.ca/docs/journal/46/c0403.pdf> (Accessed June 2023)
- Awosile, B. B., J. T. McClure, J. Sanchez, J. VanLeeuwen, J. C. Rodriguez-Lecompte, G. Keefe and L. C. Heider. 2017.** Short communication: Extended-spectrum cephalosporin-resistant *Escherichia coli* in colostrum from New Brunswick, Canada, dairy cows harbor blaCMY-2 and blaTEM resistance genes. *J. Dairy Sci.* **100**(10): 7901-7905. doi: 10.3168/jds.2017-12941.
- Brezinski K. 2018.** High Performance Size-Exclusion Chromatography (HPSEC) as a Natural Organic Matter (NOM) property indicator in Ion-Exchange (IX) applications. Doctoral thesis, University of Manitoba. Retrieved from: [https://mspace.lib.umanitoba.ca/bitstream/handle/1993/33316/brezinki\\_kenneth.pdf?sequence=1](https://mspace.lib.umanitoba.ca/bitstream/handle/1993/33316/brezinki_kenneth.pdf?sequence=1) (Accessed June 2023).

- Briceño, G., R. Demanet, M. de la Luz Mora and G. Palma. 2008.** Effect of liquid cow manure on andisol properties and atrazine adsorption. *J. Environ. Qual.* **37**(4): 1519-1526. doi: 10.2134/jeq2007.0323.
- Charles, S. M., H. Li, B. J. Teppen and S. A. Boyd. 2006.** Quantifying the availability of clay surfaces in soils for adsorption of nitrocyano benzene and diuron. *Environ. Sci. Technol.* **40**(24): 7751-7756. doi: 10.1021/es0611700.
- Chen, K.-L., L.-C. Liu and Chen, W.-R. 2017.** Adsorption of sulfamethoxazole and sulfapyridine antibiotics in high organic content soils. *Environ. Pollut.* **231**: 1163-1171. doi: 10.1016/j.envpol.2017.08.011.
- Chen, Y., Y. Inbar, Y. Hadar and R. L. Malcolm. 1989.** Chemical properties and solid-state CPMAS <sup>13</sup>C-NMR of composted organic matter. *Sci. Total Environ.* **81–82**: 201-208. doi: 10.1016/0048-9697(89)90126-5.
- Chikkamath, S., J. Manjanna, N. Momin, B. G. Hegde, G. P. Nayaka, A. S. Kar and B. S. Tomar. 2022.** Na-montmorillonite to Fe(II)-Mt using ferrous citrate/ascorbate obtained by dissolving iron powder. *Appl. Clay Sci.* **217**: 106396. doi: 10.1016/j.clay.2021.106396.
- De Mastro, F., C. Cacace, A. Traversa, M. Pallara, C. Coccozza, F. Mottola and G. Brunetti. 2022.** Influence of chemical and mineralogical soil properties on the adsorption of sulfamethoxazole and diclofenac in Mediterranean soils. *Chem. Biol. Technol. Agric.* **9**(1): 34. doi: 10.1186/s40538-022-00300-8.
- Durce, D., N. Maes, C. Bruggeman and L. Van Ravestyn. 2016.** Alteration of the molecular-size-distribution of Boom Clay dissolved organic matter induced by Na<sup>+</sup> and Ca<sup>2+</sup>. *J. Contam. Hydrol.* **185-186**: 14-27. doi: 10.1016/j.jconhyd.2015.12.001.
- Esfahani, M. R., H. A. Stretz and M. J. M. Wells. 2015.** Abiotic reversible self-assembly of fulvic and humic acid aggregates in low electrolytic conductivity solutions by dynamic light scattering and zeta potential investigation. *Sci. Total Environ.* **537**: 81-92. doi: 10.1016/j.scitotenv.2015.08.001.
- Gerasimowicz, W. V. and D. M. Byler. 1985.** Carbon-13 CPMAS NMR and FTIR spectroscopic studies of humic acids. *Soil Sci.* **139**(3): 270-278.
- Giles, C. H., D. Smith and A. Huitson. 1974.** A general treatment and classification of the solute adsorption isotherm. I. Theoretical. *J. Colloid Interface Sci.* **47**(3): 755-765. doi: 10.1016/0021-9797(74)90252-5.
- Gu, L., J. Xu, L. Lv, B. Liu, H. Zhang, X. Yu and Z. Luo. 2011.** Dissolved organic nitrogen (DON) adsorption by using Al-pillared bentonite. *Desalination*, **269**(1-3): 206-213. doi: 10.1016/j.desal.2010.10.063.
- Gulkowska, A., M. Krauss, D. Rentsch and J. Hollender. 2012.** Reactions of a sulfonamide antimicrobial with model humic constituents: Assessing pathways and stability of covalent bonding. *Environ. Sci. Technol.* **46**(4): 2102-2111. doi: 10.1021/es202272w.

- Hansima, M. A. C. K., A. T. Jayaweera, J. Ketharani, T. Ritigala, L. Zheng, D. R. Samarajeewa, K. G. N. Nanayakkara, A. C. Herath, M. Makehelwala, K. B. S. N. Jinadasa, S. K. Weragoda, Y. Wei and R. Weerasooriya. 2022.** Characterization of humic substances isolated from a tropical zone and their role in membrane fouling. *J. Environ. Chem. Eng.* **10**(3): 107456. doi: 10.1016/j.jece.2022.107456.
- Hernández, D., L. Lazo, L. Valdés, L. C. de Ménorval, Z. Rozynek and A. Rivera. 2018.** Synthetic clay mineral as nanocarrier of sulfamethoxazole and trimethoprim. *Appl. Clay Sci.* **161**: 395-403. doi: 10.1016/j.clay.2018.03.016.
- Beamson, G. and D. Briggs. 1993.** High Resolution XPS of Organic Polymers: The Scienta ESCA300 Database. *J. Chem. Educ.* **70**(1): A25. doi: 10.1021/ed070pA25.5.
- Hu, S., Y. Zhang, G. Shen, H. Zhang, Z. Yuan and W. Zhang. 2019.** Adsorption/desorption behavior and mechanisms of sulfadiazine and sulfamethoxazole in agricultural soil systems. *Soil Tillage Res.* **186**: 233-241. doi: 10.1016/j.still.2018.10.026.
- Huang, Z., P. Wu, B. Gong, S. Yang, H. Li, Z. Zhu and L. Cui. 2016.** Preservation of glutamic acid-iron chelate into montmorillonite to efficiently degrade Reactive Blue 19 in a Fenton system under sunlight irradiation at neutral pH. *Appl. Surf. Sci.* **370**: 209-217. doi: 10.1016/j.apsusc.2016.02.126.
- Jacquin, C., G. Lesage, J. Traber, W. Pronk and M. Heran. 2017.** Three-dimensional excitation and emission matrix fluorescence (3DEEM) for quick and pseudo-quantitative determination of protein- and humic-like substances in full-scale membrane bioreactor (MBR). *Water Res.* **118**: 82-92. doi: 10.1016/j.watres.2017.04.009.
- Janek, M., D. Zich, J. Molloy and M. Naftaly. 2014.** THz spectroscopy of amines and aminoacids intercalated in clays. *International Conference on Infrared, Millimeter, and Terahertz Waves, IRMMW-THz.* doi: 10.1109/IRMMW-THz.2014.6956053.
- Joo, P. and K. Antal. 1998.** Transport processes in clay and humate treated clay layers: An electrochemical and radioabsorption survey. *Colloids Surf. A: Physicochem. Eng. Asp.* **141**(3): 365-377. doi: 10.1016/S0927-7757(98)00340-9.
- Kabadagi, A., S. Chikkamath, J. Manjanna and S. Kobayashi. 2018.** In-situ complexation of o-phenanthroline in the interlayer of Fe(II)-montmorillonite. *Appl. Clay Sci.* **165**: 148-154. doi: 10.1016/j.clay.2018.08.014.
- Karickhoff, S. W. 1984.** Organic pollutant sorption in aquatic systems. *J. Hydraul. Eng.* **110**(6): 707-735. doi: 10.1061/(asce)0733-9429(1984)110:6(707).
- Kim, D-S. 2003.** Measurement of point of zero charge of bentonite by solubilization technique and its dependence of surface potential on pH. *Environ. Eng. Res.* **8**(4): 1226-1025. doi: 10.4491/eer.2003.8.4.222.

- Klučáková, M. 2018.** Size and charge evaluation of standard humic and fulvic acids as crucial factors to determine their environmental behavior and impact. *Front. Chem.* **6**(Jul). doi: 10.3389/fchem.2018.00235.
- Lado, M., A. Paz and M. Ben-Hur. 2004.** Organic matter and aggregate size interactions in infiltration, seal formation, and soil loss. *Soil Sci. Soc. Am. J.* **68**: 935-942. doi: 10.2136/sssaj2004.9350
- Li, G. F., W. J. Ma, Z. Q. Ren, Y. Wang, J. P. Li, J. W. Zhao, S. T. Li, Q. Liu, Y. N. Gu, Y. F. Cheng, B. C. Huang and R. C. Jin. 2021.** Molecular insight into the binding property and mechanism of sulfamethoxazole to extracellular proteins of anammox sludge. *Environ. Sci. Technol.* **55**(24): 16627-16635. doi: 10.1021/acs.est.1c05203.
- Li, S., H. Ju, M. Ji, J. Zhang, K. Song, P. Chen and G. Mu. 2018.** Terrestrial humic-like fluorescence peak of chromophoric dissolved organic matter as a new potential indicator tracing the antibiotics in typical polluted watershed. *J. Environ. Manage.* **228**: 65-76. doi: 10.1016/j.jenvman.2018.09.013.
- Liu, J. lin, X. yan Li, Y. feng Xie and H. Tang. 2014.** Characterization of soluble microbial products as precursors of disinfection byproducts in drinking water supply. *Sci. Total Environ.* **472**: 818-824. doi: 10.1016/j.scitotenv.2013.11.139.
- Machado, W., J. C. Franchini, M. de Fátima Guimarães and J. T. Filho. 2020.** Spectroscopic characterization of humic and fulvic acids in soil aggregates, Brazil. *Heliyon*, **6**(6): e04078. doi: 10.1016/j.heliyon.2020.e04078.
- Makehelwala, M., Y. Wei, S. K. Weragoda, R. Weerasooriya and L. Zheng. 2019.** Characterization of dissolved organic carbon in shallow groundwater of chronic kidney disease affected regions in Sri Lanka. *Sci. Total Environ.* **660**: 865-875. doi: 10.1016/j.scitotenv.2018.12.435.
- McCarty, P. L., M. Reinhard and B. E. Rittmann. 1981.** Trace organics in groundwater. *Environ. Sci. Technol.* **15**(1): 40-51. doi: 10.1021/es00083a003.
- Miao, X. S., F. Bishay, M. Chen and C. D. Metcalfe. 2004.** Occurrence of antimicrobials in the final effluents of wastewater treatment plants in Canada. *Environ. Sci. Technol.* **38**(13): 3533-3541. doi: 10.1021/es030653q.
- Monteil-Rivera, F., E. B. Brouwer, S. Masset, Y. Deslandes and J. Dumonceau. 2000.** Combination of X-ray photoelectron and solid-state <sup>13</sup>C nuclear magnetic resonance spectroscopy in the structural characterisation of humic acids. *Anal. Chim. Acta.* **424**(2): 243-255. doi: 10.1016/S0003-2670(00)01139-9.
- Murphy, E. M. and J. M. Zachara. 1995.** The role of sorbed humic substances on the distribution of organic and inorganic contaminants in groundwater. *Geoderma.* **67**(1-2): 103-124. doi: 10.1016/0016-7061(94)00055-F.

- Murphy, E. M., J. M. Zachara and S. C. Smith. 1990.** Influence of mineral-bound humic substances on the sorption of hydrophobic organic compounds. *Environ. Sci. Technol.* **24**(10): 1507-1516. doi: 10.1021/es00080a009.
- Nyiraneza J., M. H. Chantigny, A. N. Dayegamiye and M. R. Laverdière. 2009.** Dairy cattle manure improves soil productivity in low residue rotation systems. *Agron. J.* **101**(1). doi: 10.2134/agronj2008.0142.
- Ou, X., S. Chen, X. Quan and H. Zhao. 2009.** Photochemical activity and characterization of the complex of humic acids with iron(III). *J. Geochem. Explor.* **102**(2): 49-55. doi: 10.1016/j.gexplo.2009.02.003.
- Ou, X., X. Quan, S. Chen, H. Zhao and Y. Zhang. 2007.** Atrazine photodegradation in aqueous solution induced by interaction of humic acids and iron: Photoformation of iron(II) and hydrogen peroxide. *J. Agric. Food Chem.* **55**(21): 8650-8656. doi: 10.1021/jf0719050.
- Peng, X., Z. Luan, F. Chen, B. Tian and Z. Jia. 2005.** Adsorption of humic acid onto pillared bentonite. *Desalination.* **174**(2): 135-143. doi: 10.1016/j.desal.2004.09.007.
- Piccolo, A., P. Zaccheo and P. G. Genevini. 1992.** Chemical characterization of humic substances extracted from organic-waste-amended soils. *Bioresour. Technol.* **40**(3): 275-282. doi: 10.1016/0960-8524(92)90154-P.
- Reddy, T, R., S. Kaneko, T. Endo and S, L. Reddy. 2017.** Spectroscopic Characterization of Bentonite. *J. lasers opt. photonics .* **4**(3). doi: 10.4172/2469-410X.1000171.
- Rees, H. W., T. L. Chow, B. Zebarth, Z. Xing, P. Toner, J. Lavoie and J.-L. Daigle. 2014.** Impact of supplemental poultry manure application on potato yield and soil properties on a loam soil in north-western New Brunswick. *Can. J. Soil Sci.* **94**(1): 49-65. doi:10.4141/cjss2013-009.
- Samson, M. É., M. H. Chantigny, A. Vanasse, S. Menasseri-Aubry, D. A. Angers. 2020.** Coarse mineral-associated organic matter is a pivotal fraction for SOM formation and is sensitive to the quality of organic inputs. *Soil Biol. Biochem.* **149**: 107935. doi: 10.1016/j.soilbio.2020.107935.
- Smith, M., L. Scudiero, J. Espinal, J. S. McEwen and M. Garcia-Perez. 2016.** Improving the deconvolution and interpretation of XPS spectra from chars by ab initio calculations. *Carbon.* **110**: 155-171. doi: 10.1016/j.carbon.2016.09.012.
- Soto, H. S. J. S., I. D. Amarakoon, N. J. Casson, D. Kumaragamage and H. F. Wilson. 2023.** The fate of dissolved sulfamethoxazole during spring-thaw snowmelt in a field with a history of manure application. *Can. J. Soil Sci.* doi: 10.1139/cjss-2023-0006.
- Sposito, G. 1980.** Derivation of the Freundlich equation for ion exchange reactions in soils. *Soil Sci. Soc. Am. J.* **44**: 652-654. doi: 10.2136/sssaj1980.03615995004400030045x
- Thurman, E. M. 1985.** *Organic Geochemistry of Natural Waters.* USA. W. Junk Publisher. doi: 10.1007/978-94-009-5095-5.

- Topp, E., R. Chapman, M. Devers-Lamrani, A. Hartmann, R. Marti, F. Martin-Laurent, L. Sabourin, A. Scott and M. Sumarah. 2013.** Accelerated biodegradation of veterinary antibiotics in agricultural soil following long-term exposure, and isolation of a sulfamethazine-degrading microbacterium sp. *J. Environ. Qual.* **42**(1): 173-178. doi: 10.2134/jeq2012.0162.
- Walter, R. H.** Polysaccharide Dispersions **1998**. 123–155. Academic Press. doi: 10.1016/B978-012733865-1/50008-5.
- Wang, L., H. Li, Y. Yang, D. Zhang, M. Wu, B. Pan and B. Xing. 2017.** Identifying structural characteristics of humic acid to static and dynamic fluorescence quenching of phenanthrene, 9-phenanthrol, and naphthalene. *Water Res.* **122**: 337-344. doi:10.1016/j.watres.2017.06.010.
- Wang, R., S. Yang, J. Fang, Z. Wang, Y. Chen, D. Zhang and C. Yang. 2018.** Characterizing the interaction between antibiotics and humic acid by fluorescence quenching method. *Int. J. Environ. Res. Public Health.* **15**(7): 1458. doi: 10.3390/ijerph15071458.
- Weishaar, J. L., G. R. Aiken, B.A. Bergamaschi, M.S. Fram, R. Fujii and K. Mopper. 2003.** Evaluation of specific ultraviolet absorbance as an indicator of the chemical composition and reactivity of dissolved organic carbon. *Environ. Sci. Technol.* **37**(20): 4702–4708. doi: 10.1021/es030360x.
- Wieland, E., H. Wanner, Y. Albinsson, P. Wersin and O. Kamland. 1994.** A surface chemical model of the bentonite-water interface and its implications for modelling the near field chemistry in a repository for spent fuel. SKB-TR-94-26. Swedish Nuclear Fuel and Waste Management Co., Stockholm (Sweden). Retrieved from: <https://www.osti.gov/etdeweb/biblio/38842> (Accessed June 2023).
- Zhang, L., L. Luo and S. Zhang. 2012.** Integrated investigations on the adsorption mechanisms of fulvic and humic acids on three clay minerals. *Colloids Surf. A: Physicochem. Eng.* **406**: 84-90. doi:10.1016/j.colsurfa.2012.05.00.
- Zheng, S., S., Dou, H. Duan, B. Zhang and Y. Bai. 2021.** Fluorescence spectroscopy and <sup>13</sup>C NMR spectroscopy characteristics of HA in black soil at different corn straw returning modes. *Int. J. Anal. Chem.* **2021**: 9940116. doi: 10.1155/2021/9940116.

### **3. OVERALL SYNTHESIS**

#### **3.1 Summary of Findings and Contributions to Knowledge**

Livestock excretory products contain harmful environmental contaminants, including veterinary antimicrobials. Application of stored or non-stored liquid swine manure in agricultural lands results in manure-derived sulfamethoxazole (SMX) contamination in water bodies and terrestrial environments across the Canadian prairies (Awosile et al. 2017; Miao et al. 2004; Topp et al. 2013). A major concern of environmental accumulation and prolonged exposure to these pharmaceuticals is antimicrobial resistance in bacteria. The World Health Organization has identified antimicrobial resistance as one of the top ten global health threats to the human population (WHO, 2020). Manure organic matter, particularly the mobile dissolved organic carbon (DOC) fraction, affects the sorption of contaminants and hence determines their fate and transport. This thesis focuses on understanding the effects of organic matter derived from fresh liquid swine manure on the sorption of SMX into a smectite clay fraction and extends to elucidating the SMX sorption mechanisms onto bentonite clay minerals in the presence of swine manure DOC.

This study comprehensively identified the subtle differences in the physicochemical properties of fresh liquid swine manure humic substances and functional group orientations in their secondary structures for the first time. The sorption study, in combination with organic matter characterization, resolved a vast range of partial sorption mechanisms, including the SMX sorption onto humic acid (HA), fulvic acid (FA), DOC fraction, pure bentonite, HA-coated bentonite, FA-coated bentonite, and DOC-coated bentonite. These mechanisms ultimately elucidated the SMX sorption mechanisms onto 2:1 type smectite clays in the presence of fresh liquid swine manure DOC fraction.

Sorption data fitted well with Freundlich isotherm except for SMX sorption onto swine manure FA. Partition constant  $K_f$  was not significantly varied among the clay and adsorbent combination treatments tested. The linearity constant  $n$  closer to 1 indicated sulfamethoxazole sorption on bentonite is linear for the concentrations considered. SMX sorption on HA and DOC exhibited non-linear ( $n \neq 1$ ) Freundlich isotherms whereas SMX sorption on organic matter-coated bentonite exhibited  $n > 1$  Freundlich isotherms despite the type of organic matter.

The composition of fresh liquid swine manure DOC fraction is rich in young/less humified FA and HA in approximately 10:1 ratio by weight. The other components are aromatic amino acids (i.e., tryptophan and tyrosine) and multivalent metal ions (i.e.,  $Mg^{2+}$ ,  $Ca^{2+}$ ,  $Fe^{3+}$ ,  $Zn^{2+}$ ). The average molecular weight of humic acid fraction lies between 1600 and 2000 Da, whereas, for FA, the range is between 600 and 1100 Da. The molecular weight of the amino acids is between 100 and 450 Da. Fresh liquid swine manure humic substances displayed similarities in their bulk chemical properties, including hydrophobicity, hydrophilicity, aliphaticity, and aromaticity. Differences were observed in the composition of functional groups and the orientation of functional groups when making secondary structures. In summary,

- i- Carboxylic content in swine manure FA (22.1%;  $^{13}C$ -NMR) is higher than that of swine manure HA (13.5%;  $^{13}C$ -NMR), and amide quantity in HA (90.5%; XPS) is higher than in FA (45.1%; XPS).
- ii- XPS data suggested the hydrophobicity of the FA is determined by surface-oriented unsubstituted aliphatic groups, whereas surface-oriented unsubstituted aromatic groups in HA determined their hydrophobicity.
- iii- FA made larger aggregates (even for small concentrations as  $0.01 \text{ g L}^{-1}$ ) and exhibited a poly-modal distribution in the aqueous phase. Larger aggregation is due to inter-molecular

interactions facilitated by carboxyl groups; however, they are unstable and susceptible to breakdown in the aqueous phase.

- iv- HA aggregates in solutions are comparatively smaller and fall in the sub-microparticle region/closer to the nanoparticle region, showing a mono-modal distribution ( $0.1 \text{ g L}^{-1}$  and  $0.01 \text{ g L}^{-1}$ ), providing a larger surface area for the sorption.
- v- SEM surface morphology suggested solid FA aggregates have a rigid cuboid shape, while HA aggregates are spherical.
- vi- Relatively higher negative zeta potential of HA secondary structures makes them stable in aqueous solutions compared to FA.

The subtle differences between functional group orientation in humic and fulvic secondary structures resulted in different polar and non-polar SMX binding mechanisms. Further, these differences allowed humic substances to orient differently on mineral surfaces. Organic matter coating on mineral surfaces is found to be via a ligand exchange mechanism. HA and FA coating interrupted the surface of the original crystalline structure. HA coating enhanced the micro aggregation. SMX showed a similar quantity of adsorption with organic matter-coated mineral surfaces as indicated by  $K_f$  values despite the type of organic matter (i.e., DOC/HA/FA). Following binding mechanisms were involved when SMX sorb onto FA- and HA-coated bentonite surface and free organic matter in the aqueous phase.

- i. The primary SMX sorption mechanism onto FA is via fluorophore quencher complex formation facilitated by surface-oriented phenolic groups in fulvic secondary structures. These mechanisms involved  $\pi$ - $\pi$  electron donor-acceptor interactions between electron-rich fulvic phenolic functional groups and electron deficit aminobenzene groups in SMX,

water/cation bridging, and direct H-bonding between the phenolic groups and *p*-amino group in SMX.

- ii. SMX sorption onto FA also involved non-polar hydrophobic alkyl- $\pi$  interactions between surface-oriented alkyl groups in fulvic structure and the aminobenzene group in SMX.
- iii. Contrary to the fluorophore quencher mechanisms with FA, SMX sorption onto HA is via non-fluorophore quencher mechanisms. The mechanisms involved H-bonding and water/cation bridging between surface-oriented amide groups in humic secondary structures and amino benzene groups in SMX.
- iv. Non-polar hydrophobic sorption of SMX onto HA involved  $\pi$ - $\pi$  interactions between surface-oriented aromatic groups in humic structure and aminobenzene functional group in SMX.
- v. Surface-oriented O-alkyl groups in both fulvic and humic structures facilitated H-bonding with the *p*-amino group in SMX.

Multivalent metal ions in fresh liquid swine manure DOC fraction enhanced the sorption via ion bridging as indicated by  $n > 1$  value for the linearity constant. XRD data revealed interlayer exchangeable cationic species are generated as a result of metal ion complexation with aromatic amino acids, i.e., tryptophan and tyrosine. A higher ratio of fulvic acid in DOC fraction determined most of the organic matter coating on mineral surfaces and SMX binding. Aqueous FA-SMX is unstable and extractable, whereas aqueous HA-SMX is non-extractable and stable. Fresh liquid swine manure contaminated with sSMX in a smectite mineral-rich soil could enhance the transport of unstable FA-SMX in runoff and leaching water. Desorption of SMX from FA-SMX complexes can disperse the antimicrobial, increasing the ecological risks and antimicrobial resistance in bacteria.

### 3.2 Implications of the Research

The results showed that the FA fraction dominates the fate of SMX in fresh liquid swine manure in smectite clay-rich soils (i.e., typical Canadian prairie soils). Aqueous FA-SMX is mobile and liable to transport via snowmelt runoff and leaching water. Aqueous FA-bound SMX is susceptible to desorb/extractable because of the instability of fulvic secondary structures. Desorption of SMX from transported FA-SMX into ground and surface waters would contaminate the receiving ecosystem and risk antimicrobial resistance development in bacteria (Martínez-Hernández et al. 2016; Zhang et al. 2016). SMX bound to HA in the aqueous phase appeared stable and non-extractable. They could be preserved in aqueous environments due to reduced microbial accessibility. The physicochemical characteristics were able to capture differences in the sorption mechanisms for HA- and FA-coated organo-mineral surfaces despite the similar  $K_f$  and  $n$  values obtained from Freundlich isotherm.

Results in the thesis thus suggest that isotherm coefficients all along are insufficient to interpret precise binding mechanisms when heterogeneous humic substances are involved. Thus, elucidating the physicochemical characteristics of major DOC components, i.e., HA and FA, is essential to understanding sorption data. The research appropriately used spectroscopy to reveal surface and bulk physicochemical properties of fresh liquid swine manure humic substances. The physicochemical characteristics obtained from the study will aid in interpreting sorption coefficients/observations from any other swine manure-borne contaminants (e.g., heavy metals, natural estrogens, and other pharmaceuticals) to understand their environmental fate.

Research findings can be implemented in on-farm management practices associated with liquid swine manure amendment. We identified phenolic groups in the fulvic structure as the major sorption sites for SMX binding. Hence, we suggest facilitating the oxidation of phenolic groups to

reduce the environmental impact of unstable FA-SMX complexes. Facilitating the humification processes in open lagoons under aerobic conditions is suggested to oxidize phenolic groups to benzoquinone to retard fluorophore quencher mechanisms. Allowing humification via composting process to transform unstable FA to stable HA will also reduce SMX off-site contamination. Liquid swine manure-storing lagoons can also be a source of SMX contamination since they are enriched in fresh liquid swine manure FA. Therefore, care should be taken to avoid offsite transport of FA-SMX into surface waters and leaching down to groundwaters when manure is in direct contact with soil. Implementing cost-effective wastewater treatments to remove SMX/veterinary antibiotics from the fresh liquid swine manure prior to their land application could also be effective.

### **3.3 Recommendations for Future Research and Limitations of the Current Research**

The knowledge gaps identified in the thesis are recommended as future research in this section to enhance sustainability in swine manure management practices. The potential SMX contamination from swine manure can be reduced substantially by allowing humification to evolve unstable FA to stable HA. To determine the role of aqueous HA-SMX in antimicrobial resistance gene development and their persistence in the environment needs further research. We noted HA-coating enhancing the micro aggregation of the bentonite clay structure, which might increase the potential of leaching aqueous organic matter bound-SMX complexes through micropores to reach groundwater. Therefore, research is recommended to evaluate the leaching potential of aqueous organic matter bound-SMX through enhanced microporous structure. Evaluation of the stability of the humic substances on the mineral surface requires future research since instability may lead to desorption, leaching, and runoff transportation of organic matter bound-SMX. This research

demonstrated that multivalent metal ions and amino acids combine to form interlayer exchangeable cations. There is a possibility of migrating anionic [SMX]<sup>-</sup> with these organic cations into smectite interlayers and preserving them in the soil. Hence, future research is recommended to identify SMX interlayer migration with these cations. This research did not focus on the effects of multivalent cations that can be present in the soil solution (i.e., Ca<sup>2+</sup>, Mg<sup>2+</sup>, Fe<sup>2+</sup>, Fe<sup>3+</sup>, etc.) on SMX binding mechanisms when smectite clay interacts with fresh liquid swine manure humic substances. Hence, research is recommended to understand the effects of multivalent metal ions on the sorption mechanisms.

Because of time limits and the restrictions related to COVID-19 pandemic, the study was limited to fresh liquid swine manure obtained from a single farm. Physicochemical characteristics of humic substances can vary with the livestock operation; hence, an extended study considering multiple farms/livestock operations could enhance the significance of the research findings. Further, the sorption study was carried out using commercial bentonite to represent the soil clay fraction to avoid matrix interferences that can occur when using real soils. However, employing field soils varying in chemical and physical properties could also augment the understanding of the sorption mechanisms.

### 3.4 References

- Awosile, B. B., J. T. McClure, J. Sanchez, J. VanLeeuwen, J. C. Rodriguez-Lecompte, G. Keefe and L. C. Heider. 2017.** Short communication: Extended-spectrum cephalosporin-resistant *Escherichia coli* in colostrum from New Brunswick, Canada, dairy cows harbor blaCMY-2 and blaTEM resistance genes. *J. Dairy Sci.* **100**(10): 7901-7905. doi: 10.3168/jds.2017-12941.
- Martínez-Hernández, V., R. Meffe, S. H. López and I. de Bustamante. 2016.** The role of sorption and biodegradation in the removal of acetaminophen, carbamazepine, caffeine, naproxen and sulfamethoxazole during soil contact: a kinetics study. *Sci. Total Environ.* **559**: 232-241. doi: 10.1016/j.scitotenv.2016.03.131.

- Miao, X. S., F. Bishay, M. Chen and C. D. Metcalfe. 2004.** Occurrence of antimicrobials in the final effluents of wastewater treatment plants in Canada. *Environ. Sci. Technol.* **38**(13): 3533-3541. doi: 10.1021/es030653q.
- Topp, E., R. Chapman, M. Devers-Lamrani, A. Hartmann, R. Marti, F. Martin-Laurent, L. Sabourin, A. Scott and M. Sumarah. 2013.** Accelerated biodegradation of veterinary antibiotics in agricultural soil following long-term exposure, and isolation of a sulfamethazine-degrading microbacterium sp. *J. Environ. Qual.* **42**(1): 173-178. doi: 10.2134/jeq2012.0162.
- World Health Organization (WHO), 2020.** Antimicrobial resistance: key facts. Retrieved from: <https://www.who.int/news-room/fact-sheets/detail/antibiotic-resistance> (accessed 12 May 2023).
- Zhang, Y., J. Geng, H. Ma, H. Ren, K. Xu and L. Ding. 2016.** Characterization of microbial community and antibiotic resistance genes in activated sludge under tetracycline and sulfamethoxazole selection pressure. *Sci. Total Environ.* **571**: 479-486. doi: 10.1016/j.scitotenv.2016.07.014.

## 4. APPENDICES

Table A-1 Chemical properties of fresh liquid swine manure slurry and metal ions present in fresh liquid swine manure dissolved organic carbon fraction

Chemical parameters of fresh liquid swine manure slurry sample	
Dry matter (%)	39.82
Moisture (%)	60.18
Total Kjeldahl nitrogen (ppm)	28772.05
NH <sub>4</sub> <sup>+</sup> -N (ppm)	2761.53
P (ppm)	5533.36
S (ppm)	5084.45
K (ppm)	268.32
Metal ions present in fresh swine liquid manure dissolved organic carbon fraction	
Na (ppm)	620.15
Zn (ppm)	2.22
Mn (ppm)	BDL
Fe (ppm)	1.21
Mg (ppm)	36.96
Cu (ppm)	0.10
Ca (ppm)	54.38
K (ppm)	1121.90

BDL - below detection limit

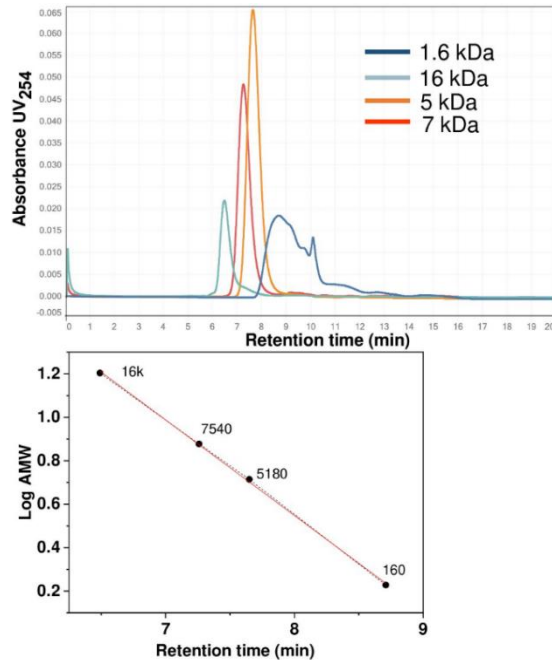


Fig A-1 The calibration curve for High Performance Size-Exclusion chromatography analysis for the polystyrene sulphonate standard

Table A-2 Peak positions of Infrared bands of bentonite (Bt) Si-O vibrations when changing the sulfamethoxazole (SMX) concentration as 0, 20, 40, 60, and 100  $\mu\text{g L}^{-1}$  in the presence of fresh liquid swine manure-derived organic matter (dissolved organic carbon fraction (DOC)/fulvic acid (FA)/humic acid (HA)) obtained from equilibrated sorption solids.

Sample	Replicate	Organic matter concentration ( $\text{mg L}^{-1}$ )	SMX concentration ( $\mu\text{g L}^{-1}$ )	FTIR band				
				Si-O in-plane stretching at $1050 \text{ cm}^{-1}$	Si-O in-plane stretching at $1119 \text{ cm}^{-1}$	Overtone ( $\nu_4$ ) of $\text{SiO}_4$ vibration at $618 \text{ cm}^{-1}$	Combination band of $\text{SiO}_4$ vibrations at $2850 \text{ cm}^{-1}$	Combination band of $\text{SiO}_4$ vibrations at $2925 \text{ cm}^{-1}$
Bt	1	0	0	1051.14	1122.38	614.54	2849.94	2922.34
Bt	1	0	20	1058.09	1122.65	616.03	2850.05	2928.54
Bt	1	0	40	1069.07	1116.65	621.10	2849.45	2928.33
Bt	1	0	60	1063.02	1120.53	616.82	2850.25	2922.99
Bt	1	0	100	1051.40	1123.64	614.16	2848.20	2923.15
Bt+HA	1	25	0	1047.77	1123.79	610.97	2849.70	2922.92
Bt+HA	1	25	20	1048.07	1122.96	611.31	2847.38	2922.49
Bt+HA	1	25	40	1050.76	1123.32	616.40	2851.97	2922.37
Bt+HA	1	25	60	1051.64	1122.97	617.59	2849.58	2922.4
Bt+HA	1	25	100	1046.87	1123.52	625.30	2847.42	2922.76
Bt	2	0	0	1050.18	1118.87	623.43	2852.98	2922.15
Bt	2	0	20	1050.31	1119.62	622.29	2852.66	2921.59
Bt	2	0	40	1053.69	1118.13	621.63	2853.64	2923.17
Bt	2	0	60	1051.79	1119.61	623.26	2852.65	2921.94
Bt	2	0	100	1051.50	1119.47	624.42	2852.62	2920.26
Bt+HA	2	25	0	1051.62	1119.79	623	2852.35	2921.17
Bt+HA	2	25	20	1052.03	1119.89	623.73	2852.97	2921.97
Bt+HA	2	25	40	1050.27	1119.54	623.17	2852.7	2922.41
Bt+HA	2	25	60	1048.89	1120.21	624.89	2853.03	2922.01
Bt+HA	2	25	100	1049.63	1120.08	622.41	2853.13	2921.94
Bt	1	0	0	1049.16	1118.15	624.85	2848.8	2921.48
Bt	1	0	20	1048.42	1121.23	626.72	2850.05	2919.93
Bt	1	0	40	1048.39	1120.94	622.13	2849.09	2921.37
Bt	1	0	60	1047.85	1120.78	626.05	2851.67	2920.18
Bt	1	0	100	1048.81	1121.47	626.78	2849.85	2922.88
Bt+FA	1	25	0	1048.94	1120.86	623.26	2855.02	2925.02
Bt+FA	1	25	20	1048.48	1121.37	625.85	2850.14	2919.22

Bt+FA	1	25	40	1048.46	1121.82	625.78	2851.02	2920.47
Bt+FA	1	25	60	1048.61	1121.26	627	2850.51	2920.81
Bt+FA	1	25	100	1048.38	1121.18	622.81	2850.04	2925.87
Bt	2	0	0	1055.34	1119.71	623.75	2854.58	2924.77
Bt	2	0	20	1059.51	1125.31	621.99	2853.72	2922.52
Bt	2	0	40	1055.43	1124.3	621.24	2855.27	2919.78
Bt	2	0	60	1059.14	1123.59	623.36	2851.11	2924.9
Bt	2	0	100	1059.05	1124.34	626.4	2852.93	2920.29
Bt+FA	2	25	0	1054	1123.96	624.35	2847.88	2920.47
Bt+FA	2	25	20	1058	1124.84	621.68	2852.03	2922.11
Bt+FA	2	25	40	1053.34	1125.89	621.05	2854.1	2922.75
Bt+FA	2	25	60	1058.78	1124.26	621.65	2851.21	2922.35
Bt+FA	2	25	100	1057.61	1124.94	624.03	2850.93	2923.29
Bt	1	0	0	1054.59	1125.03	627.96	2855.34	2920.53
Bt	1	0	20	1056.07	1125.00	627.61	2851.79	2921.31
Bt	1	0	40	1054.81	1125.52	625.44	2852.08	2919.51
Bt	1	0	60	1057.43	1124.94	623.23	2853.65	2923.74
Bt	1	0	100	1056.65	1125.59	624.38	2850.89	2923.31
Bt+DOC	1	25	0	1055.57	1120.6	625.01	2853.16	2920.44
Bt+DOC	1	25	20	1053.59	1120.37	626.08	2854.76	2923.13
Bt+DOC	1	25	40	1058.96	1124.75	623.96	2850.68	2925.19
Bt+DOC	1	25	60	1058.63	1116.7	627.01	2849.55	2924.92
Bt+DOC	1	25	100	1056.71	1126.05	626.73	2850.49	2927.82
Bt	2	0	0	1055.26	1124.94	622.64	2851.56	2920.57
Bt	2	0	20	1054.73	1125.94	622.82	2850.39	2919.94
Bt	2	0	40	1054.81	1126.89	625.6	2851.92	2920.74
Bt	2	0	60	1057.07	1126.19	625.5	2853.04	2919.57
Bt	2	0	100	1058.17	1126.98	626.8	2853.15	2921.02
Bt+DOC	2	25	0	1056.80	1126.26	626.37	2847.03	2922.55
Bt+DOC	2	25	20	1059.54	1126.46	620.9	2854.66	2922.55
Bt+DOC	2	25	40	1066.15	1124.51	626.1	2849.68	2924.16
Bt+DOC	2	25	60	1058.56	1125.65	624.10	2852.09	2920.92
Bt+DOC	2	25	100	1054.92	1126.53	624.78	2850.23	2919.97

Table A-3 Full width at half maximum values of basal reflection peak ( $d_{001}$ ) of bentonite X-ray diffraction pattern when changing the sulfamethoxazole (SMX) concentration as 0, 20, 40, 60, and 100  $\mu\text{g L}^{-1}$  in the presence of fresh liquid swine manure derived organic matter (dissolved organic carbon fraction (DOC)/fulvic acid (FA)/humic acid (HA)) obtained from equilibrated sorption solids.

Sample	Replicate	Organic matter concentration ( $\text{mg L}^{-1}$ )	SMX concentration ( $\mu\text{g L}^{-1}$ )	FWHM of $d_{001}$ peak ( $\text{\AA}$ )		
				HA	FA	DOC
Bt	1	0	0	1.27	1.74	2.89
Bt	1	0	20	1.44	1.73	2.82
Bt	1	0	40	1.76	1.69	2.98
Bt	1	0	60	1.90	2.00	3.19
Bt	1	0	100	1.84	2.12	2.83
Bt+OM	1	25	0	1.53	2.16	2.41
Bt+OM	1	25	20	1.72	1.99	2.10
Bt+OM	1	25	40	1.59	2.03	2.35
Bt+OM	1	25	60	1.87	2.03	2.99
Bt+OM	1	25	100	1.54	2.14	2.62
Bt	2	0	0	1.40	1.71	2.20
Bt	2	0	20	1.64	2.26	2.27
Bt	2	0	40	1.33	1.99	2.44
Bt	2	0	60	1.34	1.76	2.27
Bt	2	0	100	1.35	1.45	2.66
Bt+OM	2	25	0	1.35	1.46	2.26
Bt+OM	2	25	20	1.33	1.61	2.38
Bt+OM	2	25	40	1.35	2.06	2.36
Bt+OM	2	25	60	1.44	1.57	2.45
Bt+OM	2	25	100	1.29	1.53	2.15